Seismic Retrofit of Reinforced Concrete Frames with Diagonal Prestressing Cables

By

Ali Molaei

A thesis presented to the School of Graduate Studies and Research of the University of Ottawa in partial fulfillment of the requirement for the degree of Master's in Applied Science

Ottawa-Carleton Institute for Civil Engineering
Department of Civil Engineering
Faculty of Engineering
University of Ottawa
February 2014

Acknowledgement

I would like to thank Dr. Murat Saatcioglu for his continues support and supervision. It has been an honor to be his student.

My gratitude goes to PhD candidate Mansour Navidpour for his continues assistance during my program.

My special thanks to my parents, my wife and my daughter for their encouragement and support.

Abstract

A large number of building inventory in Canada and elsewhere in the world consists of non-ductile reinforced concrete frames, with or without masonry infill panels. These structures suffer damage when seismic force demands are higher than their force capacities. Therefore, seismic retrofitting of such frame buildings for drift control remains to be a viable option for improved building performance. A retrofit methodology has been developed in the current research project, which involves diagonal bracing of frames with prestressing strands. An experimental research project has been conducted to assess the effectiveness of diagonal prestressing in non-ductile reinforced concrete frame buildings.

The experimental program consists of two large-scale single-bay single-storey reinforced concrete frames, with a height of 3.0m and a span length of 3.5 m. The frames were designed and built to reflect the 1960's practice in Canada, without the seismic requirements of current building codes, and hence are seismically deficient. They were retrofitted with diagonally placed prestressing strands, having two different areas of steel, prestressed to 40% of the strand capacity. One of the frames was retested after the failure of the strands, with a new set of strands without any prestressing, forming the third test.

The results indicate that lateral bracing reinforced concrete frames with high-strength prestressing strands is an effective strategy for controlling lateral drift and hence potential damage in buildings during strong earthquakes. Prestressing of the strands increases initial stiffness, as compared to non-prestressed cables, and provide superior performance. The area of diagonally placed steel (including the number of strands) and the level of initial prestressing depend on the required level of upgrade in the building in terms of seismic force requirements. The design procedure recommended in this thesis may be employed for implementing the technology. The thesis presents the details of the experimental program, and the test results. It also provides analytical verification of the approach, with a step-by-step design procedure.

Table of Contents

List of Figures

Chapter 2 Figures

Chapter 3 Figures

Chapter 4 Figures

Chapter 5 Figures

Chapter 1

Introduction

1.1 General

A large inventory of existing civil engineering infrastructure includes seismically deficient buildings. These buildings were either designed prior to the enactment of modern seismic codes or they were built recently in regions where code requirements were not enforced. Buildings designed and built in Canada prior to 1970's are especially vulnerable to seismic forces as earlier editions of the National Building Code of Canada did not address seismic design adequately. These buildings often lack sufficient strength and/or ductility (inelastic deformability). The seismic design force levels used in older codes were significantly below those required to meet the current Canadian seismic hazard. These design forces have increased over the years (Mitchell et al. 2011), making older buildings seismically deficient. Furthermore, the design and detailing requirements for structural elements, specified in material standards, have become more stringent over the years. In the Canadian practice, there was a significant improvement in design and detailing requirements in 1985 for concrete buildings and 1990 for other buildings (NRCC 1992). Therefore, older buildings pose significant seismic risk to the occupants and the society in general. Currently, a large volume of building inventory falls in this category. Unfortunately, due to economic reasons, it is not feasible to replace the existing inventory of seismically deficient structures with those that comply with current seismic codes. Therefore, retrofitting remains to be the only viable option for such structures. Depending on the retrofit goals, different methodologies can be implemented.

Many retrofit techniques have been developed over the last three decades, as discussed in Chapter 2. These techniques have different application areas with different levels of effectiveness. There are needs to develop economically superior and structurally sound seismic retrofit systems, providing practical solutions with minimum time and effort for implementation. The research project that is reported in this thesis is intended to meet this challenge and develop a new retrofit methodology, involving high-strength steel strands as tension-only braces.

1.2 Seismic Retrofit Techniques

In a seismically deficient structure, where elements, connections, and assemblies are designed for lower seismic forces than required, and lack proper design and detailing, the elastic design capacity may be exceeded and the structure may experience local or global failure during a strong seismic event. If the structure consists of a large number of problematic members, then the structural mitigation strategy may have to be applied at the system level. This task can be accomplished by limiting the overall lateral deformation of the structure through lateral stiffening and strengthening. Sometimes, drift control is accompanied by improved ductility and energy dissipation capacity of elements. If both are achieved without exceeding the deformation capacity of the seismically deficient elements of the system, then superior seismic performance of the building can be obtained.

When seismic deficiencies are limited to a few elements, seismic retrofitting can be implemented at the element or component level, without interfering with the overall system behaviour. This type of retrofitting often offers a cost effective solution. A significant portion of seismically deficient structures requires system level retrofitting. Proper selection of a retrofit technique is dependent on the specifics of the problem at hand, practical limitations, and the selected target performance level. The current research project, reported in this thesis, focuses on a system level retrofit methodology.

1.3 Objective

The objective of the current research project is to develop a seismic retrofit methodology for non-ductile reinforced concrete frame buildings involving the use of diagonally placed high-strength prestressing strands as bracing elements, with or without prestressing. This objective is

intended to be achieved primarily through experimental research that includes tests of large-scale reinforced concrete frames.

1.4 Scope

The scope of the research project consists of the following:

- Design and construction of two large-scale reinforced concrete frames, representing 1960's practice in Canada, to be seismically deficient both from strength and ductility perspectives.
- Instrumentation of the frames for strain and deformation measurements.
- Application of the proposed seismic retrofit technique by placing diagonally placed prestressing strands on the specimens.
- Testing of the frames under slowly applied lateral deformation reversals to assess the performance of each frame.
- Evaluation of test data and presentation of results in the form of force-deformation hysteretic relationships, as well as plots of strain and rotation measurements.
- Analyses of frames, comparisons of frame performances and assessment of the effectiveness of the proposed retrofit methodology.
- Development of a design methodology and recommendations for design of diagonal cable braces as a seismic retrofit strategy.

Chapter 2

Literature Review

2.1 General

The emphasis in previous seismic risk mitigation efforts has been placed on the development of retrofit methodologies for seismically deficient civil engineering infrastructure. A number of techniques have been developed over the last three decades, ranging from more conventional techniques, such as bracing existing structures by adding new shear walls or structural steel bracing elements, to new and evolving technologies that involve energy dissipation systems, dampers and control systems. Review of existing retrofit methodologies was conducted first, and included in this Chapter prior to undertaking the current research effort. The review of current state-of-the-art and previous research is presented in this Chapter with emphasis on seismic retrofitting through lateral bracing.

2.2 Structural Mitigation at Global Level

Seismic risk mitigation for non-ductile older buildings or newly built but non code-compliant buildings often requires intervention at the system or global level. These retrofit techniques are intended to reduce the overall seismic drift demand on the structure, while also enhancing its lateral load resistance. They consist of lateral bracing systems, such as shear walls and structural steel braces, supplementary damping devices, base isolation and active control systems. Most of these methods aim to improve properties of the original structure for improved performance. Semi-active or active-control methods adjust the properties of the supplementary devices according to external excitations through a central control unit. Since the performance of these methods is quite sensitive to the algorithm employed, quality of the implemented device and the

reliability of power source, these methods are not explored further for the purpose of this research. In addition, these methods may not be the most cost efficient approaches until they are fully developed.

The energy exchange between a structure and the ground during a seismic event can be explained by using the principles of the conservation of energy. According to Uang and Bertero (1988), the total energy is broken down to the following components:

$$E = E_k + E_s + E_h + E_d \tag{2.1}$$

Where;

E: Total input energy by earthquake;

E_k: Absolute kinetic energy;

E_s: Recoverable elastic strain energy;

E_h: Irrecoverable energy dissipated by the structural system through inelastic deformation or other inelastic forms of damping;

E_d : Energy dissipated by structural protective systems.

Commonly used and recently researched global retrofit options are presented in the following sections. Each of these methods has contribution(s) to one or more of the structural response terms given in the equation above.

2.2.1 Shear Walls

The performance of non-ductile seismically deficient structures is usually improved by either enhancing strength or ductility. A considerable percentage of existing non-code compliant structures consist of frame structures with or without masonry infill walls. When permitted by the layout and geometry of the building, adding and integrating properly designed and detailed shear walls can enhance both the lateral force resisting capacity and the ductility of the structure. However, application of this technique requires certain conditions for implementation. First, the layout of the structure should allow for placing sufficient number of shear walls in a manner not to generate significant torsion during seismic response. These walls can be placed in empty bays

or as replacement of infill masonry walls. Second, the existing structure should have the capability to transfer in-plane diaphragm forces to the added shear walls. Proper interlocking of the new elements and the existing structure can be achieved by detailing the connections. A sample of implementation of this retrofit technique is illustrated in Fig. 2.1 (Thermou and Elnashi 2006). The reinforcement should be detailed according to the current seismic provisions with special attention given to the reinforcement in potential plastic hinges in boundary elements for confinement of concrete. A convenient approach for implementing shear walls is to use the existing beams and columns while adding a web by placing concrete in the selected bay either by shotcreting or placing cast-in-place concrete. Figure 2.1 illustrates the application of the method.

Fig. 2. 1 Adding shear walls as a retrofit technique (Thermou and Elnashi 2006)

An important aspect of this technique is to provide a sufficiently strong link for load transfer to the foundation. Often times, the existing foundation is not adequate, and it becomes necessary to enlarge the size and depth of these foundations, which requires significant work and considerable budget.

Repair and retrofitting of RC walls using selective techniques was studied by Elnashai and Pinho (1998). In their study various retrofit methodologies, including the addition of external unbounded steel plates or externally unbounded steel reinforcement on the surface of existing walls, were researched for increase in strength without affecting the stiffness. The other experimental study included the addition of U-shaped external confinement steel plates when

additional ductility is required. This methodology only affects the ductility of the retrofitted wall. In addition to improving flexural response of shear walls, the researchers also retrofitted shear-dominant walls with horizontally epoxy glued steel plates for improved shear capacity. These specimens exhibited ductile behaviour because of the retrofit strategy implemented.

Jiang and Kurama (2013) studied retrofitting of medium-rise buildings designed in 1960's and 1970's, located in high seismic regions in the US. A series of analytical models of shear-deficient walls were developed using a micro-fibre plane element to capture the nonlinear interaction of axial force flexure and shear forces in walls. ASCE 41-06 was used to provide retrofit alternatives, including: i) reduction of flexural strength, ii) addition of concrete confinement, and iii) increasing shear strength. Each approach enhanced the performance of walls while showing deficiencies in lateral displacement capacities. The deficiencies related to large displacements were resolved by implementing a combination of these methods.

The use of steel plates on concrete shear walls as a seismic retrofit methodology was studied analytically by Elnashai and Elghazouli (1993). The researchers provided a reliable tool in evaluating response under earthquake loading. The non-linear cyclic concrete model developed incorporates concrete confinement. The software used by the researchers also captured the effects of local buckling and variable amplitude cyclic degradation of steel. The analytical results were subsequently compared with the results of pseudo dynamic tests, which showed good correlations.

Cortés and Palermo (2010) studied the performance of new and repaired/retrofitted shear walls using VecTor 2, a two dimensional nonlinear finite element analysis (FEM) software. The repair and retrofit methodology considered involve replacing damaged concrete with new concrete and adding diagonal reinforcement and externally placed steel plates and FRP sheets. This research aimed to provide a simple yet effective tool, capable of capturing the condition of the wall after experiencing damage and carry forward the correct properties to the post-retrofit model. It also integrated the existing material with new repair material such as concrete replacement, diagonal reinforcing bars, externally bolted steel plates and externally bonded fiber reinforced polymer sheets. The research also took into consideration the aspect ratio of the shear wall and extended the scope to include squat, slender-squat and slender walls. The results of analytical study showed good correlation with observed wall tests in laboratory. The program showed to be more

accurate when dealing with walls which do not have low aspect ratio. It should be noted that the model used smeared reinforcement to represent steel bars. Further studies were recommended to study the effects of bar buckling.

2.2.2 Diagonal Braces

Similar to the lateral bracing by concrete shear walls, buildings can be retrofitted using diagonal braces as illustrated in Fig. 2.2. Normally steel braces are placed in orthogonal directions in clear bays to provide additional lateral force resisting capacity as well as keeping lateral drift under control. The lateral force, whether it is caused by wind or earthquake, is transferred through the diaphragm to the braced frames, and subsequently to the diagonal members. The diagonal members would form tension ties and compression struts, which would help resist lateral forces. Often these members are strong enough to withstand forces elastically or in near elastic state. However, in cases where the demand is significantly high, exceeding the elastic capacity of the bracing elements, tension ties may yield and compression struts may buckle, while maintaining their lateral force resisting capacities and dissipating seismic induced energy.

Fig. 2. 2 Examples of using steel braces as a retrofit methodology
University of California dormitory, Berkley, CA., USA (Left)
Parking garage in Berkley, CA., USA (Right)

Brace retrofits often create challenges at connections, especially in tension. To overcome this, Caron et al (2010) developed compression-only braces. The braces only resisted compression, and were made sufficiently rigid to prevent buckling. This approach offers the advantage of eliminating costly tension connections.

Ozcelik et al. (2012) used chevron braces as a seismic retrofit technique for non-ductile reinforced concrete frames. The application was verified through experimental and numerical studies of two as-built and five strengthened frames. The reverse cyclic loading test results showed improvements in stiffness and lateral strength of about 3.5 times the unretrofitted frame and maintained it for a drift ratio of up to 2%. Although the specimens experienced rapid strength degradation, the results showed significant energy dissipation capability. The specimens retrofitted with square HSS showed the least susceptibility and performed better. They also concluded that the post-buckling capacity of the braces can be relied on as long as the inter-storey drift is kept below 1% for seismically induced lateral loads.

Moghaddasi et al. (2012) explored the idea of utilizing Glass fiber reinforced polymer tube to confine concrete infill with a steel inner core as braces. The composite brace enhanced the lateral force resisting capacity and frame stiffness largely. Subsequently, OpenSees, a finite element analysis software, was used to generate a computer model of the retrofitted frame. The analytical investigation included push-over analysis and time-history analysis of a single frame and expanded to a three-storey structure to determine the efficiency of this approach in large scale construction. The results indicated that this methodology is capable of reducing peak deformation demands for an average ratio of 81% while the base shear was only increased by about a factor ranging between 0.35 to 0.65, depending on the nature of the simulated excitation. It should be noted that the steel core area to gross sectional area ratio has the most influence in the performance of this technique.

Varum et al. (2013) evaluated the performance of seismically deficient RC buildings using steel braces. The experimental results generated showed the effect of lateral bracing on global structural response, with and without the presence of infill walls. The researchers also conducted a numerical study using rigid strut models and reproduced graphs matching the experimental values. The research was extended to investigate the non-linear dynamic response of structures

under various excitation scenarios using a calibrated model. The study highlighted the significance of masonry infill panels on the global response of structures.

The application of self-centering braces as a retrofit technique was studied by Tremblay et al. (2010). The particular self-centering characteristic of this seismic retrofit option provides additional preventative measures against instability and progressive collapse. The technique is further studied for improved performance (Tremblay et al. 2008, Merzouq and Tremblay 2006, Filiatrault et al. 2004).

2.2.3 Strengthening of Unreinforced Masonry (URM) Infill Walls using Fibre Reinforced Polymer (FRP) Sheets

Some of the existing non-ductile frame systems in buildings have at least several unreinforced masonry (URM) infill walls. These walls are intended to be non-structural elements. Hence they are not designed for lateral force resistance. However, since they are not fully isolated from the frames, they interact with the surrounding structural elements when subjected to lateral forces. Lack of proper reinforcement in URM walls lead to brittle failures, sometimes even under moderate levels of lateral forces, or due to the out-of plane forces. An effective retrofit strategy for such walls, hence for the entire structural system, is the use of surface-bonded FRP. The application of FRP sheets on the surface of URM provides reinforcement to the wall, increasing its diagonal tension capacity, while also contributing towards the integrity of URM units. This transforms URM into an effective shear wall, especially if integrated with the enclosing frame elements, adding lateral stiffness and strength to the system. FRP sheet(s) can be applied on the entire surface of URM infill walls or as diagonals where they provide diagonal tension ties (Shalouf and Saatcioglu 2006). Tests of URM walls, retrofitted with FRP either as full coverage of the wall surface, or in the form of diagonal strips are shown in Fig. 2.3.This methodology is easy to install and is not considered to be intrusive. However, though it increases strength and stiffness, it does not increase the ductility of the system, as both URM and FRP are brittle materials. This method is also sensitive to the bond characteristics of FRP sheets on existing URM walls and frames. Surface bonding is effective until debonding occurs at about 0.6% tensile strain. The use of FRP anchors provides additional anchorage to masonry and concrete, significantly improving tensile capacity of diagonal ties (Saatcioglu et al. 2005, Ozbakkaloglu and Saatcioglu 2009). Ozbakkaloglu and Saatcioglu (2009) illustrated that FRP fan anchors can

be used successfully in seismic retrofit applications. Fig. 2.4 illustrates the application of FRP anchors in a URM infill wall, tested at the University of Ottawa.

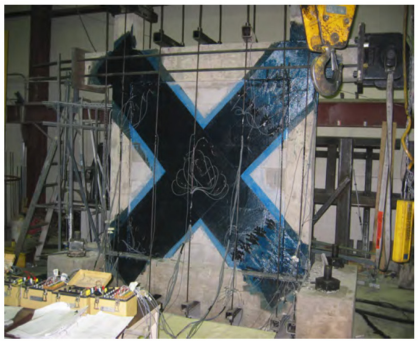

Fig. 2.3 Full surface and diagonal application of FRP sheets on URM walls (Shalouf and Saatcioglu 2006)

a) Anchor tests

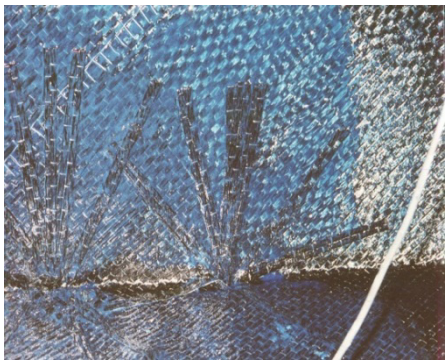

b) Installed anchor

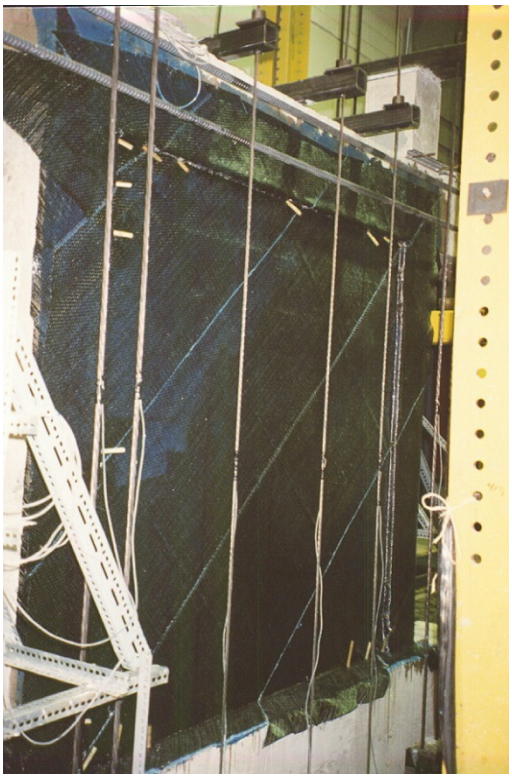

c) Locations of frame elements for anchors

Fig. 2.4 Development and use of FRP anchors for masonry walls (Saatcioglu et al. 2005, Ozbakkaloglu and Saatcioglu 2009)

2.2.4 Bracing with Prestressing Strands

As an alternative to conventional steel bracing systems, which are often in the form of structural steel members, prestressing strands or cables can be used to provide tension ties along the diagonals of frames. These cables can be placed snug-tight or can be prestressed based on the required design methodology. If the cables are attached to the structure without applying initial forces, the system is designed as a passive system and the magnitude of the cable force is dependent on the lateral deformation of the frame. If there are no lateral deformations, then the diagonal cables provided in both directions are stress-free. When the frame sways laterally, then the cables in one of the diagonals stretch while the others sag. When the direction of the lateral load changes, the cables in two diagonal directions switch roles. On the other hand, when the cables are prestressed, they are in tension prior to sway. The net horizontal force on the frame is initially zero since the horizontal components of diagonal forces are equal and opposite to each other, cancelling the effect of prestressing. However, when the frame sways under lateral loading, one of the cables stretches further while the other cable starts unloading itself. This additional force difference results in higher lateral force resistance at the same lateral drift level. It should be noted that, while both un-prestressed and prestressed cable applications provide the same maximum lateral load resistance to the frame, prestressed cables provide the same level of resistance at a significantly smaller lateral drift level, essentially improving the stiffness of the system. This aspect of cable bracing may be important in terms of controlling lateral drift and associated damage in brittle elements.

Shalouf (2005) investigated the seismic performance of a half-scale frame-brick wall assembly using diagonal prestressing cables as a retrofit option. The initial wall-frame assembly was built as per 1970's NBCC, and was tested as a benchmark. The subsequent specimen used two diagonal cables on each side, one in each direction per side, with 75 kN/cable initial prestress force. This option showed significant improvement in the lateral force resisting capability, adding over 75% additional capacity. Finally, the last retrofitted wall-frame assembly utilized 2 diagonal prestressing cables per wall side with 125 kN force per cable, resulting in a total of 4 cables in each diagonal. Upper portions of columns were jacketed using FRP sheets to provide additional confinement/shear capacity. This specimen exhibited almost the same level of lateral

force resisting capacity but failed with limited lateral deformation compared to the previous two samples.

The research project was extended to include an analytical study of the cable retrofit application in buildings where NBCC-2005 compatible earthquake records were used to evaluate building performance (Shalouf and Saatcioglu 2006). The results indicated that unretrofitted buildings developed 60% of the required lateral force capacity and failed in a brittle manner, as opposed to diagonally prestressed braced frames, which developed lateral force capacities in excess of that required by NBCC-2005 at a drift ratio of 2% to 2.5%.

Pincheira and Jirsa (1992) conducted an analytical investigation to study the effectiveness of post-tensioning braces. Five different ground motions were used to perform dynamic analyses of retrofitted frames with foundations on different types of soils. They considered various layouts of cable placement on the frames, with alternative cable arrangements, including cables spreading across the face of the building to form diagonal tension braces on the entire face of the structure. This is shown in Fig. 2.5. The researchers subsequently extended their scope to study the efficiency of diagonal pre-stress cables as a retrofit technique in three prototype buildings (Pincheira and Jirsa 1992). The prototype buildings were selected to represented low and medium-rise seismically deficient structures. The research provided satisfactory results as long the lateral deformation of the structure was controlled within the range that was tolerable by the entire structure, including gravity only members. The results were verified against various soil conditions and it was concluded that the method might require strengthening of framing/foundation elements to sustain additional shear/axial/flexural demands on certain elements.

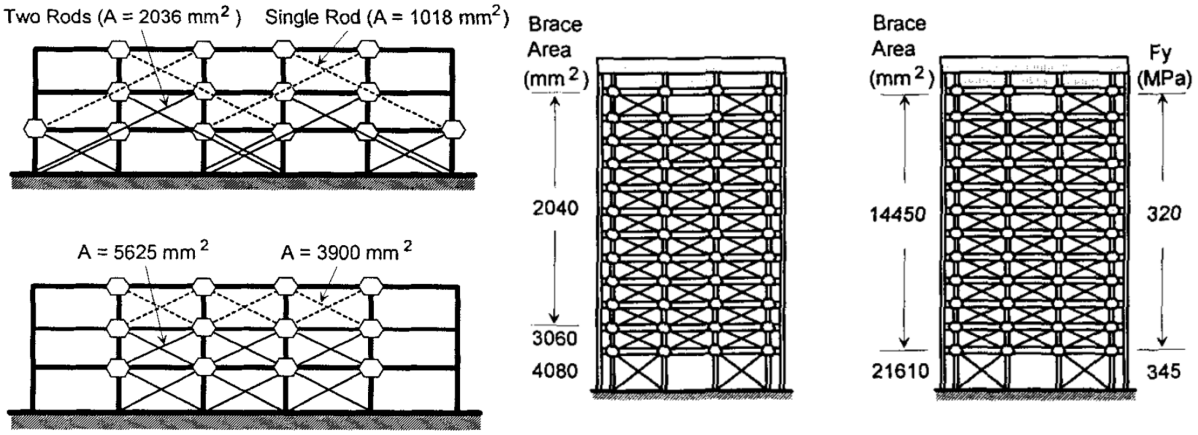

Fig. 2.5 Different retrofit schemes for a seismically deficient structure using cables; left) providing diagonal tensions on the entire face of the structure in selected bays; right) mid-rise prototype structure using prestress cablesas retrofit technique Pincheira and Jirsa (1992 and 1995)

The researchers also modeled a seven-storey building and applied the same retrofit strategy using different patterns of cable layout. The results indicated that the lateral force resisting capacity was significantly increased and either one of the two arrangements shown in Fig. 2.5 could be used, if designed properly. They also noted that applying this method should take into consideration the localized effect of presstressing, and might require enhancement of few selected elements, i.e. jacketing of columns.

Carriere (2007) continued on Shalouf's research by generating a series of computer models for seismically deficient structures in Vancouver, designed using the NBCC-1970. The models included 5, 10 and 15 story buildings with various patterns of prestress cables. A limit of 1% lateral drift was selected to ensure elastic performance of the entire building. The results indicated that by placing adequate number of cables in proper configuration, it was possible to limit the lateral drift demands to approximately 1%. His research also showed that this method is sensitive to building mass and is best suited for building of lower mass since relationship between increased mass and number of cables is not linear. Finally, it was indicated that, while the method provided additional lateral force resisting capacity, the building elements has to be checked for adequate shear resistance, especially near the base.

Buckling Restrained Braces (BRB)

One of the more recent seismic retrofit techniques that have been developed involves buckling restrained braces (BRB) in both concrete and steel frame structures. This method is used to overcome inherently low energy dissipation capability of conventional steel braces by preventing compression buckling. As a result, stable tension-compression hysteretic cycles are achieved with substantial improvements in energy dissipation when BRB's are implemented in the structure. A schematic view of a typical BRB system is shown in Fig. 2.6.

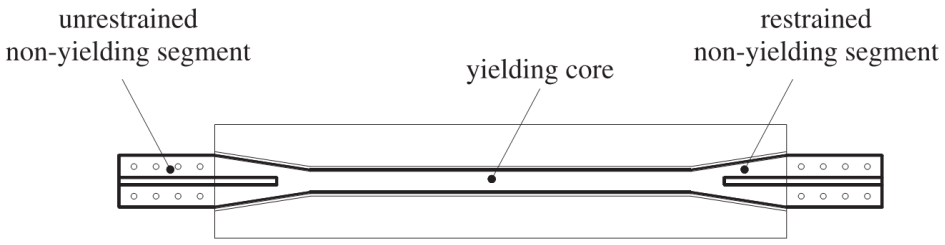

Fig. 2.6 Components of buckling restrained brace (BRB) – Bosco and Marino (2012)

Even though the concept of BRB was considered decades ago, national codes and standards just recently started to consider and adopt this approach as a recognized approach. Initially, the Structural Engineers Association of Northern California (SEAONC) introduced the "recommended provisions for buckling restrained braced frames" in 2001 to promote BRB applications. This was followed by NEHRP "Recommended Provisions for Seismic Regulations for New Buildings and Other Structures" in FEMA-450 (2004) and then "Seismic Provisions for Structural Steel Buildings" in AISC-2005. The concept has since evolved further and adopted by few seismic codes. Several companies in the world developed their own BRBs for use in the construction industry.

The research on BRB is mainly focused on two areas: i) the effect of using BRB systems as a global lateral force resisting system and the level of improvement achieved; and ii) the connection details/issues.

The design methodology of a BRB system as a global lateral force resisting system was investigated by Bosco and Marino (2012). In their research, they emphasized the efficiency of the method and suggested that codes like EuroCode 8 should recognize the method as a standard

practice. In addition, they looked at various documents and proposed new/improved behaviour factors for various storey drift values.

Sarno and Manfredi (2011) performed experimental studies on full-scale unretrofitted reinforced concrete frames using BRBs. Two 2-storey 2-bay specimens were designed, detailed and constructed for gravity loads only. One was tested without a BRB as benchmark and the other was equipped with a BRB system. The samples were tested under monotonically increasing static lateral loads (push over) and dynamic loads. The results indicated more than twice the capacity in both lateral strength and ductility. Fig. 2.7 shows a brace element after yielding.

Fig. 2.7 Retrofitted specimen; close-up view (left) and yielding of BRB element (right) - Sarno and Manfredi (2011)

Prinz et al. (2012) studied the seismic performance of BRB frames with eccentric configurations. This approach basically combined eccentrically braced frames (EBF) and BRB in one application. In their analytical study, the economical/technical aspects of using BRB in EBF were looked at. It was concluded that even though the hybrid system had a greater residual drift than a comparable EBF system and required more steel for construction, the novel hybrid system was less susceptible to failure at connections, and more economical in design, fabrication and erection stages. The schematic view of the proposed connection details and the overall global system for their analytical studies is shown in Figs. 2.8 and 2.9, respectively.

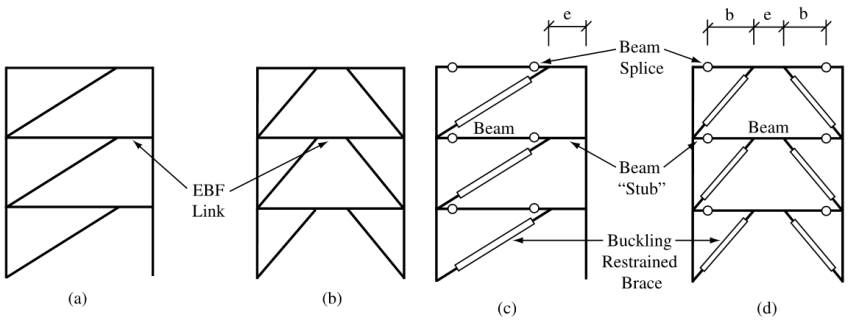

Fig. 2.8 Conventional EBF (a and b) vs. Hybrid BRB and EBF (c and d) - Prinz et al. (2012)

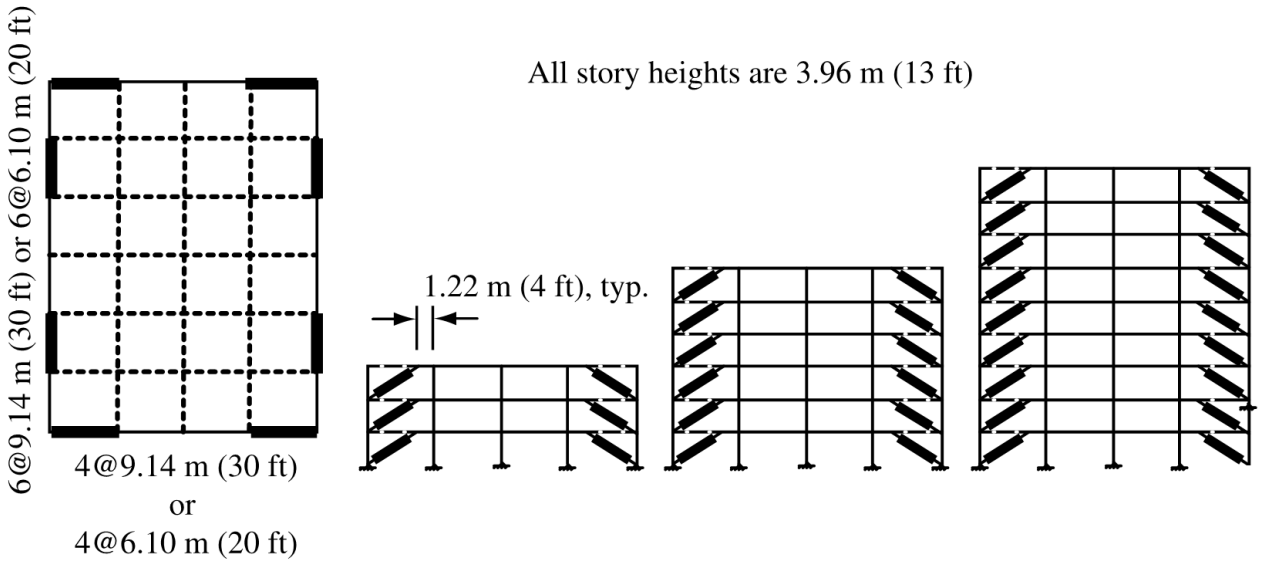

Fig. 2.9 Building plan and elevation views of the analytical model - Prinz et al. (2012)

Li et al. (2013) conducted a two part study involving both theoretical and experimental investigations on BRB connection detailing and performance in concrete structures. Fig. 2.10 illustrates the BRB connection to steel reinforce concrete. The study compared experimental and analytical results against the Chinese Code, and proposed details for connections.

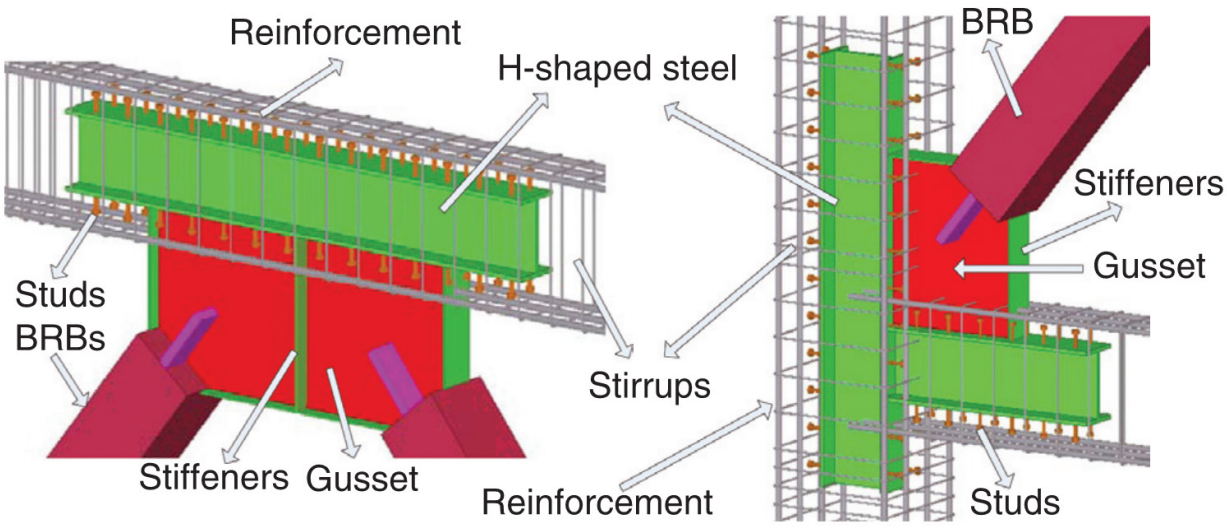

Fig. 2.10 BRB Connection to Steel Reinforced Concrete, Li et al. (2013)

The researchers concluded that under various loading scenarios, the yield displacement of connection was very small, and hence the anchorage connection performed elastically during the seismic event considered. In other words, the energy dissipation at the connection was negligible. They also noted that the anchorage connection capacity was highly dependent on the bending stiffness of the upper anchor plate. Fig. 2.11 shows the schematic diagram of the anchorage connection used and a picture of the failed connection.

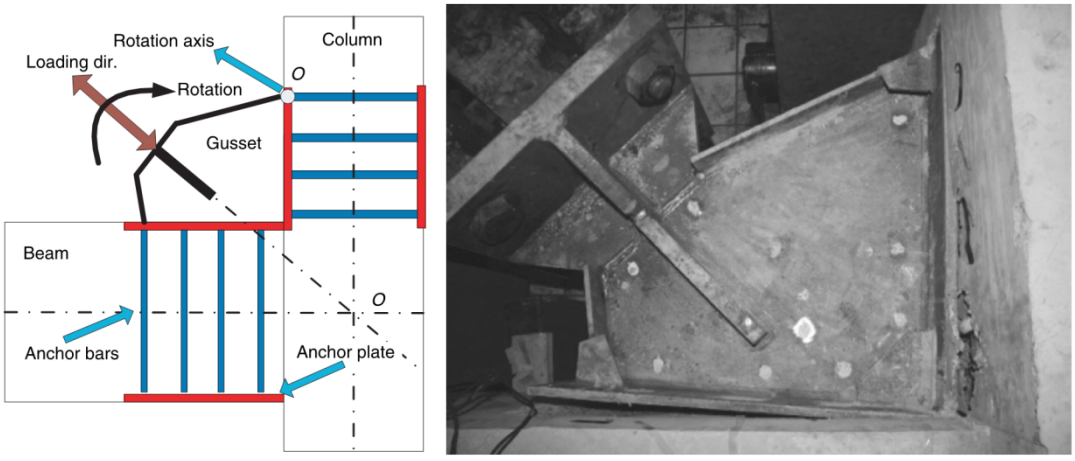

Fig. 2.11 schematic diagram of anchorage connection (Left) and failed connection (Right) - Li et al. (2013)

Berman and Bruneau (2009) tested a series of BRB braces where a single diagonal member was placed in the designated bay, and was designed to yield in both tension and compression. Their application is shown schematically in Fig. 2.12. The researchers indicated that BRB systems conventionally used strong gusset-plates to connect the brace element to the frame. This could potentially lead to some problems. Gusset plates produce local strengthening of the frame at beam-column connection. This results in a higher framing action and a negative impact on seismic performance of the system. It may also increase the base-shear during seismic response and transfers moments to braces though the brace elements are not designed for bending. To eliminate these potential deficiencies of gusset plates, an offset BRB connection was proposed where the BRB would connect to the beam directly. The test results conducted by Berman and Bruneau (2009) indicated significant improvements in the deficiencies indicated above. Fig. 2.13 illustrates a sample BRB installed connection. Hysteretic relationship obtain for such a system under reversed cyclic loading is shown in Fig. 2.14. The hysteretic cycles show stable and fat hysteresis loops with considerable energy dissipation capability.

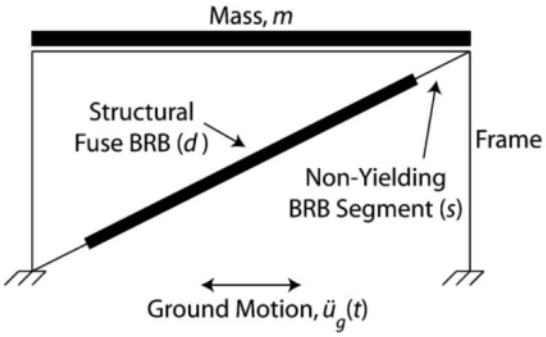

Fig. 2.12 Schematic view of a frame system using BRB (Berman and Bruneau 2009)

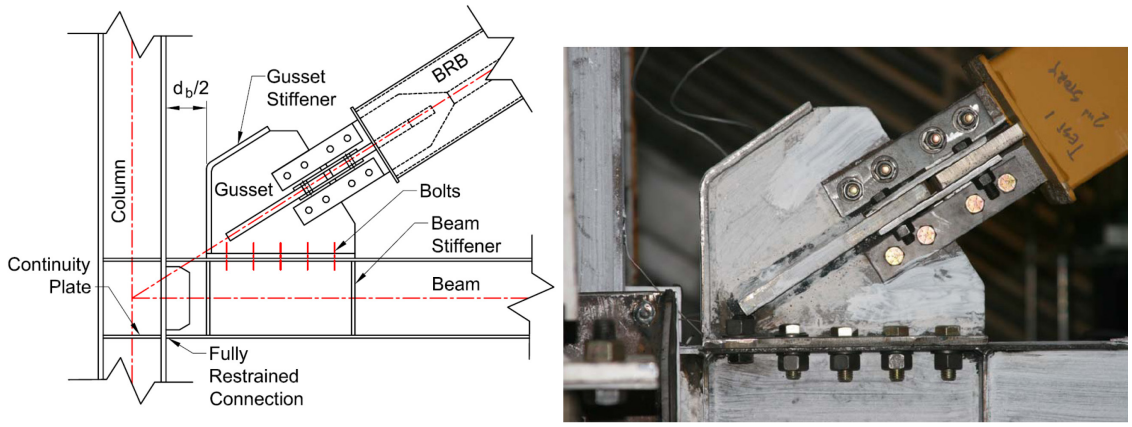

Fig. 2.13 Schematic and in-place views of the proposed BRB connection (Berman and Bruneau 2009)

Extensive reviews of the state of the art on BRB are presented by other researchers, especially involving steel frames (Della Corte and et. al 2011, Uang and Nakashima 2004, Xie 2005 and Di Sarno and Manfredi 2009).

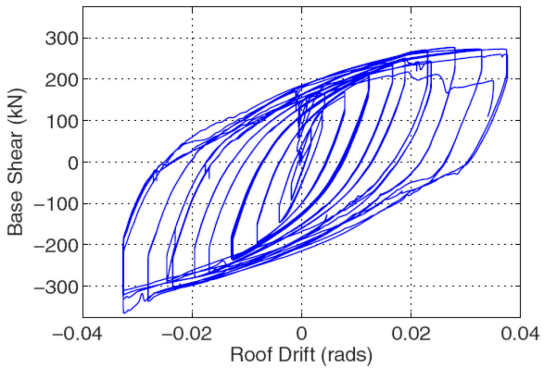

Fig. 2.14 Hysteretic response of a BRB system (Berman and Bruneau, 2009)

Chapter 3

Experimental Research

3.1 Introduction

Experimental research was conducted to investigate the strength and deformability of non-ductile reinforced concrete frames, braced with diagonal prestressing cables. Two large-scale reinforced concrete frames were designed and built based on the ACI 318-1963 building code, reflecting pre-1970's practice. This implies that the frames were built without particular considerations for seismic design requirements and represent the conditions of a seismically deficient existing structures built prior to the enactment of modern seismic codes.

The experimental research included two identical 2/3rd scale single-bay single-storey frames, braced diagonally with different number of cables, prestressed to approximately 40% of the cable capacity. One of the frames was also re-tested with strands placed snug-tight, without prestressing. The frames were companion to that designed and tested by Al-Sadoon (2013) without any retrofit, which was used as a reference frame. The results are compared in terms force and deformation capacities.

The current research project forms the second phase of an earlier research that was conducted at the University of Ottawa on smaller scale reinforced concrete frames with brick masonry infill walls, retrofitted with diagonal prestressing (Shallouf 1999). It aims to determine the effectiveness of diagonal prestressing cables in bare reinforced concrete frames as a seismic retrofit lateral bracing system for use in practice.

3.2 Specimen Description

The specimens consisted of ~~a~~ single storey single bay 2/3rd scale reinforced concrete frames with 300 mm by 300 mm square columns supporting a beam with 300mm width and 350mm depth ~~at the top~~. The entire frame was cast on an I-shaped foundation with holes matching the pre-existing holes on the strong floor of the Structures Laboratory at the University of Ottawa. High strength steel bolts with 75 mm diameter were used to mount the foundation through these holes, and fix the frame to the laboratory strong floor, providing full-fixity at the column footing locations. The reinforcement details, based on the ACI 318-1963 requirements, are shown in Fig. 3.1.

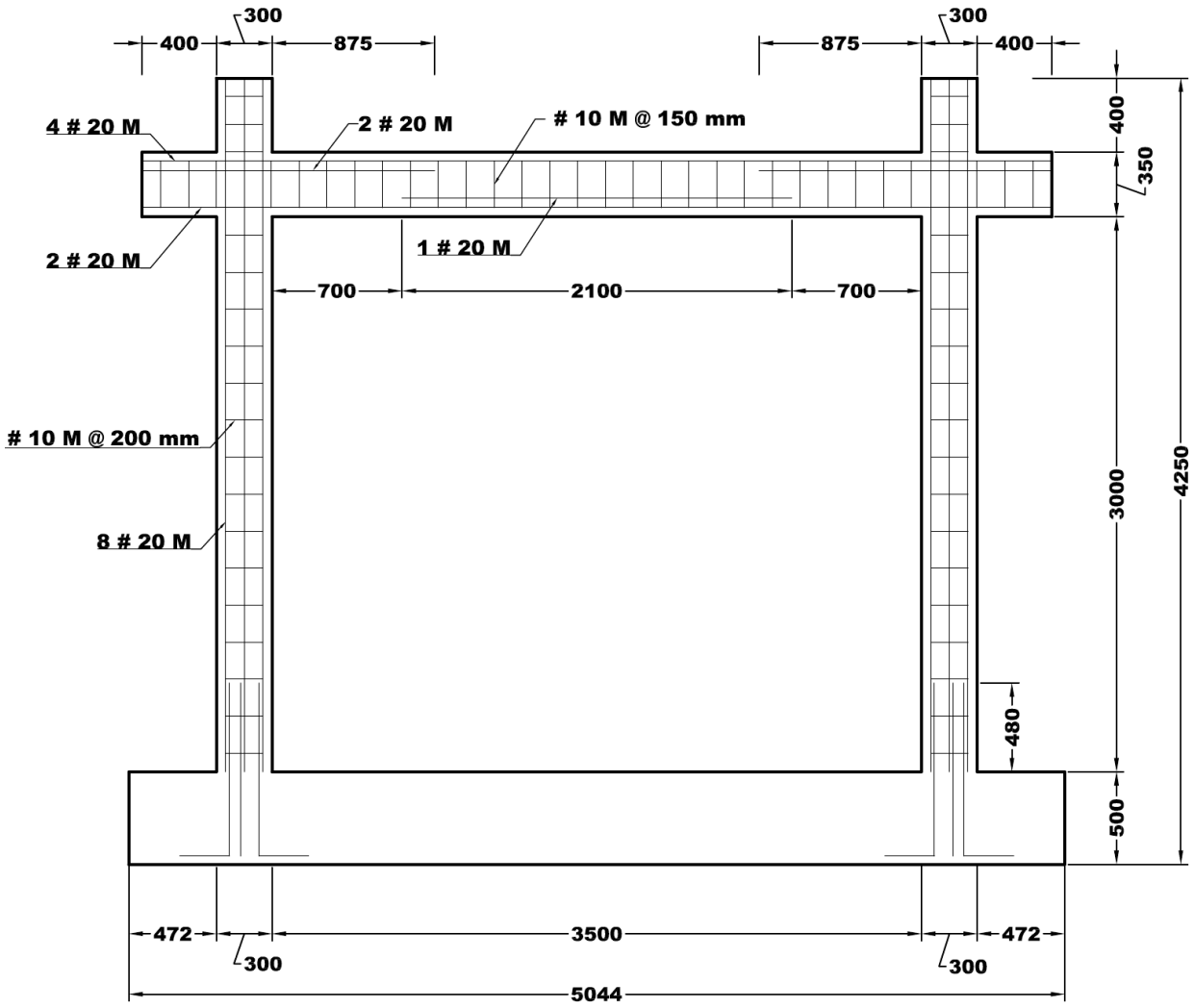

Fig. 3.1 Reinforcement layout of a typical test frame (Al-Sadoon 2013)

The longitudinal reinforcement in columns consisted of 8-20M bars ($A_s = 2400\,mm^2$) which correspond to 2.67% reinforcement ratio. The beam longitudinal reinforcement at mid-span consisted of 4-#20M top bars and 3-#20M bottom bars; and at the supports it consisted of 6-#20M top bars and 2-#20M bottom bars. The geometric and reinforcement details for the beam and the column cross sections are illustrated in Fig. 3.2.

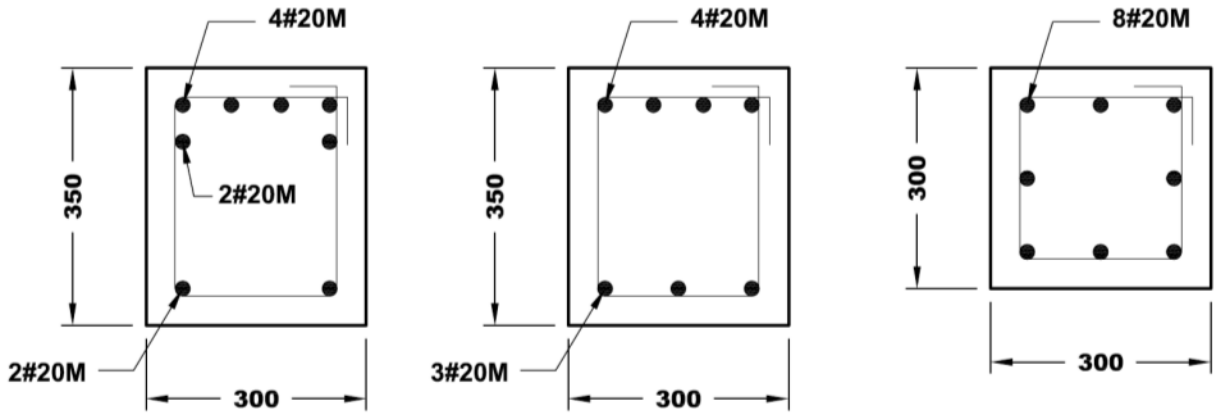

a) Beam section at support b) Beam section at mid-span c) Column section

Fig. 3.2Cross-section details of frame members

The transverse reinforcement of the beams and columns were selected as #10M (11.3 mm diameter) closed stirrups with 90-degree bends having $6d_b = 68\,mm$ (2¾ inches) extensions. The stirrups were placed at 150 mm, equal to one half of the minimum cross-sectional dimension of the beam, as per the shear design requirements of the ACI 318-1963 code. Column ties were also made out of the same size reinforcement (#10M) and were placed as perimeter ties with 90-degree bends. The tie bends had the same extensions as those used for the beam stirrups. The column ties were placed at a spacing of 200 mm. The column longitudinal reinforcement was lap spliced according to the ACI 318-1963 requirements with a $24d_b$ (d_b: diameter of the longitudinal bar in column) lap length. Hence, a lap length of 480 mm was provided immediately above the foundation as shown in Fig. 3.1.

The specimen was subjected to gravity loads prior to the application of incrementally increasing reversed cyclic lateral loading. The axial load consisted of 800 kN of concentric compression on each column, plus three concentrated loads of 40 kN each on the beam with equal spacing. The

column axial load corresponded to 21% of column concentric capacity (P_0).The axial loads were applied by means of prestressing strands, using six vertical tendons at each column, and two tendons at each load point on the beam. This is shown in Fig. 3.3.

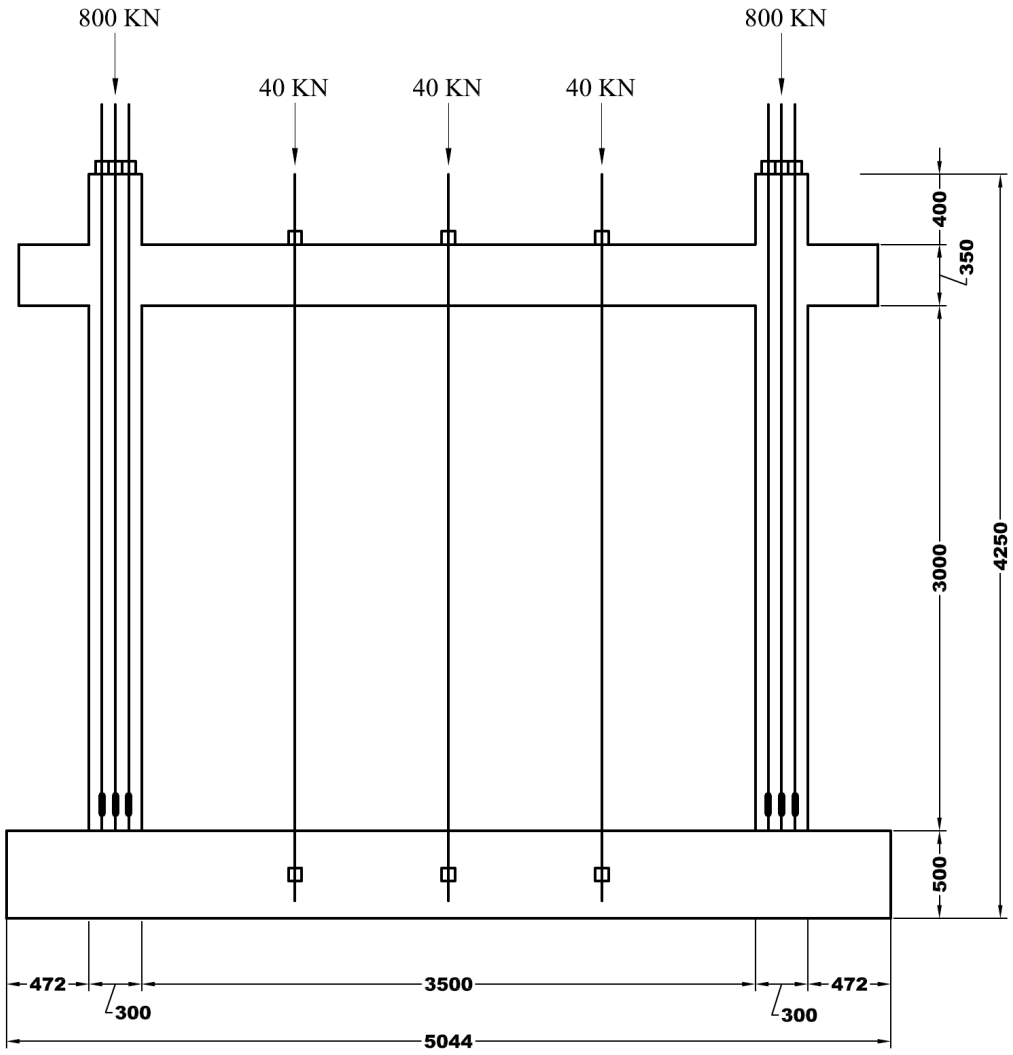

Fig. 3.3 Application of gravity loads

3.3 Behaviour of Seismically Deficient Reinforced Concrete Frames

It is important to understand the behaviour of reinforced concrete frames prior to constructing and testing laboratory specimens. This 1960's frame is expected to perform similar to a seismically designed frame during its elastic response. The shortcomings of a seismically deficient frame would become obvious at higher lateral deformation levels when inadequate confinement of core concrete, combined with insufficient lap splice would lead to premature

failure of the frame. Lack of proper lap splicing in columns generally becomes apparent starting at approximately 1% lateral drift, depending on the splice length and the level of axial compression. It was observed in earlier tests that bridge columns under low levels of axial compression, with 20 d_b splice length, started experiencing strength degradation at about 1% lateral drift (Beausejour 2000, Saatcioglu et al. 2002). Similar bridge columns without a splice deficiency, but with lack of concrete confinement did not show strength decay until after 2% lateral drift (Mess 1999, Saatcioglu et al. 2002). This implies that a maximum design drift ratio should not exceed 1% to 2% drift ratios depending on the degree of deficiency in the structure.

The possible failure mechanisms of a reinforced concrete frame include:

- Buckling of longitudinal column bars under combined axial compression and bending moment due to lack of closely spaced ties;
- Spalling and crushing of column concrete due to lack of confinement.
- Flexural failure of columns or beams;
- Shear failure of columns or beams where transverse shear reinforcement is insufficient or poorly detailed;
- Column failure at splice regions where the splice length is insufficient to develop the full capacity of re-bars (bar slippage);

In addition to the practice for design and detailing, our knowledge of Canadian seismicity has improved over the years, and seismic hazard levels in the National Building Code of Canada (NBCC) have increased relative to 1960's. Therefore, a frame building designed based on the 2010 NBCC is likely to require approximately up to 3 times higher forces, depending on the location, relative to buildings designed in the 1960s (Mitchel et al. – 2010). Therefore, the focus on current research is placed on increasing strength, while controlling lateral drift. Lateral bracing of frames with diagonal prestressing strands, with and without prestressing, can fulfil this combined goal of increasing lateral resistance, while controlling lateral drift.

Preparation of Specimens

The specimens for this project were built in the Structural Laboratory of the University of Ottawa. The initial steps included the preparation of formwork, ordering steel with specific

dimensions as required by design, assembling the steel cage, and concrete casting. The underside of the formwork was built using ¾ inch tongue-and-groove plywood to form a platform under the foundation. The sides were cut to 500 mm to match the foundation height and accommodate the existing test set-up in the lab. The formwork is illustrated in Fig. 3.4(a).

Conventional Grade 400 MPa reinforcement was ordered through a local supplier. The reinforcement came pre-bent, based on the specified dimensions. The reinforcement was then tied together to assemble the foundation cage as illustrated in Fig. 3.4. An extra set of bars were placed in the foundation to provide cast-in anchors to tie vertical prestressing tendons for the application of axial loads. These cast-in anchors were designed to provide sufficient capacity to allow the development of the ultimate capacity of cables. A similar approach was used to provide support for diagonal cables that are used for retrofitting the frame.

A total of four 3-inch plastic pipes, two per side, were placed in the formwork prior to casting. These holes matched the locations of existing holes on the laboratory strong floor. They were used to insert 3-inch diameter high-strength steel bolts to connect the foundation to the strong floor. The plastic pipes and the overall view of the formwork are shown in Fig. 3.4.

(a) Formwork with 3 inch pipes (b) Steel cage in formwork

Fig. 3.4 Overall view of formwork

The foundation concrete was poured and vibrated thoroughly. Several cylinders were cast with each frame to monitor the strength gain in concrete with time. Fig 3.5(a) shows the foundation immediately after casting. The forms were removed two days after casting. The foundation

concrete was moist cured for seven days. The entire exposed concrete surface was covered with burlaps, and watered frequently to maintain the moist environment for continued curing. This is shown in Fig. 3.5(b).

a) Fresh concrete after finishing b) Wet burlap covering for concrete curing

Fig. 3.5 Placement and curing of foundation concrete

The second phase of construction involved the construction of the columns and the beam for each frame. Column cages were assembled separately and tied to the starter bars to complete the assembly of the cage. Column formwork was prepared from wood. It was laterally supported by steel straps to ensure sufficient strength against wet concrete pressure. Similarly, the beam formwork was built and assembled to complete the entire frame formwork. The formwork was oiled and sealed prior to casting concrete. Fig. 3.6 illustrates the completed frame formwork and the frame after the removal of the formwork.

For the first frame (Frame No. 1), holes were provided in beam-column joints to insert the prestressing strands for retrofitting. Fig. 3.4(b) illustrates the foundation formwork ready for casting. It can be seen in the figure that two inclined small diameter plastic pipes were placed in the formwork diagonally with the same angle as the frame hypotenuse to create holes in concrete. These holes were used to run prestressing tendons in the retrofitted specimen, with one diagonal cable in each direction.

Fig. 3.6 Frame formwork and frame after formwork removal

In the second frame (Frame No. 2), two cables were used in each diagonal. The cables were positioned so that each cable would pass on one side of the column. The cables were connected to one inch high-strength threaded bolts that had been cast in concrete near the base of each column. The cylindrical prestressing anchors were threaded at their ends and connected to the bolts. This is illustrated in Fig. 3.7.

Fig. 3.7 Cable connection mechanism to the foundation

Hollow steel sections were placed at top joints on the opposite side of beam-column joint. The steel sections had pre-drilled holes to accommodate the strands. The cable is run through these holes and locked in by friction wedges. The prestressing operation was done at the top end of the strands. Fig. 3.8 illustrates the diagonal cables in place for Frame No. 2.

Fig. 3.8Frame 2 with installed double cables

The specimens were painted with diluted white paint prior to testing for better visibility of cracks, and to simplify marking of cracks. Strain gauge cables were extended and connected to the data acquisition system. A total of forty strain gauges were placed on longitudinal and transverse reinforcement to monitor internal strains and stresses. A few redundant strain gauges were placed in critical locations as back-ups, in case some gauges were damaged or failed during casting or testing. The frame was cast using 30 MPa concrete (which reached 31 MPa after 28 days), as representative of the practice in 1960s, and moist cured for three days. Concrete cylinder samples were taken and tested after 7, 14 and 28 days to monitor strength gain. These details are given in the material properties section.

The frames were subjected to vertical forces representing gravity loads 28 days after casting. These loads were applied by means of externally placed prestressing strands. The prestressing operation included the use of two hydraulic jacks, one at each side of the wall, to stress the cables simultaneously with equal forces. The bottom of each cable was secured to an HSS section that had been placed underneath the foundation, extending towards each side of the wall. The HSS sections had holes, fitted with anchor wedges to allow the seven wire strands to be secured. The top of the strands was pulled by hollow hydraulic jacks to a level slightly higher than the required tension force because of the subsequent anchorage slip expected upon the removal of the jack. The level of prestressing applied was established through trial and error until

the correct level of permanent prestress was attained. The prestress level in a cable was measured using the strain gauges installed on each cable and by comparing the readings with the calibration sheet of that particular cable. In addition, the effect of prestressing new cables on previously prestressed cables was monitored through reading of the strain gauges throughout the prestressing process, since adding a new vertical strand could reduce or increase the stress in other cables, albeit slightly.

3.4 Material Properties

The concrete was supplied by a local ready mix concrete company, with concrete compressive strength of30 MPa and20 mm maximum aggregate size. It had a slump of 90 mm and was poured and vibrated thoroughly to assure consistent quality throughout the sample. The actual capacity of the concrete was monitored by taking standard cylinders and testing them at 7, 14 and 28 days after casting. Additional concrete cylinders were cast to establish concrete strength on the day of frame tests. The strength gain with time is presented in Fig. 3.9.

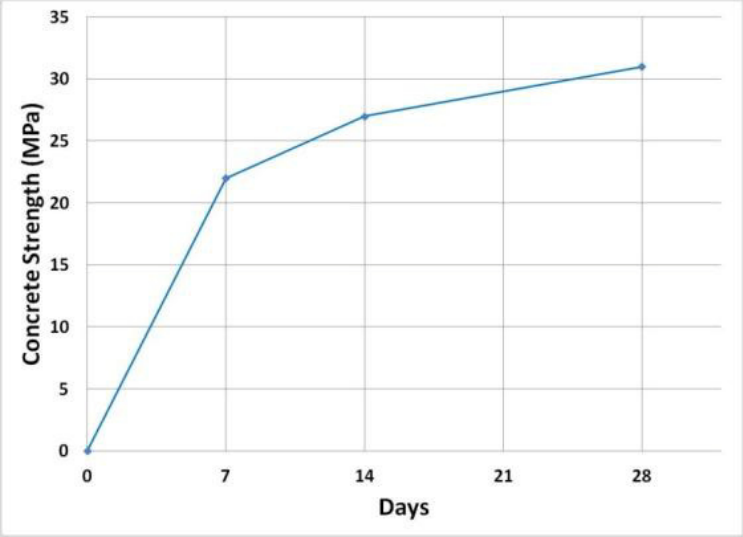

Fig. 3.9 Concrete compressive strength gain with time

Concrete stress-strain relationship was modeled using Hognestad's model (Hognestad 1956). In this model, the concrete is assumed to fail by reaching $\varepsilon_{cu} = 0.0038$. The strain at peak compressive strength, ε_0 is calculated by the following equation:

$$\varepsilon_0 = 1.8f''_c/E_c$$

The parabolic ascending branch of the curve is expressed by the following expression:

$$f_c = f''_c \left[\frac{2\varepsilon_c}{\varepsilon_0} - \left(\frac{\varepsilon_c}{\varepsilon_0} \right)^2 \right]$$

The descending linear portion for the stress-strain diagram starts from the peak stress and reduced to $0.85f''_c$ at ultimate compressive strain of $\varepsilon_{cu} = 0.0038$.The model for the concrete used in the frames is illustrated in Fig. 3.10.

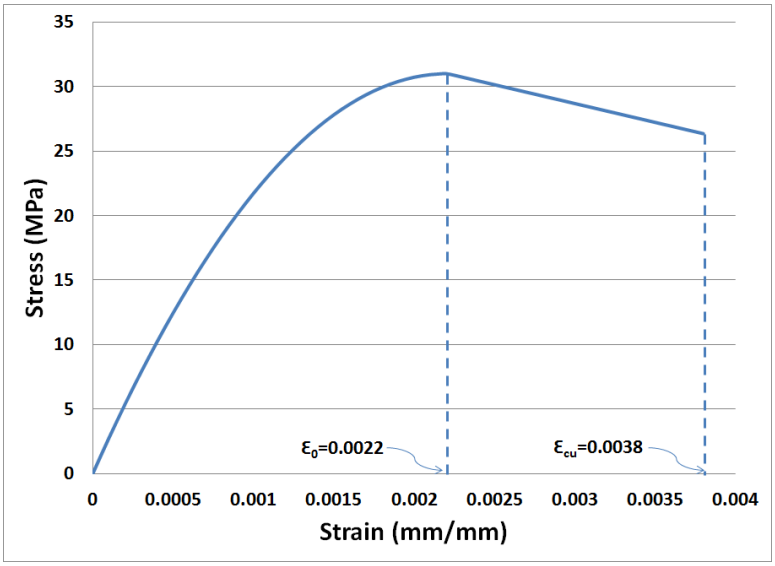

Fig. 3.10 Concrete stress-strain relationship

Standard tension coupon tests were performed to determine the properties of #20 steel re-bars with a nominal area of 300 mm^2, and No 15 seven wire prestressing strands with a nominal cross-sectional area of 140 mm^2. The stress-strain diagrams for the reinforcing bars and the prestressing strands in tension are illustrated in Figs. 3.11 and 3.12, respectively. Three samples were tested for each material and the average was used to obtain the plots.

3.5 Instrumentation , Test Set-up and Test Procedure

The test frames were secured on the laboratory strong floor by means of high-strength steel bolts for testing. Gravity loads, as described in Section 3.2 were first applied through vertical prestressing. The lateral displacement reversals were applied by a 1000 kN capacity MTS actuator supported by a meccano set, which was also fixed on the laboratory strong floor. The specimen end of the actuator was attached to a steel plate bearing against the end of the top beam

during pushing. When pulling, additional horizontal members were required to transfer the load to the far end of the beam.

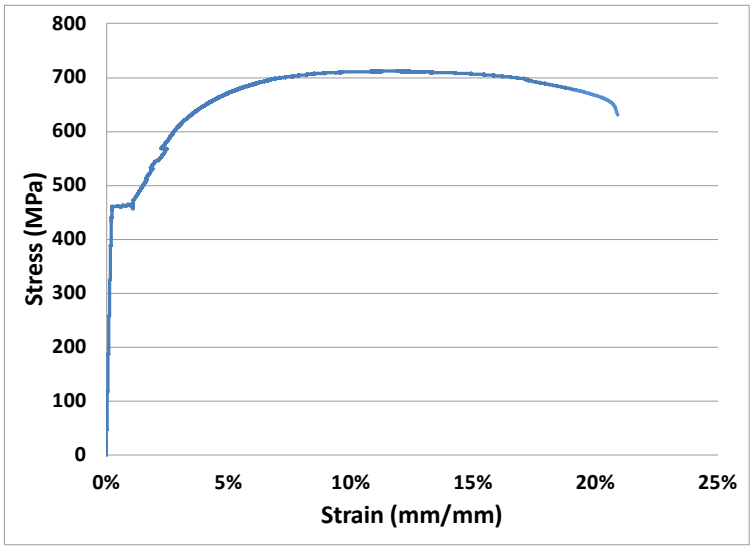

Fig. 3. 11 Stress-strain relationship for #20 bars in tension

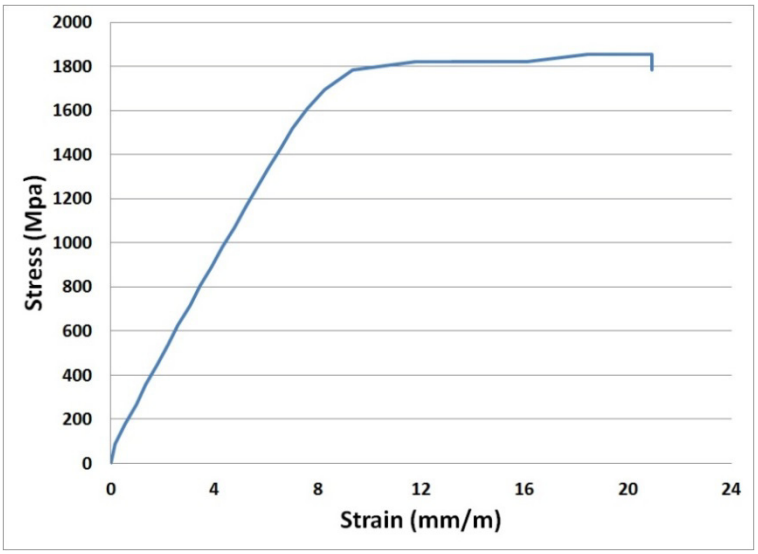

Fig. 3.12 Stress-strain diagram for No. 15 seven wire prestressing strands (A_{ps}=140 mm2)

Four high strength DYWIDAG bars with 1-½ inch diameter and1000 MPatensile capacity were positioned parallel to the beam to transfer the load to the far end of the beam. The DYWIDAG bars were locked in place using double nuts and washers at the interface with the steel end bearing plates. The actuator was capable of travelling 500 mm in total which would translate into

250 mm stroke in push and pull directions. This was adequate for the tests. The Actuator was controlled in displacement-control mode, which allowed the user to indicate the required travel length for each cycle while sufficient force was provided to achieve the desired displacement level. The loading program used during the tests is detailed in the next section. The lateral deformation of the frame was accurately measured by means of displacement transducers attached to a light steel frame that had been placed adjacent to the frame specimen. The top horizontal displacement was measured at the center line of the top beam, which coincided with the centre of application of the top horizontal force. The lateral displacement was measured relative to the laboratory floor. The lateral movement of the foundation was also monitored during testing, and the actual frame displacement was found by subtracting the movement of the foundation (however small it may be) from the frame displacement relative to the floor. Sliding supports were provided along the top beam to prevent any potential out-of-plane movement of the frame.

A total of twenty strain gauges were placed on longitudinal and transverse reinforcement to monitor internal strains and stresses. Additional four or eight strain gauges were placed on diagonal strands, depending on if single or double strands were used. This is shown in Figs. 3.13 and 3.14 for Frames 1 and 2, respectively. The frames were also instrumented by vertically placed LVDTs at the base of both columns to record the rotations of the potential plastic hinge regions and anchorage slip (rotations associated with the extension of longitudinal column reinforcement in column footings). This is shown in Fig. 3.15. In addition, a cable transducer is placed on the foundation to monitor the horizontal sliding of the foundation during testing, as also shown in Fig. 3.15.

3.6 Loading Program

The walls were tested for seismic performance under constant gravity loads, applied through vertically placed prestressing cables, and lateral displacement reversals applied using a horizontally placed MTS actuator. Each displacement level was repeated 3 times in both push and pull directions (3 complete cycles) as cracks were marked at the end of each cycle and observations were recorded concerning the behaviour and damage of each frame.

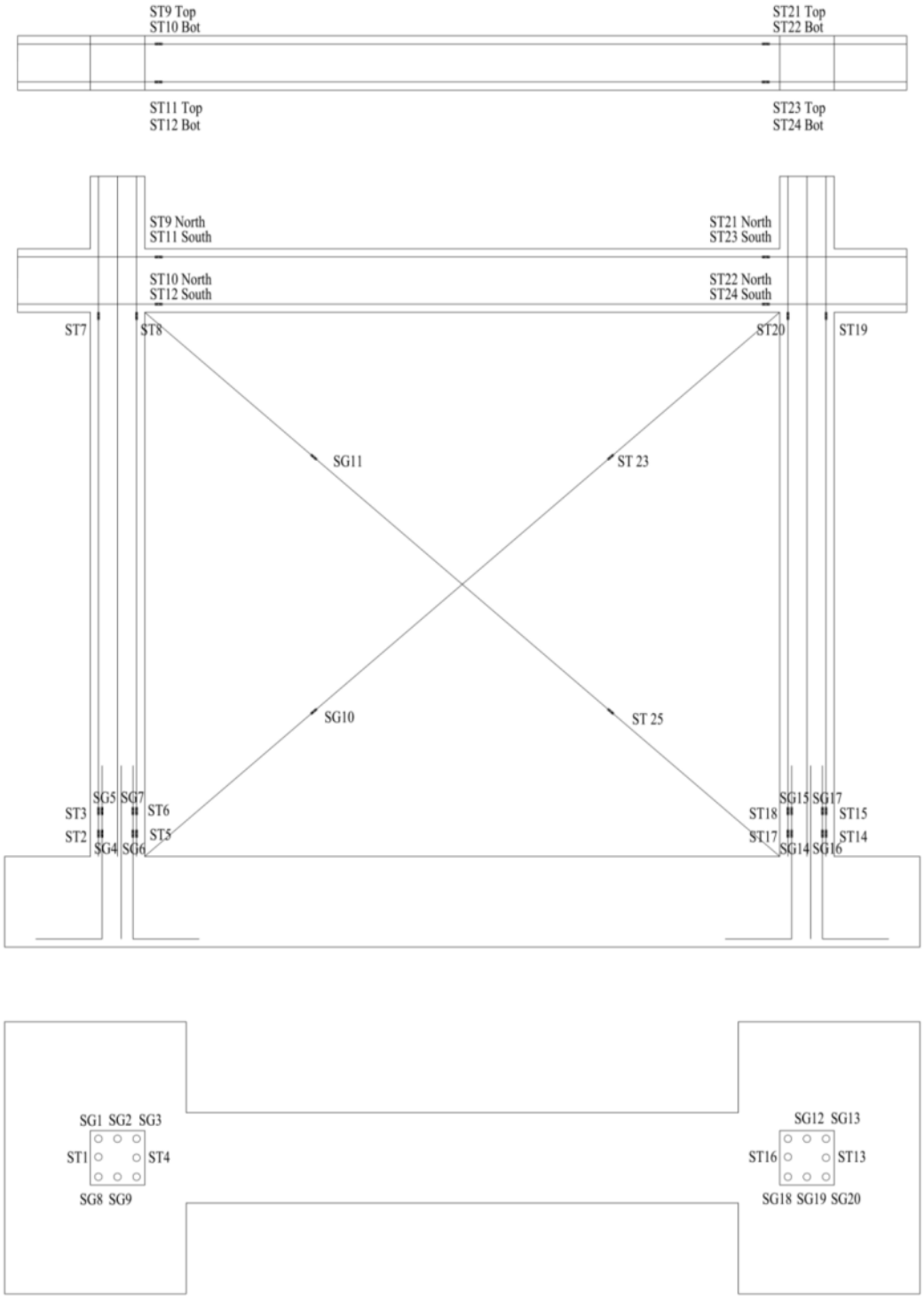

Fig. 3.13 Strain gauge layout on Frame No. 1

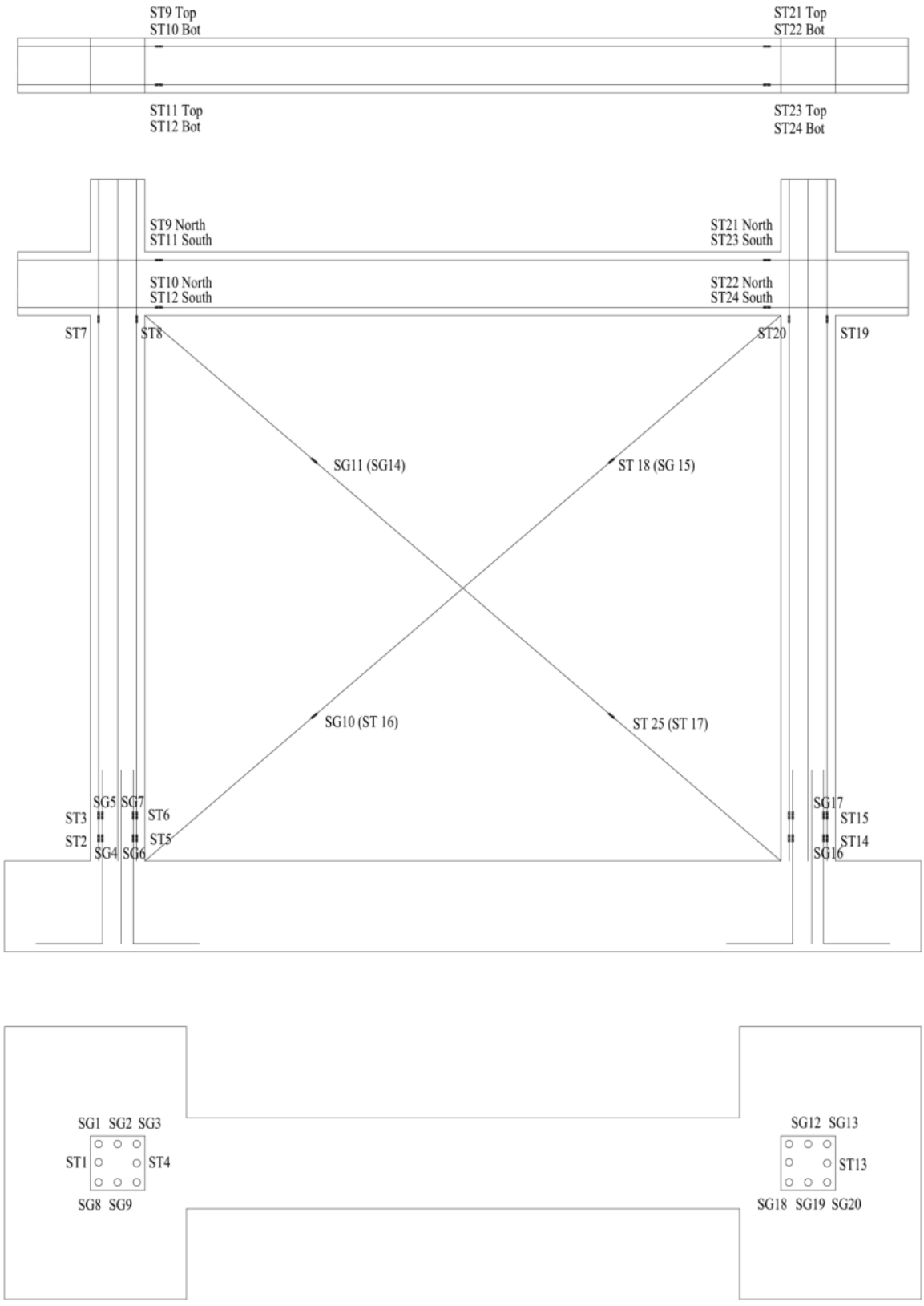

Fig. 3.14 Strain gauge layout on Frame No. 2

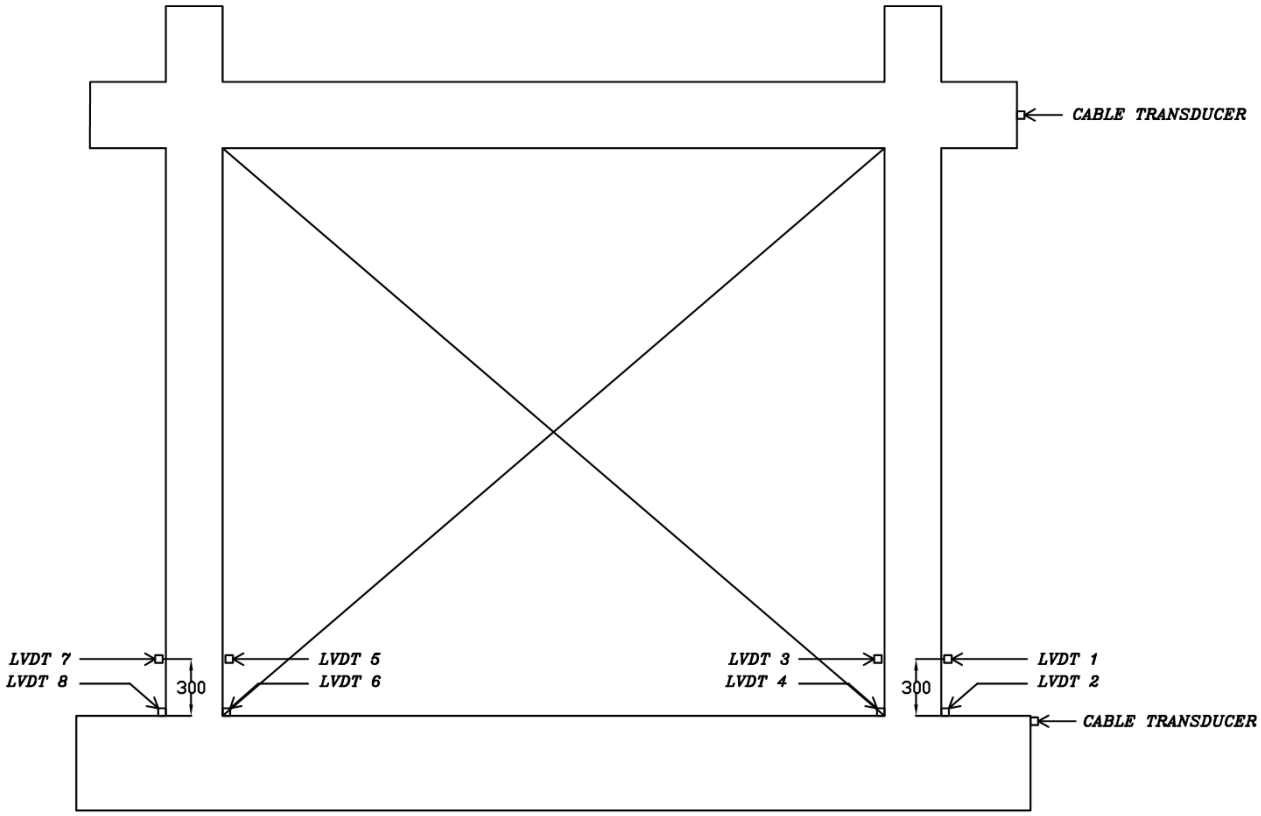

Fig. 3.15 LVDT and Cable Transducer Positioning for Test Frames 1 and 2

During the push cycle, the actuator applied force on the beam directly, whereas during the pull cycles, the actuator force was transmitted through high-strength DYWIDAG bars to a bearing plate at the other end of the beam. The loading procedure was repeated under incrementally increasing displacement levels until the full capacity of the specimen was achieved, followed by full destruction of the specimen as indicated by significant strength decay. The force-displacement response of the frame was plotted to illustrate the full behaviour of frames under reverse-cyclic loading. Fig. 3.16 shows the loading program used in all tests. The initial step was applied at 0.25% drift ratio to monitor the initial elastic behaviour of the frame. After that, the specimen was subjected to displacement cycles that increased with an increment of 0.25% drift ratio up to 2.0% drift, followed by increasing displacements with 0.5%drift ratio. The loading continued until the frame showed substantial strength loss and considered to have failed.

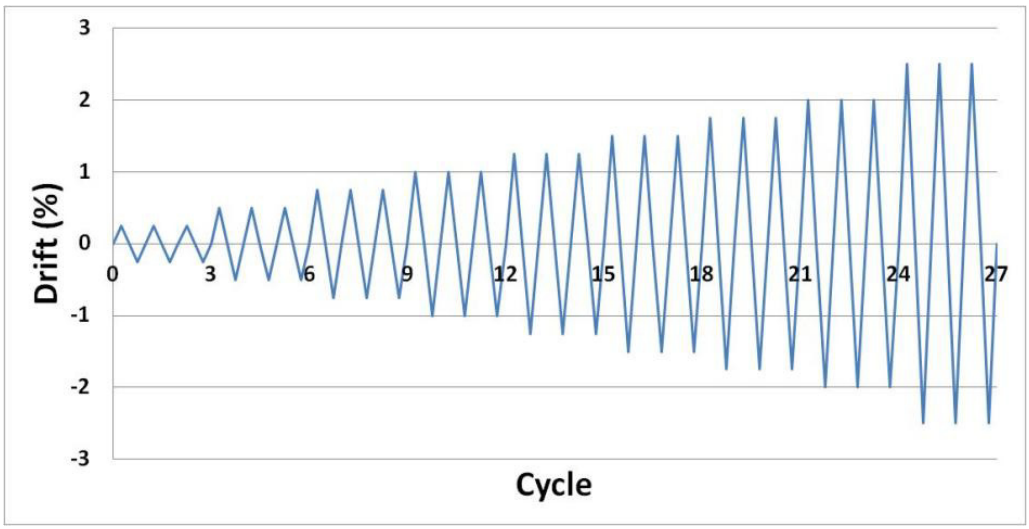

Fig. 3.16 Lateral Loading Program

Chapter 4

Test results and Observed Behaviour

4.1 General

Test results and observed behaviour of two seismically deficient frames retrofitted with either one or two diagonal cables are presented in this chapter. In addition, the hysteretic relationship of a companion unretrofitted frame, tested by Al-Sadoon (2013) in another phase of the same overall research program, is provided for comparison.

The results include recorded lateral force-lateral deformation hysteretic relationships, strain gauge readings, and observations of damage in terms of crack patterns and failure modes. The strain gauge data is presented to assist in determining internal forces, and also to better understand the material behaviour during the experiments. The strain values of the diagonal prestressing cables are shown in graphs.

4.2 Performance of Unretrofitted Frame

A companion unretrofitted frame, designed based on the 1960's code was designed and tested by Al-Sadoon (2013) as part of another phase of the same overall research program at the University of Ottawa. This wall had the same characteristics as the two retrofitted walls tested in the current project, and was used as a bench mark test to evaluate the effectiveness of the retrofit technique employed in the current project. The force-displacement hysteretic relationship of the unretrofitted frame is shown in Fig. 4.1. This frame resisted approximately a maximum lateral load of 265 kN at 2.5% lateral drift ratio and started experiencing strength loss during 3% drift

cycles. The frame subsequently failed at about 4% drift ratio when it developed significant strength decay. The frame represented a prototype building, which did not meet the seismic force requirements of the current National Building Code of Canada (NBCC 2010), as illustrated by Al-Sadoon (2013). Therefore it had to be strengthened and stiffened for drift control.

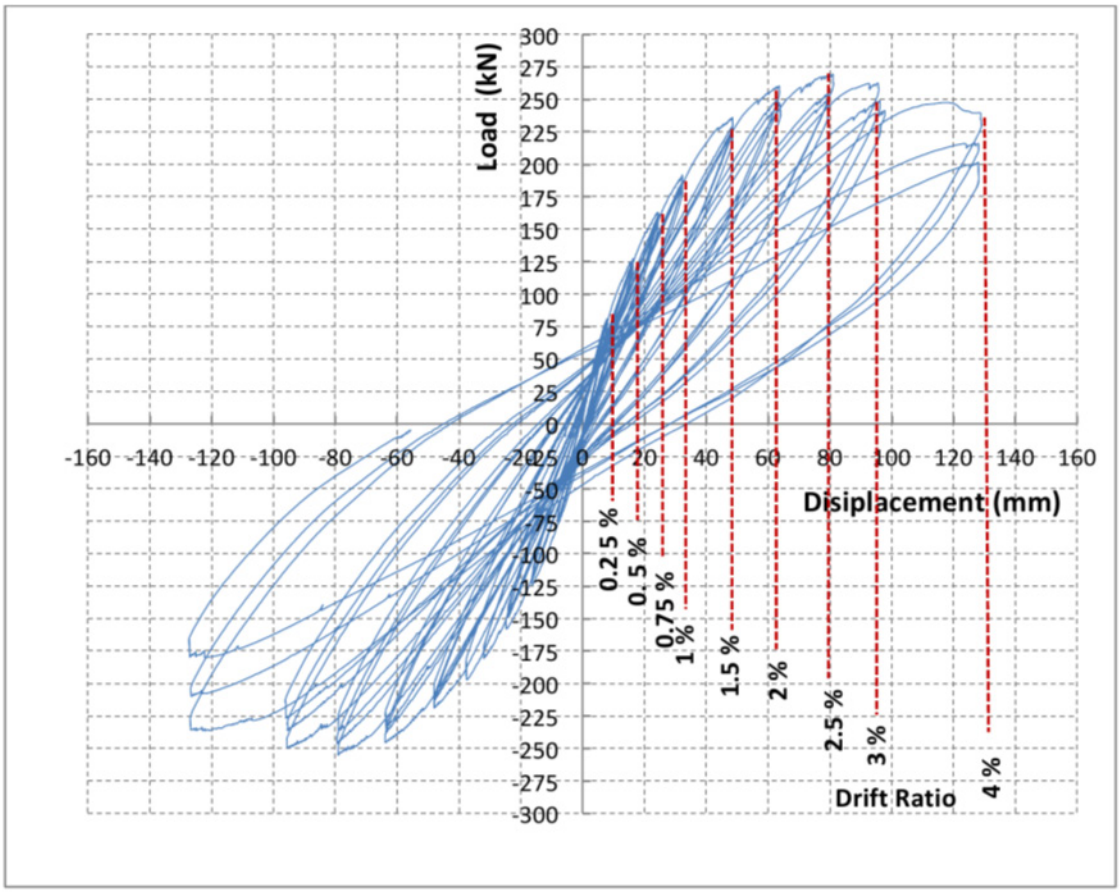

Fig. 4. 1 Hysteretic force-displacement response of an unretrofitted frame (Al-Sadoon, 2013)

4.3 Performance of Frame No. 1, Braced with Single Diagonal Prestressing Strand in Each Direction (100 kN Prestress Force Per Tendon)

The first specimen consisted of a frame designed based on the 1960 edition of ACI-318(60), strengthened and stiffened by one diagonal cable in each of the two frame diagonals. Each cable was prestressed to 100 kN as initial level of prestressing before it was subjected to reversed cyclic loading. This level of prestressing corresponded approximately to 40% of the strand capacity. The overall hysteretic force-displacement response of Frame No.1 is shown in Fig. 4.2. As shown in the figure, each drift increment was repeated three times. The test was stopped

when the frame showed substantial decay in capacity and the concrete core in the column suffered significant damage leading to the buckling of longitudinal bars.

Each step of loading and its effect on the behaviour of specimen is explained in the following paragraphs.

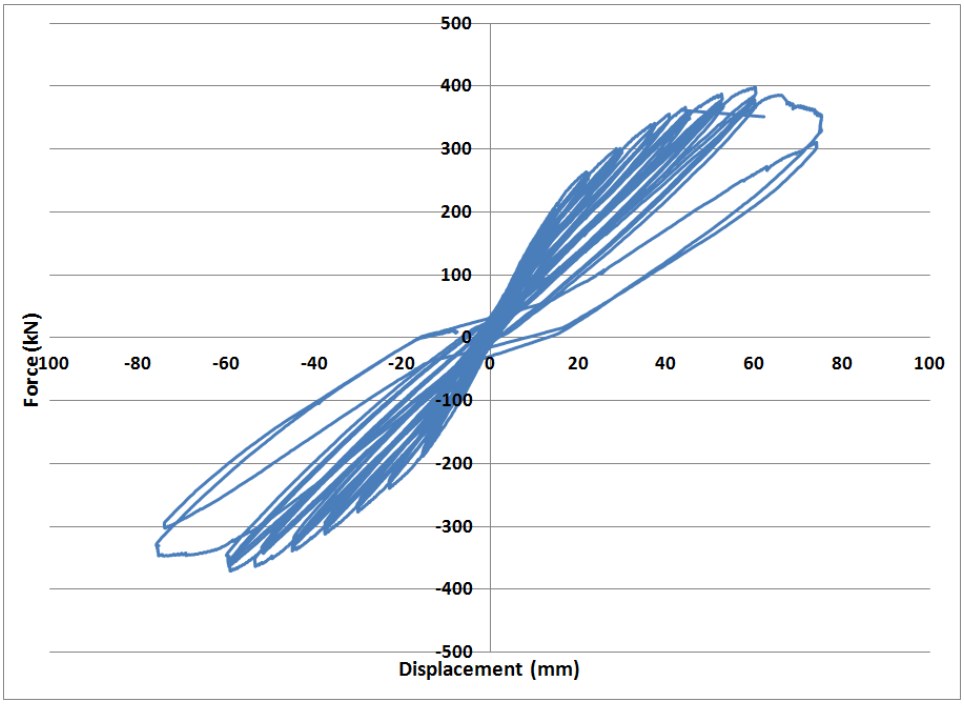

Fig. 4.2 Hysteretic force-displacement relationship of Frame No. 1

The strain in diagonal cables were measured and plotted as shown in Figs. 4.3 and 4.4. These strains are used to determine the contribution of cables to lateral load resistance, while also indicating the stage of loading at which the cable along the compression diagonal has lost its initial tension and became slack. The strain data also provides an indication of the additional stiffness provided to the frame by means of prestressing. Figs. 4.3 and 4.4show the strain values in the strands during push and pull. It can be seen in the figures that the strains became constant when the initial prestress was completely released along the compression diagonal. The initial displacement increment was selected to be 0.25% lateral drift, corresponding to 7.5 mm lateral displacement of the top beam relative to the base of the column. In this step the specimen behaved elastically with high initial stiffness and no observed cracks. The displacement was subsequently increased to 0.5% drift ratio, corresponding to 15 mm lateral displacement. No cracks were observed at this deformation level.

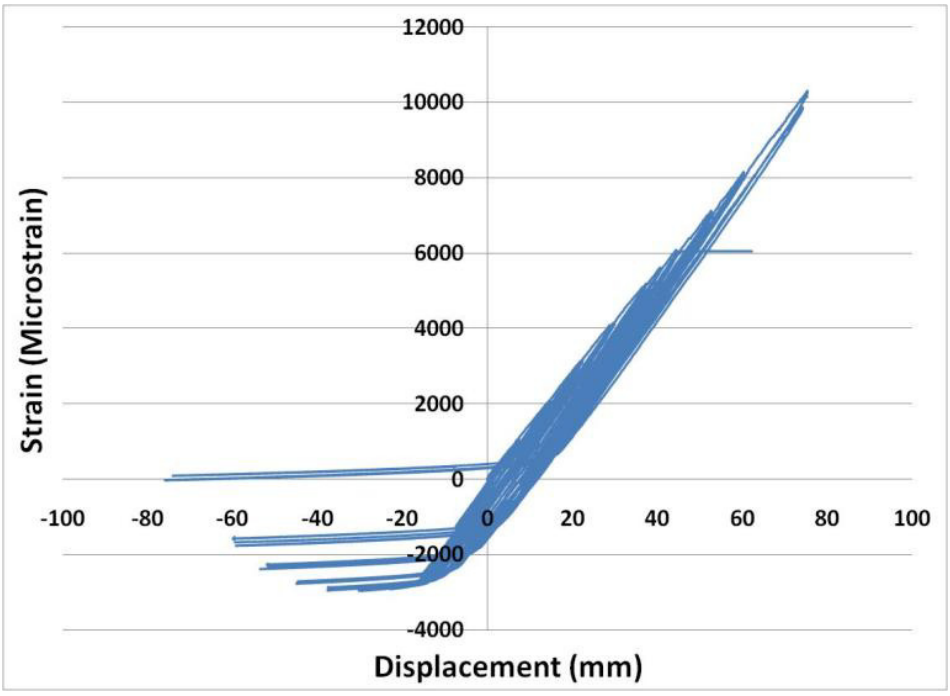

Fig. 4.3 Diagonal cable strain vs. lateral frame displacement for Frame No. 1 in the cable where tension increases during push

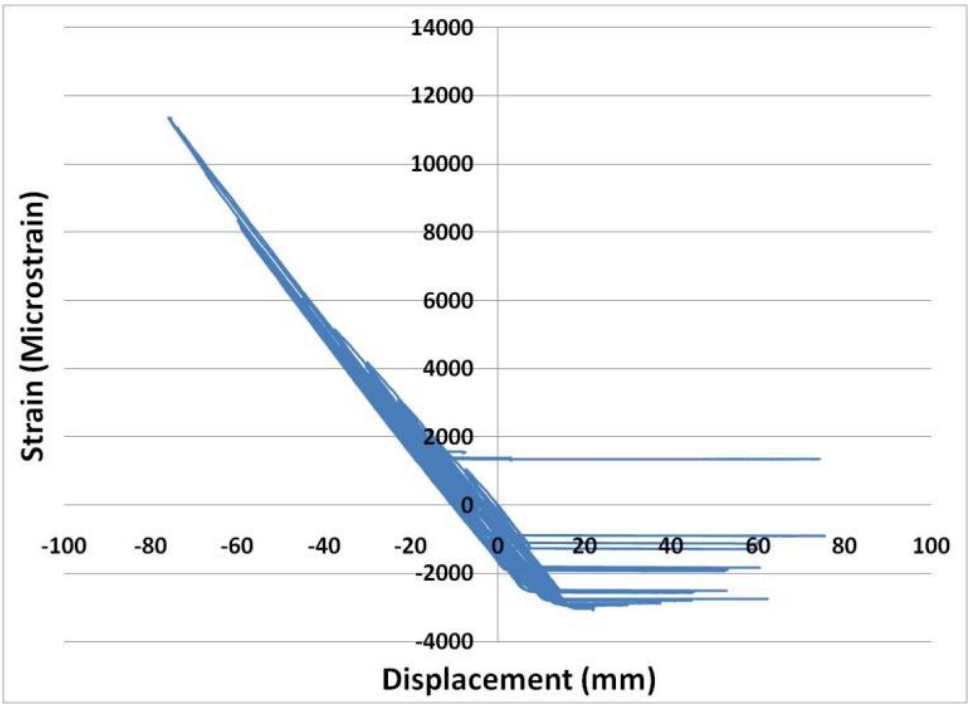

Fig. 4.4 Diagonal cable strain vs. lateral frame displacement for Frame No. 1 in the cable where tension increases during pull

When the displacement cycles increased to 0.75% lateral drift ratio, corresponding to 22.5 mm lateral displacement, the initial prestressing was lost in the strand along the compression diagonal. Hairline flexural cracks appeared at few locations on the tension side of columns, spaced at about 300 mm.In addition, a series of pure flexural cracks appeared in the beam at a regular spacing of about 200 mm. A couple of flexure-shear cracks were also observed in the beam end regions within a segment equal to one-quarter of the span. Beam-column joints remained in good condition without any visible crack or concrete damage.

At 1.0% drift ratio, corresponding to 30 mm lateral displacement, the column flexural cracks spread to about one third of the column height with a spacing of about 150 mm. The number and spacing of beam flexural cracks remains the same but the crack widths increased slightly. The beam also developed a few shear cracks. The beam-column joints exhibited several small diagonal cracks, criss-crossing each other. The cables along the compression diagonals showed complete loss of prestress. However, the strand in the direction of tension diagonals continued resisting significant lateral forces.

At 1.25% lateral drift ratio, corresponding to 37.5 mm of lateral deflection, the flexural cracks in columns intensified within a region exceeding half the column sectional dimension. The cracks became wide enough to allow a 0.5mm pencil lead to pass through easily. The cracks near the column mid-height started to become inclined, taking the form of flexure-shear cracks. Localized corner cracks at columns started to develop, although hardly visible at this stage of loading. The beam cracks, both flexure and shear, continued to spread and widen. The joint shear cracks increased both in numbers and widths. Overall, the frame continued resisting more load without much observed damage. The strain gauge readings indicated that the bars remained elastic.

At 1.5% drift ratio, corresponding to 45 mm lateral deflection, more cracks were detected, especially in columns. A crack has formed at the column-footing interface. In spite increased cracking, there was no concrete crushing observed anywhere in the frame.

At 1.75% drift ratio, corresponding to 52.5 mm lateral deflection, column and beam cracks expanded slightly. New wider cracks appeared in column corners, giving the signs of the onset of cover spalling.

At 2.0% drift, corresponding to 60 mm lateral deflection, the column cracks became quiet extensive, covering all four faces of columns within the lower one-third of column height, with few additional cracks at higher locations. The joint and beam cracking continued, but otherwise no substantial damage was observed in concrete. The concrete cover in column corners started spalling off. A couple of pieces of concrete, with approximate dimensions of 20x30x70 mm were detached from the columns. Signs of concrete compression crushing became more evident. The peak lateral force resistance was attained at this stage of loading with 420 kN resistance in push and 400 kN resistance in pull directions. The force capacity attained was 160% of the capacity of the companion unretrofitted frame.

At 2.5% drift ratio, corresponding to 75 mm lateral deflection, the column base exhibited significant damage during the first push cycle. Large pieces of concrete cover separated and thick diagonal shear cracks appeared at the base of the column. The extent of damage increased significantly during the subsequent cycles at the same maximum deformation level. This was accompanied by a sudden drop in peak capacity. Severe damage of concrete core was observed in columns. Wide cracks were formed. Some cracks were wide enough to permit seeing through the cracks. These cracks never closed upon removal of the load. During the last cycle at 2.5%drift ratio, a piece of concrete cover became loose, exposing buckled column reinforcement. At this point the frame capacity had dropped more than 35%, and it also started to move slightly out–of–plane. The test was stopped. It was decided to provide out-of-plane support for the subsequent test. During the removal of the frame, it was confirmed that the column concrete core was severely damaged. Fig. 4.5 shows localized damage of the column base at 2.5% drift level.

The strain gauge reading taken on diagonal strands indicated that both strands reached their yield strains and slightly exceeded them by developing 0.0100 to 0.0115 strains. This implies that the yielding of diagonal prestressing strands and the failure of columns occurred at the same deformation level. When compared with the post peak behaviour of unretrofitted frame, which continued up to 4% lateral drift before the column concrete crushed and the specimen lost a significant portion of its lateral load capacity, it may be argued that the relatively early crushing of the column concrete in Wall No. 1 at 2.5% drift ratio may have been caused by the additional axial compression imposed on the columns by diagonal strands.

Fig. 4.5 Damage at column base at the end of 2.5% cycles (failure cycles)

4.4 Performance of Frame No. 2, Braced with Double Diagonal Prestressing Strands in Each Direction (200 kN Prestress Force Per Diagonal)

The second frame (Frame No. 2)was identical to the first frame (Frame No. 1) except for the use of double strands in each diagonal as opposed to the single strand used in Frame No 1. The objective of testing the second frame was to assess any further increase in the lateral load capacity associated with using higher number of strands. The use of two cables in each diagonal, one on each side of the frame, was believed to provide stability against out-of-plane movement as the cables would be self-balancing and applying corrective moments to the frame to return back to the original state. However, because the test was intended to take the frame to full destruction, it was decided to provide lateral support against out-of-plane movements. A steel frame was used for this purpose, with attachments extending to the top beam, and guiding the beam to move only in the plane of the frame.

This frame was tested in multiple stages. The initial test was conducted with each strand prestressed to 100 kN (200 kN in each diagonal). At 1.5% drift level, one of the wires that make up the 7-wire strands ruptured, when the strain reading in the middle of the strand was approximately 0.005. This was attributed to the yielding of the steel in a localized area and a potential stress concentration at the top anchor, where rupturing took place. The strand was replaced and the test was continued starting with 1.5% drift cycles. After 9 cycles, and having reached 2% lateral drift ratio, the new strand ruptured in the same manner as the previous one. At

this stage of loading, there was some damage in the frame elements, and it was decided to discontinue testing the frame with stressed strands. The overall hysteretic force-displacement response of Frame No.2 is shown in Fig. 4.6. The variation in strand strains with lateral drift is shown in Figs. 4.7 and 4.8 for strands that would develop increased tension during push and pull, respectively. It was then decided to replace the ruptured strand once again and continue the test with unstressed strands. This formed the third stage of testing, and showed the effect of initial prestressing.

Observed performance of the frame at each step of loading is discussed in subsequent paragraphs.

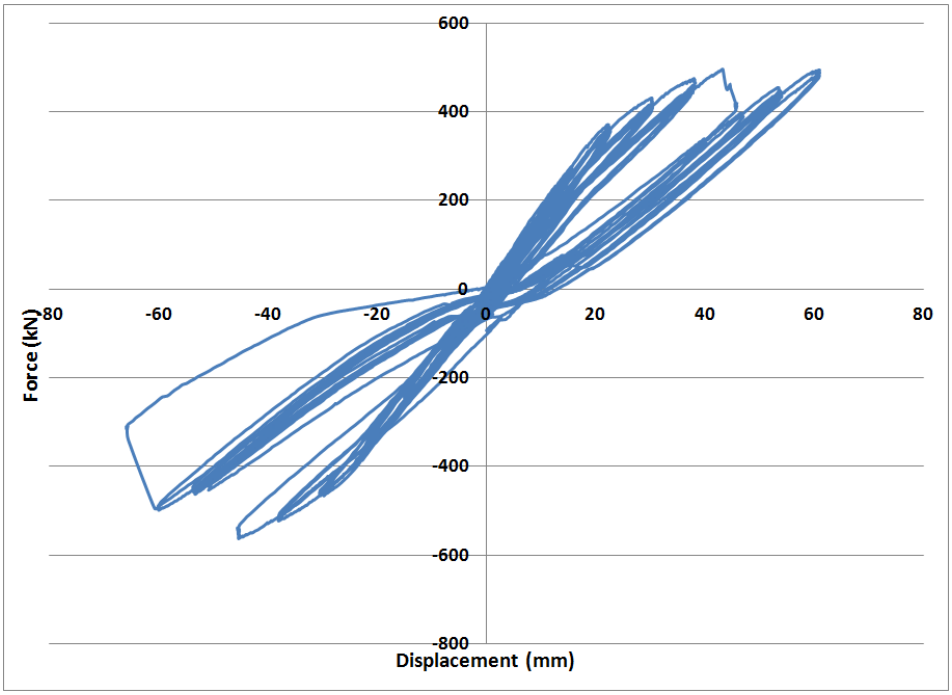

Fig. 4.6 Hysteretic force-displacement response of Frame No. 2 with double strands along each diagonal, prestressed to a total of 200 kN per diagonal

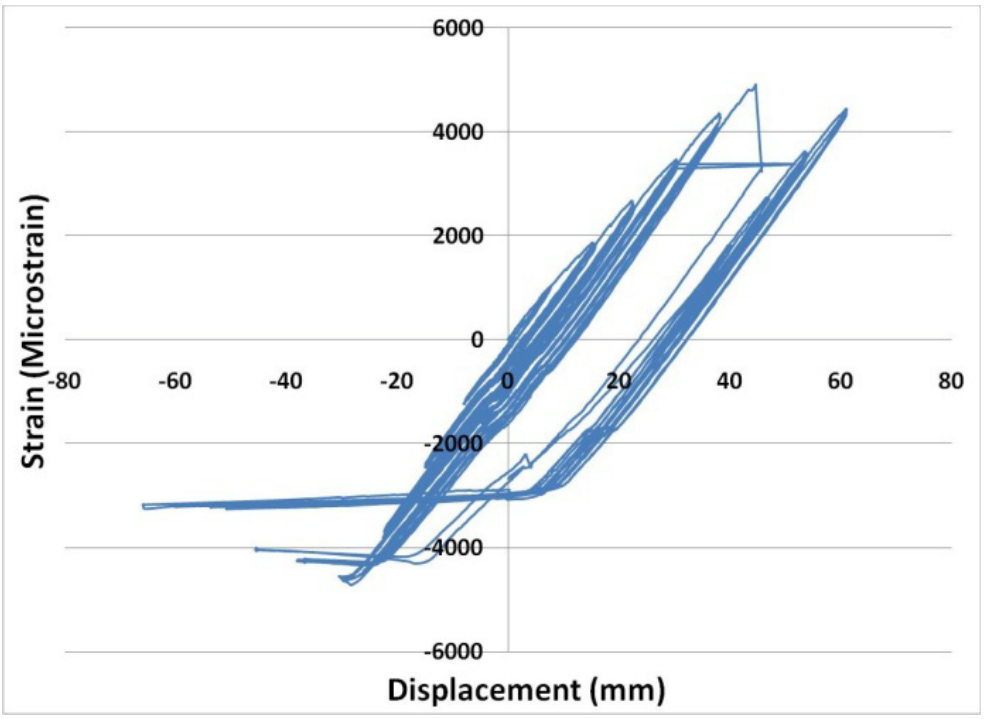

Fig. 4.7 Diagonal strain versus lateral frame defection in Frame No. 2 in strands that would develop increased tension during push

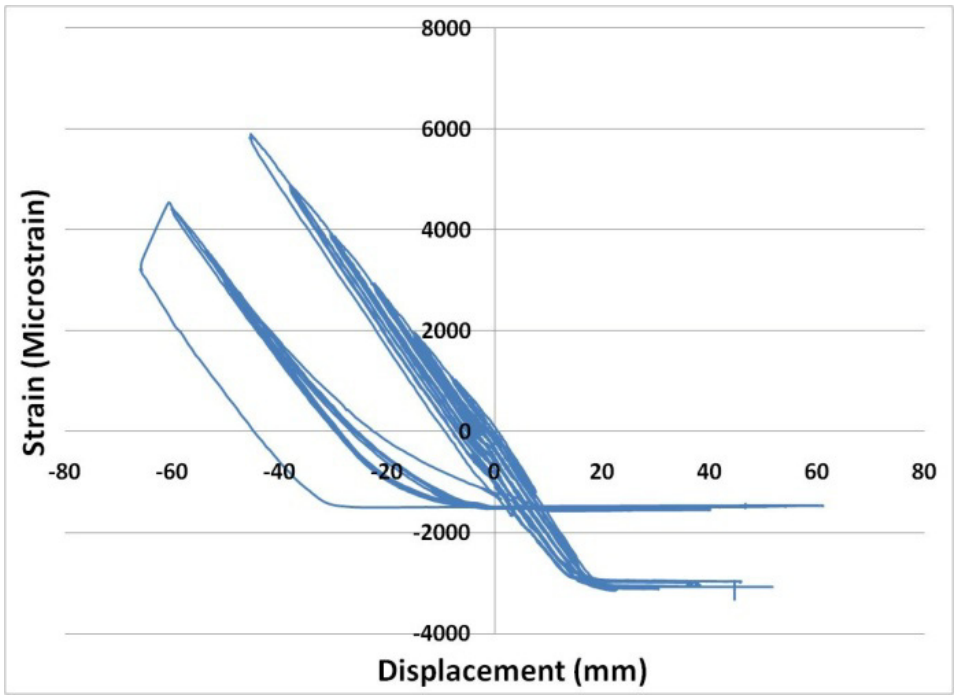

Fig. 4.8 Diagonal strain versus lateral frame defection in Frame No. 2 in strands that would develop increased tension during pull

At 0.25% drift ratio, corresponding to 7.5 mm lateral displacement, the frame barely showed any sign of cracking and remained fully elastic. The stiffness was high and the lateral deformation was not sufficient to loosen the cables as they remained in tension. At 0.5% drift ratio, corresponding to 15 mm lateral displacement, the columns started to show minor flexural cracks spaced at every 250 mm, concentrated approximately within the bottom one third of the columns. The beam also showed minor flexural cracks spaced at about 250 mm at the ends, near the beam-column joints. The cracked region was limited to 1.0 meter length from the each end (quarter of beam length).

At 0.75% drift ratio, corresponding to 22.5 mm lateral displacement, the column cracks became wider, with reduced spacing. The crack spacing was observed to be approximately 150 mm. A few shear-flexure cracks appeared on the beam. The strands in the direction of compression diagonal become completely relaxed, losing their initial prestressing.

At 1.0% drift ratio, corresponding to 30 mm lateral displacement, the frame showed little additional damage. Few cracks formed on the inner face of the columns near the ends. At 1.25% drift ratio, corresponding to 37.5 mm lateral movement, the bottom third of both columns were covered with long flexural cracks and series of flexure-shear cracks. The extent and frequency of column cracks near the ends increased. The beam-column joints developed few more cracks.

At 1.5% drift ratio, corresponding to 45 mm lateral displacement, the prestressing tendon ruptured during the first push cycle, and the test was stopped. The tendon was replaced and then prestressed to approximately the same level, matching the condition prior to the rupture. This was done to verify if the failure was caused by localized stress concentration at tendon connection, or if it was caused by reaching the rupturing strain of the tendon associated with tendon deformability. Fig. 4.9 illustrates the ruptured cables near the beam-column joint location.

The test was continued from the same lateral drift of 1.5% with the same level of prestress in diagonal cables. At this load stage the column cracks became wide enough to be able to insert the tip of a pencil. This was the case at few other locations on the beam. The joint cracks became longer, extending diagonally from corner to corner with a 45 degree inclination. The flexure-shear cracks on beams extended to almost one-third of the beam span from each end. The corner concrete cover at the base of the columns started to crush locally. A crack between the base of

the column and top of the foundation was formed. The crack depth was approximately equal to half the column cross-sectional dimension.

Fig. 4. 9 Ruptured diagonal prestressing tendon during testing of Frame No. 2

At 1.75% drift ratio, corresponding to 52.5 mm lateral deflection, the bottom half of the column was covered with significant cracks. The upper third of the columns near the joints also showed closely spaced cracks but not as intense as the bottom portions. One third of the beam was covered with flexure and shear cracks. The beam-column joints showed hairline cracks. The bearing surface between the HSS section that supported the tendons and the joint concrete showed some crushing of thin pieces of concrete cover. The column concrete near the base also crushed on the compression side, and the crack at the end of the column opened up a few millimetres on the tension side, with a crack depth of about 70% of the column dimension. The frame capacity remained the same at this stage of loading, developing yielding of the specimen. An overall view of the frame during the pull cycle is illustrated in Fig. 4.10.

At 2.0% drift ratio, corresponding to 60 mm lateral deflection, the frame showed no reduction in capacity and maintained its yield force level. Some additional concrete crushing was observed at the bottom corners of columns when subjected to compression. The crack patterns remained the same with increased crack widths. During the third cycle of 2.0% drift, the cables ruptured once again and the impact of the shock caused the attached HSS section to rupture along its length with a loud noise. This is illustrated in Fig. 4.11.

Fig. 4.10 Frame No. 2 at 1.75% drift during the pull cycle

Fig. 4.11 Failure of the HSS section as a result of tendon rupturing

At this stage, the test was stopped and it was decided to fix the cable support and continue the test with non-prestressed tendons as it was estimated that the elongation of the frame diagonals associated with this drift level was in excess of the available elongation capacity of the strands, leading to the cable rupture once again.

4.5 Performance of Specimen No.2, Braced with Two Non-Prestressed Tendons (Without Diagonal Prestressing)

Frame No. 2 was repaired and the cables were placed without prestressing. They were stretched to a snug-tight position and the strain values were monitored during testing. Since the last cycle of 2.0% drift was interrupted during the previous test, it was decided to start this test by repeating one cycle at 2.0% drift ratio. The test continued until failure during 2.5% drift reversals. The hysteretic force-displacement relationship of this segment of the test is illustrated in Fig. 4.12. It can be observed that, since the cables were not prestressed this time, the frame was softer as indicated by the reduced slope of force-displacement relationship. The variation of strains in prestressing strands is shown in Figs 4.13 and 4.14. The progression of damage during testing is discussed in the following paragraphs.

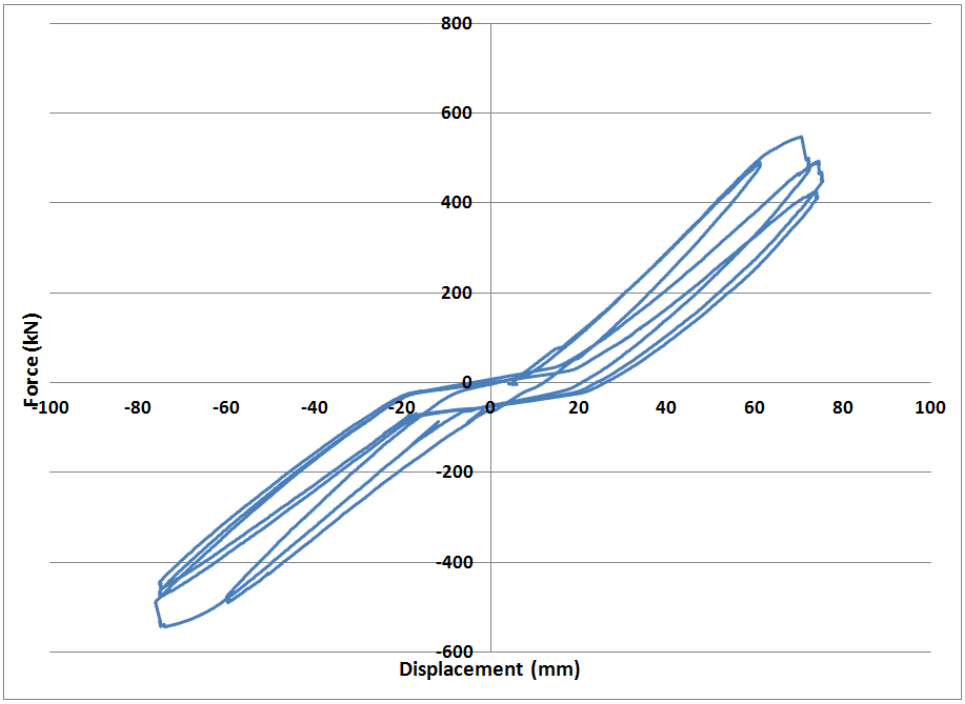

Fig. 4.12 Hysteretic force-displacement response of Frame No. 2 with non-prestressed tendons

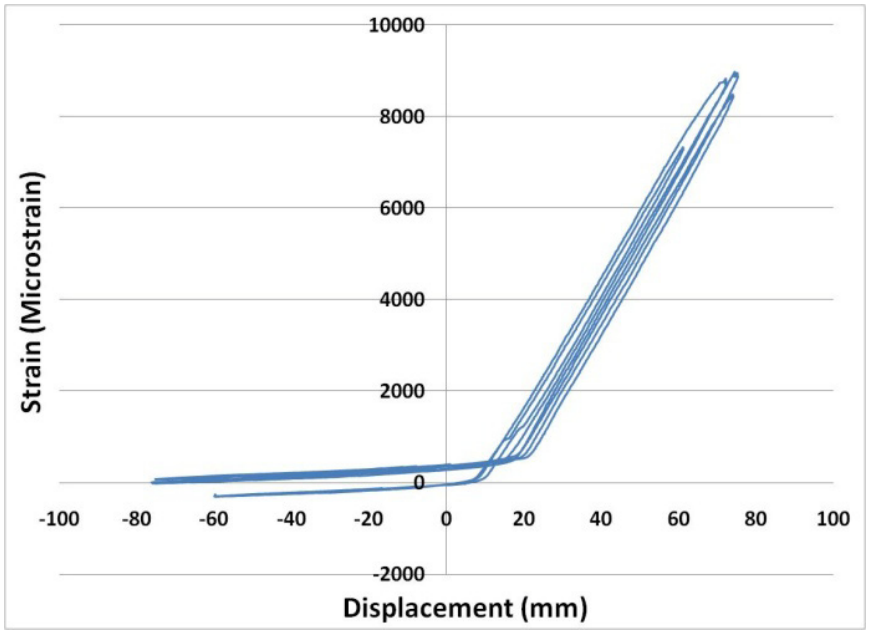

Fig. 4 13 Diagonal cable strain vs. lateral displacement for Frame No. 2 without initial prestressing in the push direction

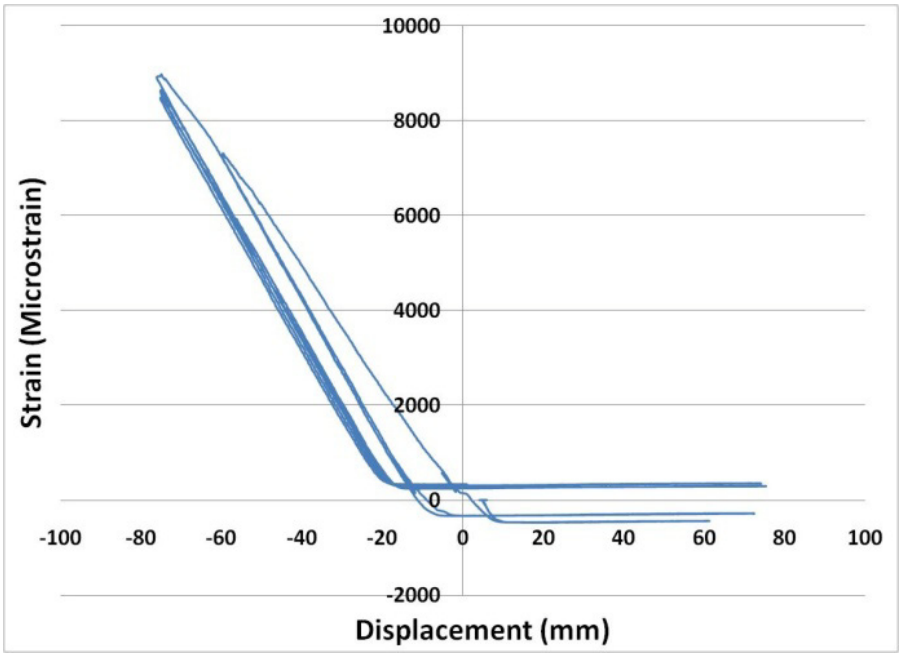

Fig. 4.14 Diagonal cable strain vs. lateral displacement for Frame No. 2 without initial prestressing in the pull direction

When subjected to 2.0% lateral drift, corresponding to 60 mm lateral deflection, the frame developed the same capacity as that developed earlier with the prestressed cables. This may be explained by the fact that, at this lateral drift level the tendons have already yielded. The bottom column concrete continued to show further crushing, but the frame maintained the same overall capacity as the earlier test with the prestressed cables. This suggests that the frame behaviour could be different during the initial stages of loading, but remains the same after the yielding of cables at higher deformation levels.

At 2.5% drift ratio, corresponding to 75 mm lateral displacement, the specimen suffered severe damage and with each additional cycle the lateral force resistance dropped progressively and the damage became more significant. During these cycles, the concrete cover at the lower portion of columns was completely crushed. In addition, the cover concrete near the top of the column on the inside face spalled off. The damage observed is illustrated in Fig. 4.15.

Fig. 4.15 Column damage at 2.5% drift; (a) crushing of column concrete near the base, (b) spalling of column cover near the top joint

The extent of damage increased during the last cycle at 2.5% drift ratio and the concrete column experienced diagonal tension failure at the top, near the beam-column joint. This is illustrated in Fig. 4.16(a). During this cycle, one of the wires of the seven-wire strand ruptured as shown in Fig. 4.16(b), this time at the bottom anchor location. This indicates that, regardless of the level of prestressing, the elongation capacity of strands allows only a limited inelastic drift capacity for the frames. The significance of initial prestressing becomes obvious during elastic load reversals, in the form of significant stiffening of the frame and associated damage control in both structural and non-structural elements.

Fig. 4.16 Damage during the last cycle of 2.5% drift; (a) diagonal tension failure of column at the top, (b) ruptured wire of a strand

During the last cycle of the test, it was also noted that a longitudinal column bar buckled in compression, near the top, following the spalling of cover concrete. This is illustrated in Fig. 4.17(a). An addition observation made was the crushing of concrete under bearing stresses generated by the HSS section that was used to support the prestressing strands. This is shown in Fig. 4.17(b).

Fig. 4. 17 (a) Buckled longitudinal bar at the top of column, (b) localized crushing of concrete under bearing stresses

Chapter 5

Analysis of Results and Design Procedure

5.1 General

This chapter provides analysis of experimental results, as well as the results of frame analysis. The first part of the chapter includes design and detailing of the frame elements and the computation of nominal capacities of beams and columns. The lateral force capacity of frames is computed when the nominal capacity is attained at member ends. The contributions of diagonal strands are computed when the maximum lateral load resistance is attained at tensile capacity of tension strand(s), while the strand(s) on the compression diagonal become loose and do not provide any load resistance. This provides analytically computed maximum force resistance of the retrofitted frames.

The second part of the chapter involves analysis of test data to establish the contributions of the frame and the diagonal strands to assess the total lateral force resistance of frames. The experimental results are compared with computed capacities and the significance of the retrofit technique is illustrated.

Finally design recommendations are made based on frame analysis and experimentally observed behaviour of frames for using diagonally placed and prestressed strands as a seismic bracing system for increased seismic force resistance.

5.2 Computed Capacity of Test Frames

The two frames tested in the experimental phase of current research, presented in Chapters 3 and 4 were designed and detailed based on the ACI 318-1963 Concrete Code of the US. The design

practice in Canada was the same as that specified by ACI 318-1963 during the same era. This design practice lacked seismic design and detailing requirements of current building codes, and was deficient in many respects. The ties were placed at large spacings, as dictated by the compression bar buckling requirement under gravity loads and/or by shear design provisions. They were not sufficient for proper confinement of core concrete for ductile behaviour. Furthermore, the longitudinal reinforcement lap splices were inadequate in two ways; i) first they were provided in potential plastic hinge regions, and ii) second they did not have sufficient lap length (lap length of 24 times the bar diameter was used). Design details of the frames tested are provided in Fig. 5.1 as designed by Al-Sadoon (2013), who designed the frames as part of the same overall research program. Because of the deficiencies in design, the frames did not have the ability to go beyond their nominal capacities significantly in the inelastic range of deformations. This was observed during tests. It was also observed that the frames did not suffer premature shear failures, prior to yielding in flexure and the development of nominal moment capacities in members. Therefore, the lateral load resistance provided by the frames were assumed to be provided at the formation of nominal flexural capacities of frame elements. The first step in frame analysis involved the computation of nominal flexural capacities of beam sections in both positive and negative bending, as well as the column capacities under combined bending and axial force. This is done in the next section.

5.2.1 Sectional Capacities

Nominal moment capacities of beam and column sections require flexural analysis using the assumption of plane sections before bending remaining plane after bending. Also required for the analysis are material strengths for concrete and reinforcing steel. This was done by conducting standard cylinder tests and steel coupon tests. Accordingly, concrete compressive strength of $f'_c = 31\,MPa$ was used as representative of concrete strength in beams and columns. The tension coupon tests for steel bars indicated a yield capacity of $f_y = 460\,MPa$. The strain at ultimate in the extreme compression fibre (crushing of concrete in flexure) was assumed to be $\varepsilon_{cu} = 0.0035$ to be consistent with CSA Standard A23.3 (2004). The equivalent rectangular stress block was used as specified in the same standard. The beam capacity was computed at the ends of beams (as well as the mid-span location) with different top and bottom reinforcement. These capacities are shown in Fig. 5.2.

The column flexural capacity was computed by establishing the axial force-bending moment interaction diagram for the column section. The nominal moment capacity of the column section was computed from the interaction diagram for different levels of accompanying axial load. Fig.5.3 illustrates the nominal interaction diagram.

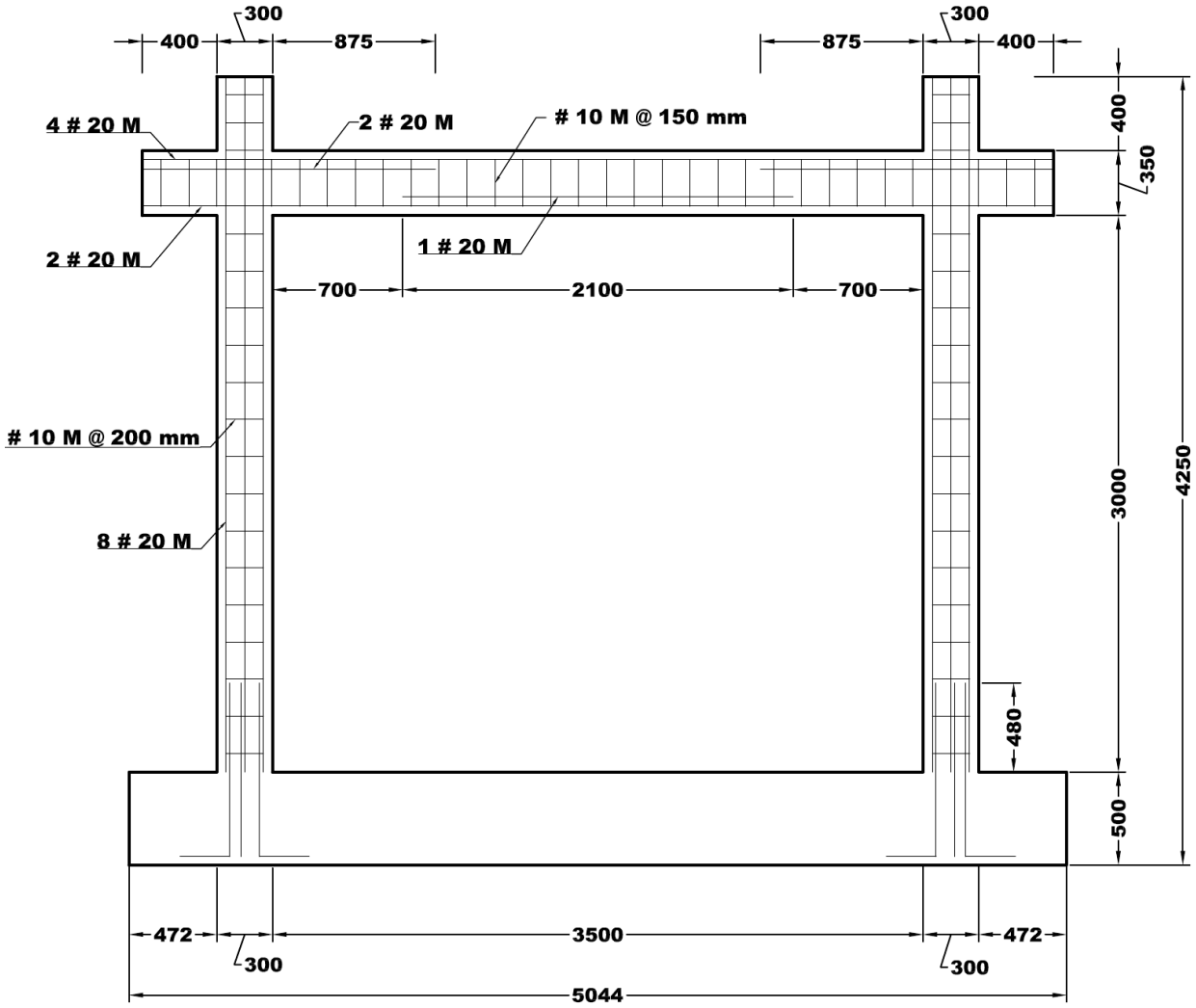

Fig. 5.1 Elevation view of test frames (Al-Sadoon 2013)

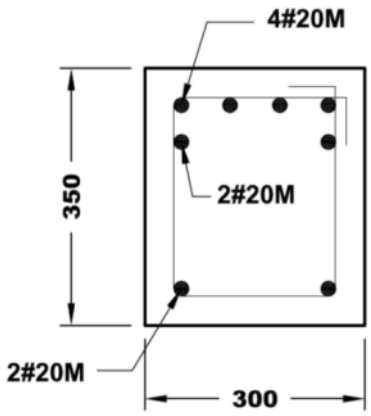

$M_n^- = 198\ kN.m$ $M_n^+ = 93$ kN.m

a) Beam section at beam end

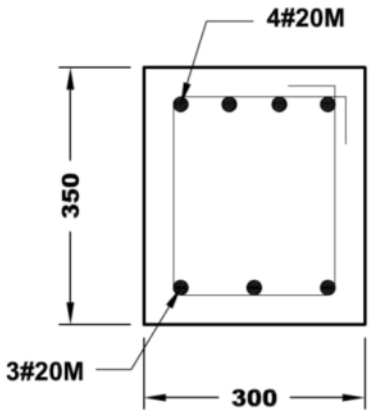

$M_n^+ = 100\ kN.m$

b) Beam section at mid-span

Fig. 5.2 Beam cross-sections and nominal capacities

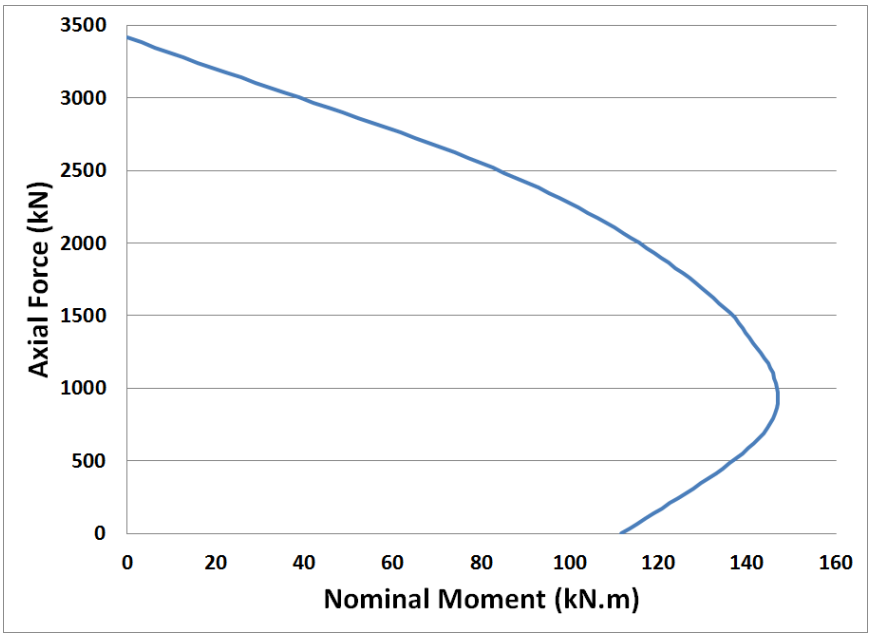

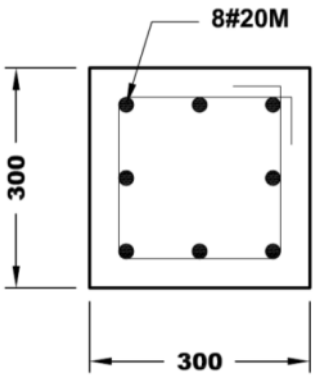

Fig. 5.3 Column axial force-bending moment interaction diagram for nominal capacity

The nominal moment capacities were used for frame analysis to establish the lateral load capacity of unretrofitted frame, as well as the contribution of frame to overall lateral force resistance in retrofitted frames at the formation of nominal moment resistances at the ends of beams and columns. This is presented in the next section.

5.2.2 Frame Analysis

The lateral force resistance of a retrofitted frame consists of two components; i) the component provided by the reinforced concrete frame alone, and ii) the component provided by the horizontal component of diagonal strands. This can be expressed as shown below:

$$F_{LATERAL} = F_{FRAME} + F_{H,CABLE}$$

While experimentally recorded contributions of each component were recorded under incrementally increasing lateral drift cycles and presented in Section 5.3, the force components are computed analytically in this section. It was experimentally observed that the frames attained their nominal lateral load capacities when the beams developed yielding at their ends and the columns reached their nominal bending capacities at their base at about 1% lateral drift ratio. This observation was used to facilitate the frame analysis as indicated in Fig. 5.4.

The following are the components of frame elements that contributed to the resistance of the frame with reference to Fig. 5.4:

Negative beam end moment due to three concentrated gravity loads, each 40 kN, assuming 50% fixity at the ends: 22 kN.m

Positive beam moment due to lateral seismic force at nominal capacity (occurring at the left end when swaying to the right): 93 kN.m

Negative beam moment due to lateral seismic force at nominal capacity (occurring at the right end when swaying to the right): 198 kN.m

Total positive beam moment at the left beam end: 93 – 22 = 71 kN.m (also equal to top left column moment).

Total negative beam moment at the right beam end: 198 + 22 = 220 kN.m (also equal to top right column moment).

Beam shear at the left end due to the end moments and the gravity load: (71 + 220)/3.5–3(40)/2 = 23 kN. Note that this shear force acts as axial tension on the left column.

Beam shear at the right end due to the end moments and the gravity load: (71 + 220)/3.5–3(40)/2 = 143 kN. Note that this shear force acts as axial compression on the right column.

Left column bottom moment at nominal capacity corresponding to 777 kN of axial compression resulting from 800 kN of externally applied axial compression and 23 kN of axial tension coming from the beam shear (from the interaction diagram shown in Fig. 5.3): 177 kN.m

Right column bottom moment at nominal capacity corresponding to 943 kN of axial compression resulting from 800 kN of externally applied axial compression and 143 kN of axial compression coming from the beam shear (from the interaction diagram shown in Fig. 5.3): 236 kN.m

Left column base shear: (71 + 142) / 3.0 = 71 kN

Right column base shear: (220 + 150) / 3.0 = 123 kN

Total lateral force resistance of the frame alone: 71 + 123 = 194 kN (without the contribution of diagonal tension strand). The effect of the diagonal strand at peak load resistance of the frame was to apply additional compression on the right column, thereby increasing its moment capacity. The additional axial compression applied by the strand was established to be 125 kN. This increased the axial load on the column from 943 kN to 1068 kN (943 kN + 125 kN) and the corresponding column base moment resistance from 150 kN.m to 154 kN.m, with a slight increase in total base shear resistance from 194 kN to 196 kN.

The above values can be compared with experimentally obtained frame resistances. Frame No. 1 developed 190 kN and 175 kN of lateral force resistance in the push and pull directions, respectively when the frame started yielding at 1% lateral drift. The frame resistance increased to 220 kN and 195 kN when the lateral drift ratio increased to 1.5%. Frame No. 2 developed 170 kN of lateral force resistance in both the push and pull directions when the frame started yielding at 1% lateral drift. The frame resistances were 170 kN and 200 kN when the lateral drift ratio increased to 1.5%. The experimental values for the frames were obtained by subtracting the contributions of tension braces (which were computed from measured strains) from the overall frame resistances recorded during testing.

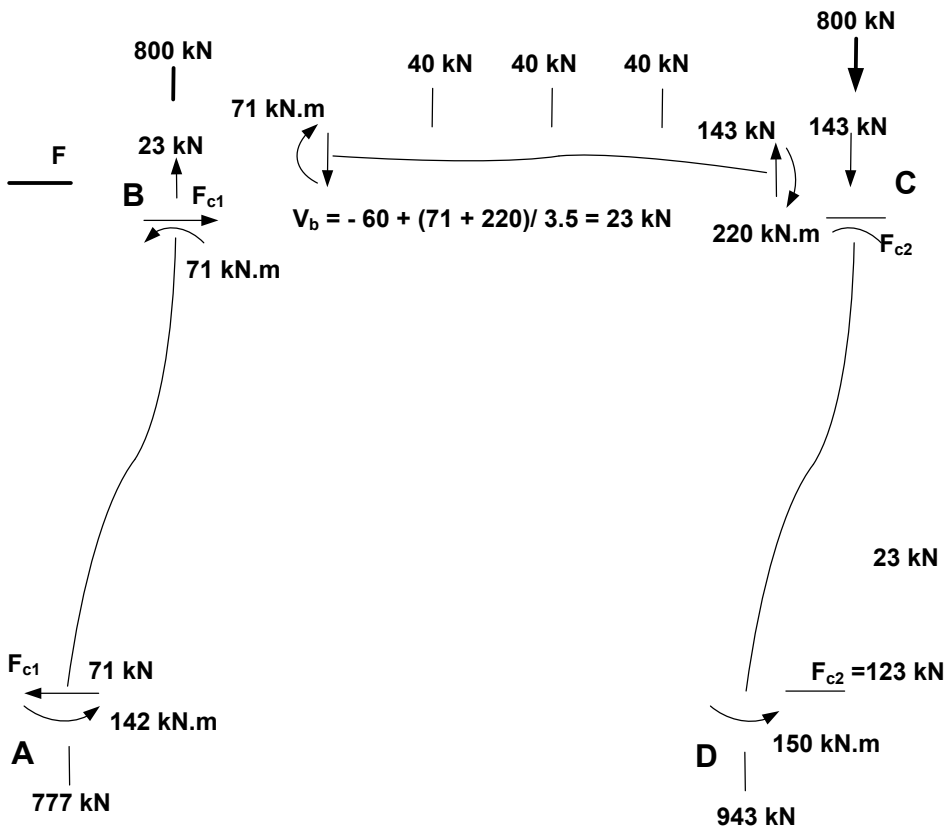

Fig. 5.4 Member-end forces in frame elements, without the braces

The contribution of diagonal strands can be computed from statics. Fig. 5.5 shows internal forces in diagonal strands. The free-body diagram of one of the joints is also drawn to compute the horizontal and vertical components of cable forces.

The inclination of diagonal strands is shown below for the frames tested:

$$\theta = tan^{-1}\left(\frac{3000}{3500}\right) = 40.6°$$

When the strands were diagonally prestressed, the initial prestressing was done by applying 100 kN of tension force to each strand. This resulted in 714 MPa initial prestress at approximately 40% of the strand capacity. At this stage, the horizontal force components in diagonal strands balanced each other. When the frame was laterally displaced in one direction, one of the diagonals was stretched further, started taking higher tensile forces, while the other gradually lost its prestress. When the frame was swayed sufficiently to relieve prestressing in one of the diagonals, the lateral load resistance was provided by only one strand.

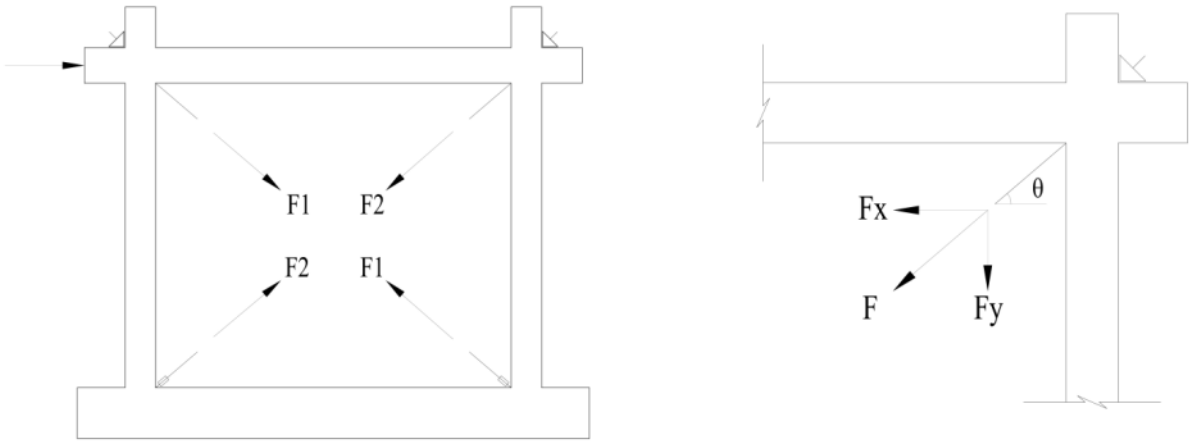

Fig. 5.5 Tendon forces

The following two load stages illustrate horizontal force resistances provided by diagonal strands at these stages of loading.

Initial load stage: Both cables are in equal tension:

$$F_{H,CABLE} = F_1.\cos\theta - F_2.\cos\theta$$

After losing stresses in one cable: Only one cable is in tension:

$$F_{H,CABLE} = F_1.\cos\theta \qquad ,F_2 = 0$$

When one of the cables approached its tensile capacity, then the maximum resistance of the strands was attained. This level of resistance is shown below:

$$f_{pu}\, A_{ps}\cos\theta = 1860\ (140)\ \cos\ (40.6) = 198 \times 10^3\ \text{N}$$

The above value agrees well with the test data. In Frame No. 1 the strands developed approximately 190 kN of horizontal resistance with a single No. 15 7-wire strand in each diagonal. They developed twice this value when double strands were used in each diagonal.

5.2.3 Significance of Diagonal Strands

In addition to the analytical approach presented above to explain the contribution of diagonal strands to lateral force resistance, experimental data was further analyzed to illustrate the significance of using single or double strands in each diagonal. Figs 5.6 and 5.7 illustrate the contributions of diagonal cables for Frame No 1 and Frame No 2, respectively. These figures

consist of bar charts, where each bar represents total lateral force resistance at each deformation level. Each bar consists of two lateral force components; i) force resisted by the horizontal components of diagonal forces, computed from measured strains, and ii) the base shear resistance provided by the frame, which is obtained by subtracting the strand contribution from the total applied net horizontal force.

The results indicate that about 60% of total resistance in Frame No. 1 is provided by the reinforced concrete frame and the remaining 40% is provided by the cables. In this frame, single No. 15 7-wire strand was used in each diagonal with a nominal area of 140 mm^2. Frame No. 2 had two strands in each direction, which provided twice as much resistance. Accordingly, the contribution of the reinforced concrete frame in Frame No. 2 was about 1/3 of total resistance, while approximately 2/3rd was provided by the strands.

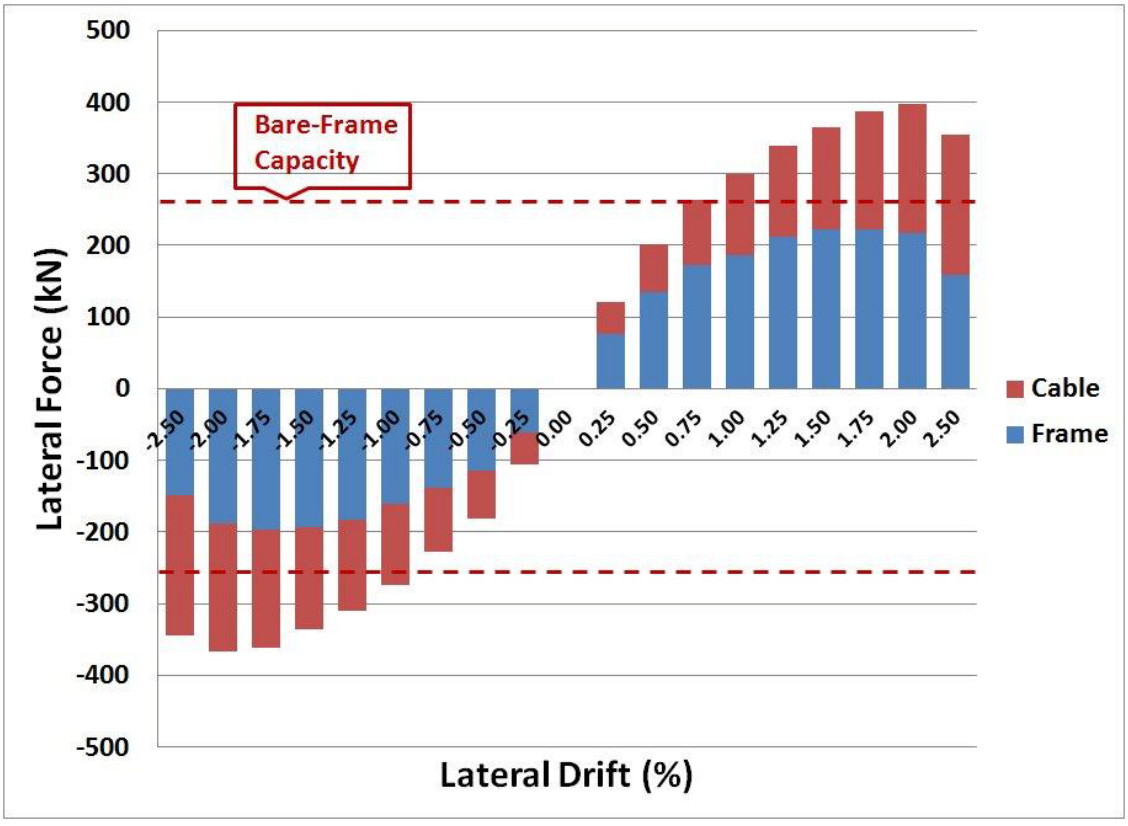

Fig. 5.6 Lateral force resistance contributions in Frame No. 1

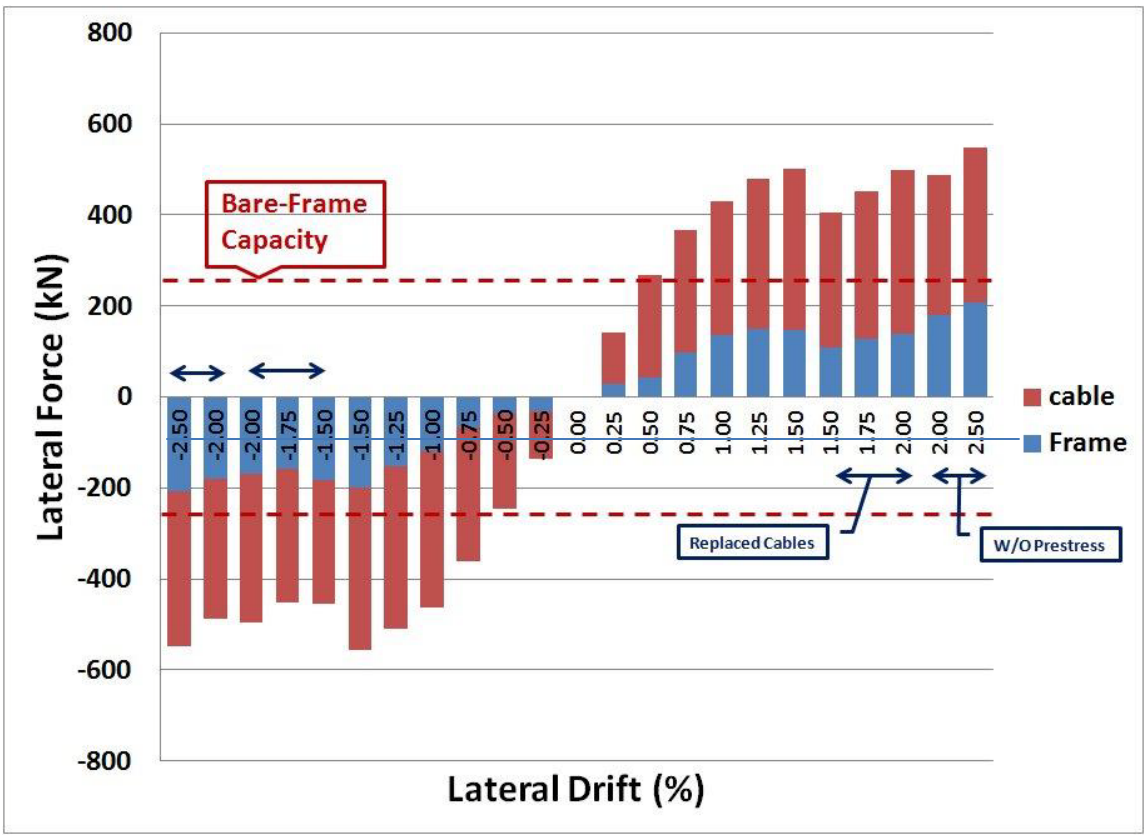

Fig. 5.7 Lateral force resistance contributions in Frame No. 2

The overall behaviour of each frame is compared in Figs. 5.8 through 5.11. Fig. 5.8 shows force-displacement hysteretic relationships for Frame No. 1 with a single prestressed strand in each diagonal (with an initial prestressing force of 100 kN), Frame No. 2 with twice as many prestressed strands (total initial prestressing force of 200 kN in each diagonal), as well as Frame No, 2 with double strands without any prestressing. It is clear in the figure that when cables in both directions were initially prestressed using double strands, it took higher forces to attain the same deformation as the companion frame with non-prestressed strands. This implies that initial prestressing makes the frame more rigid, which may be an asset for drift control and hence damage control in non-ductile frames.

However, the total possible contribution of cables did not vary significantly since the ultimate capacity of the cables remained approximately the same. It may then be concluded that, two aspects of retrofit design must be considered for application in practice; i) the number of strands (area of A_{ps}), and ii) the level of initial prestressing (f_{pi}). The former is decided based on the

additional level of force resistance required, and the latter is decided based on the lateral drift limitation.

In all tests the ductility attained was limited. The expectation that the steel strands could improve the ductility of the overall structural system could not be realized. This was attributed to the limited elongation capacity of the strands, which did not permit a significant increase in lateral drift capacity following initial yielding.

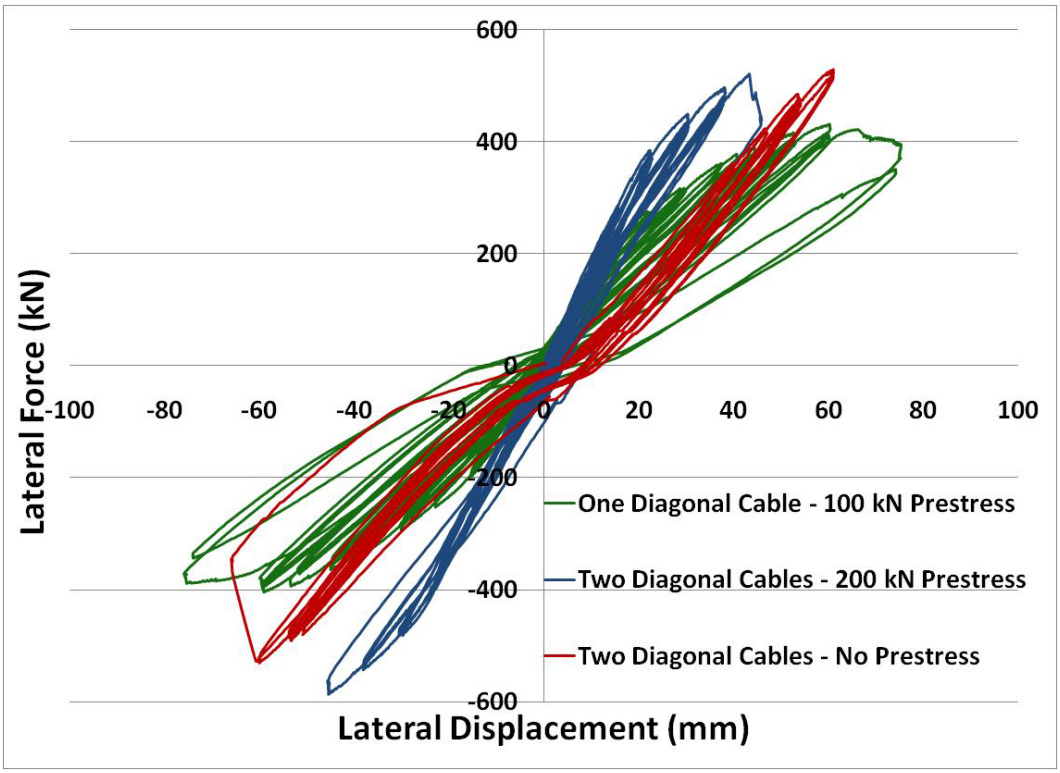

Fig. 5.8 Comparisons of force-displacement hysteretic relationships of frames

Another interesting aspect of the performance of retrofitted frames was the pinched hysteresis loops observed in the inelastic range of deformations. The strands developed plastic deformations beyond yielding, as expected. These plastic deformations could not be recovered upon unloading and the strands remain stress free in both diagonals until lateral drift is increased in the opposite direction and the strands start taking forces once again. This produces low resistance initially, followed by increased resistance, contributing towards

the pinching of hysteresis loops. Figs. 5.9 through 5.11 show moment-lateral displacement hysteretic relationships, with more pronounced pinching in Fig. 5.11 which shows the behaviour

of Frame No. 2 with non-prestressed strands. These hysteretic relationships are for total moment resistance of frames, obtained by multiplying the horizontal actuator force by the frame height. Because the axial load was applied through vertical prestressing and the vertical prestressing forces would pass through column base as the frame sways under reversed cyclic loading, they will not cause additional moments due to the P-Δ effect. This implies that the P-Δ moment associated with laterally deformed column under reverse-cyclic loading are incorporated in generating moment-displacement hysteretic relationships. The vertical load (P) in this calculation is the summation of initial axial load on columns and vertical force component of diagonal prestress cable.

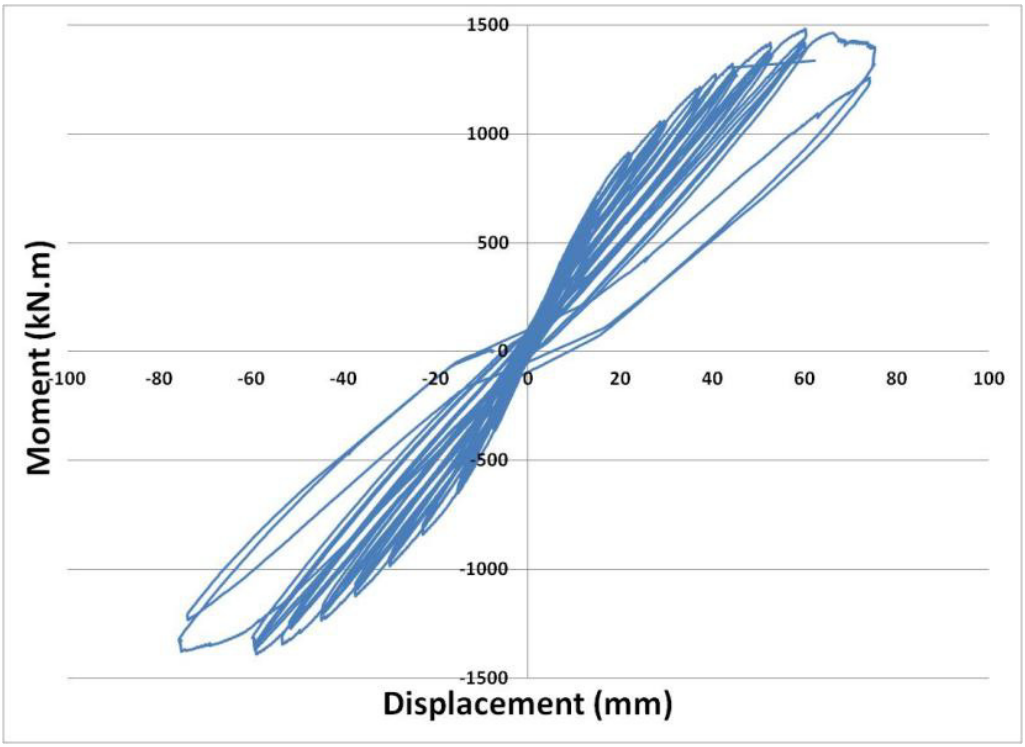

Fig. 5.9 Moment – displacement hysteretic relationship of Frame No. 1

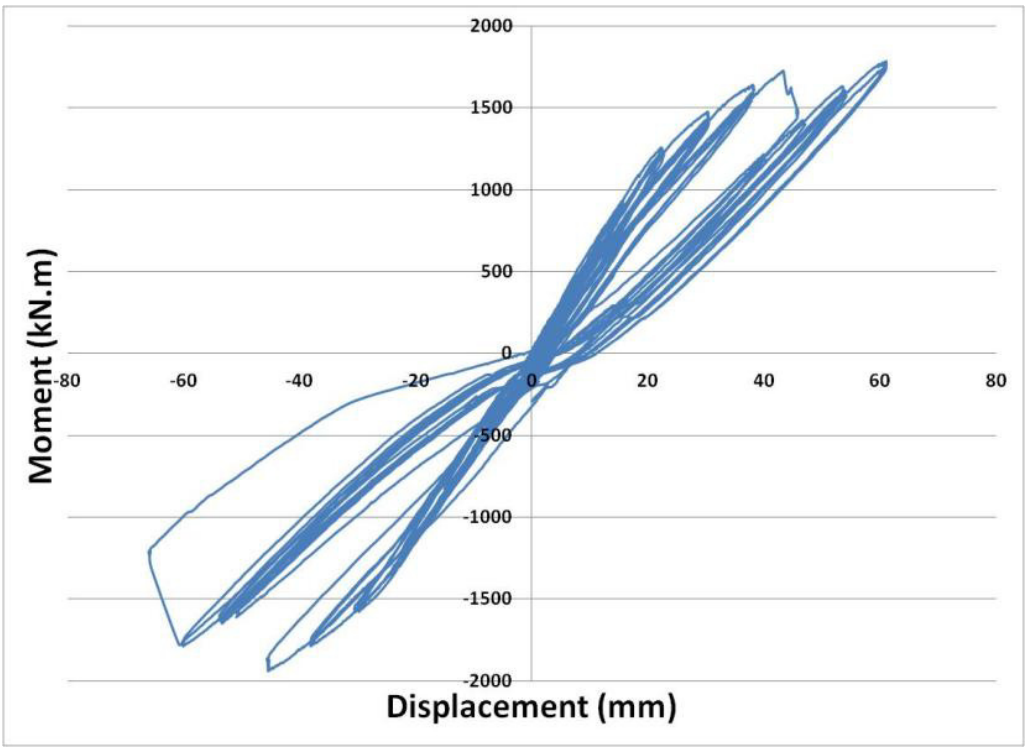

Fig. 5.10 Moment – displacement hysteretic relationship of Frame No. 2 (with prestress)

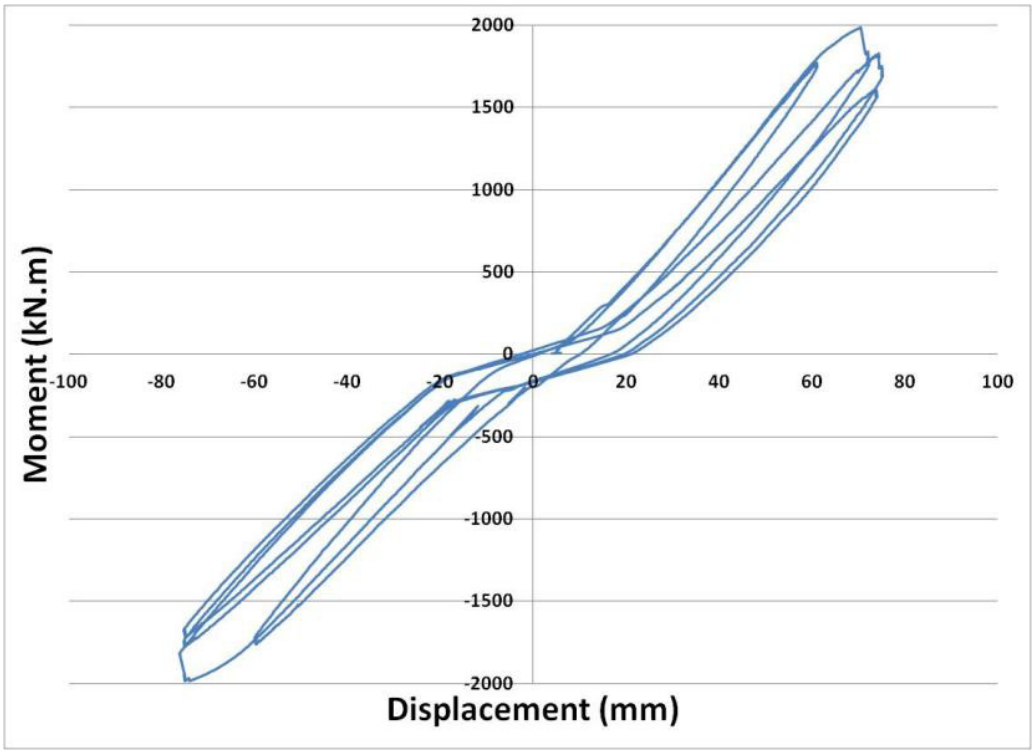

Fig. 5.11 displacement hysteretic relationship of Frame No. 2 (without prestress)

5.4 Retrofit Design Procedure

The experimental data and the frame analysis presented in Chapters 4 and 5 provide information to devise a design procedure for seismic retrofit of non-ductile reinforced concrete frames with diagonal prestressing. The design philosophy consists of lateral bracing of frames for improved strength and stiffness. The ductility achieved during the tests, with the 7-wire strands employed, was not high enough to be relied on during seismic excitations. Hence, unless more ductile prestressing steel is used, the retrofit strategy should be based on elastic response of the strands, while inelastic deformation capacity of the retrofitted frame remains as the secondary line of defence. The following steps can be followed in the retrofit design:

- Conduct seismic analysis of the frame building at hand using the current seismic hazard values (in Canada; Uniform Hazard Spectra specified in the National Building Code of Canada) and determine the elastic seismic force demands.
- Compute the available lateral force resisting capacity of the building. If the building has sufficiently high shear capacity to develop flexural yielding in critical regions of frame elements without developing shear failure, the lateral force capacity can be taken as the smaller of the force associated with nominal flexural capacity or inter-storey drift of 2%, whichever is small. If the shear capacity of critical elements in diagonal tension, diagonal compression or sliding shear is lower than the shear force associated with nominal flexural capacity, then the shear critical elements should be retrofitted first by any one of the available element retrofit methods to ensure flexure-dominant response of the building.
- Compute the required level of strength enhancement by finding the difference between the elastic force demands and the force capacities.
- Compute the required area of diagonal prestressing strand that will provide the additional seismic force capacity needed at the onset of strand yielding (horizontal component of strand force in tension).
- Compute lateral inter-storey drift ratio corresponding to the onset of yielding in the prestressing strands. If this value is within the performance level sought, while not exceeding 2% drift ratio, then the retrofit design is completed. If the lateral drift is higher than that required to control damage in structural and non-structural elements, apply

initial prestressing to the strands to stiffen the frame for reduced inter-storey drift. It is advisable not to exceed 50% of the strand rupturing capacity as the initial prestress to allow for the development of additional force resistance during seismic response.

Chapter 6

Summary and Conclusions

6.1 Summary

Experimental research was conducted to develop a cost effective and structurally sound lateral bracing system for seismic retrofit of non-ductile reinforced concrete frame systems that can be implemented with limited interference with structural and non-structural elements while keeping the construction down time to a minimum. The technique consists of providing diagonal pretstressing strands as tension braces, with or without initial prestressing. The effectiveness of the technique was investigated through experimental research by testing large-scale specimens under reversed cyclic loading.

The experimental program consisted of design, construction and testing of two large-scale reinforced concrete frames, which were representatives of the 1960's practice in North America with seismic deficiencies. The frames were retrofitted by providing either single or double No. 15 7-wire strands with or without prestressing. The frames were subjected to a constant axial gravity load, representing gravity service loads, and incrementally increasing lateral deformation reversals until failure. The frames were instrumented for displacement and strain measurements. The results were presented in the form of hysteretic force-displacement and moment displacement relationships to assess the improvements in strength, deformability and stiffness.

Analysis of the frames was conducted and compared with experimentally recorded capacities. A design procedure was developed and recommended for seismic retrofit of seismically deficient concrete frame buildings.

6.2 Conclusions

The following conclusions can be drawn from the research project reported in this thesis:

- Non-ductile reinforced concrete frame buildings may not have sufficient strength and deformability to resist earthquake forces in medium to high seismic regions. An appropriate seismic risk mitigation approach for such buildings involves seismic retrofitting. A system level retrofit is more appropriate for buildings that have a large number of seismically deficient elements. Lateral bracing for deformation control is appropriate for such buildings.
- Lateral bracing of concrete frames by means of diagonally placed prestressing strands provides significantly increased seismic force resistance, while stiffening the frames for reduced inter-storey drift and damage.
- While the level of strength enhancement in frames laterally braced with steel strands depends on the size and number of strands provided, the use of single No.15 7-wire strands with 140 mm^2 strand area resulted in 1.5 times increase of seismic force resistance in the test frame considered in the experimental phase. The use of double strands resulted in 2.1 times increase in seismic force resistance of the test frame considered.
- Initial prestressing of diagonal strands increases stiffness but does not necessarily result in increased strength. The effect of initial prestressing is to have higher lateral force resistances at lower inter-storey drifts, hence potentially controlling seismic damage associated with increased inelastic deformations in the frame.
- The 7-wire strands used in the current investigation, with 4% elongation capacity, were not able to generate sufficient ductility of the overall retrofitted frame system. The level of displacement ductility attained was limited to 2.0. Therefore, the retrofit strategy based on the use of diagonal prestressing strands may have to be limited to elastic behaviour of strands unless more ductile steel strands are employed.

- Frames braced with steel strands develop pinched hysteresis in the inelastic range of deformations with reduced energy dissipation capacity. Pinching may be eliminated or reduced if the strands are always kept in tension, without and slack upon unloading by means of specially designed connection devices at the ends.
- The retrofit technology and the design procedure proposed for lateral bracing of reinforced concrete frames, involving the use of diagonal steel strands, may be used as an effective seismic retrofit approach for non-ductile concrete frames.

6.3 Recommendations for Future Research

The following research topics/projects are recommended for further investigation:

- The effect of high-elongation tension braces, as in the case of stainless steel strands, should be investigated through experimental research to explore potential improvements in inelastic deformability and energy absorption capacity of the retrofitted system.
- Additional tests with different number of strands and levels of prestressing should be investigated, as current test data is limited to three cases.
- Application of the retrofit methodology to prototype buildings and dynamic inelastic response history analyses of buildings to assess the performance of the retrofit technique.
- Response history analyses of multi-storey buildings having different number of stories and structural layouts, retrofitted with different patterns of diagonal prestressing, subjected to different earthquake records.
- Connection details for prestressing strands.

References

- ACI 318-63: "ACI Standard – Building Code Requirements for Reinforced Concrete", aci publications.
- Al-Sadoon Z., "Seismic Retrofit of Reinforced Concrete Frames with Buckling Restrained Braces", PhD dissertation (2013), Department of Civil Engineering, the University of Ottawa, Ottawa, Canada.
- Berman, J.W. and Bruneau, M. "Cyclic testing of a buckling restrained braced frame with unconstrained gusset connections." Journal of Structural Engineering, 135:12, (2009) pp. 1499-1510.
- Bosco M. and Marino E.M. , "Design method and behavior factor for steel frames with buckling restrained braces", Earthquake Engineering and Structural Dynamics, (2013) 42: pp. 1243-1263.
- Caron, F. "Repair and retrofit of non-ductile reinforced concrete frames with diagonal steel compression struts." M.A.Sc. Thesis, Department of Civil Engineering, University of Ottawa, (2010), Ottawa, Canada.
- Carriere, J.M., "Seismic retrofit of existing reinforced concrete moment resisting frame structures using diagonal prestressing", M.A.Sc. Dissertation (2007).
- Cortés, W.L., Palermo, D., "Modelling of seismic repair and retrofit of concrete shear walls", (2010), Proceedings, Annual Conference - Canadian Society for Civil Engineering 1 , pp. 128-137.
- Christopoulos, C., Tremblay, R., Kim, H.-J., Lacerte, M., "Self-centering energy dissipative bracing system for the seismic resistance of structures: Development and validation", (2008), Journal of Structural Engineering, 134 (1), pp. 96-107.
- Di Sarno, L. and Manfredi, G. "Seismic retrofitting with buckling restrained braces: Application to an existing non-ductile RC framed building." Soil Dynamics and Earthquake Engineering, 30:11, (2009), pp. 1279-1297.
- Della Corte G., D'Aniello M., Landolfo R., Mazzolani F.M., "Review of steel buckling-restrained braces.",(2011), Steel Construction;4(2):85–93.

- Demers, M., and Neale, K.W. “Confinement of reinforced concrete columns with fibre-reinforced composite sheets-an experimental study.”, Canadian Journal of Civil Engineering, 26, (1999), pp. 226-241.
- Elnashai, A.S., Elghazouli, A.Y., “Performance of composite steel/concrete members under earthquake loading. Part I: Analytical model”, (1993), Earthquake Engineering and Structural Dynamics, 22 (4), pp.
- Elnashai A.S., Pinho, R., “Repair and retrofitting of RC walls using selective techniques”, (1998), Journal of Earthquake Engineering 2 (4) , pp. 525-568.
- Filiatrault, A., Restrepo, J., Christopoulos, C., “Development of self-centering earthquake resisting systems”, (2004), Proc. 13 th World Conf. on Earthquake Eng.
- Harajli, M.H., Khalil, Z., “Seismic FRP retrofit of bond-critical regions in circular RC columns: Validation of proposed design methods”, (2008), ACI Structural Journal 105 (6), pp. 760-769.
- Hognestad, E., “Ultimate strength of reinforced concrete in American design practice”, Proceedings of a symposium on the strength of concrete structures, London, (1956).
- Jiang, H., Kurama, Y.C., “An analytical investigation on the seismic retrofit of older medium-rise reinforced concrete shear walls under lateral loads”, (2013), Engineering Structures 46 , pp. 459-470.
- Li, G.-Q., Guo, X.-K., Sun, F.-F., Chen, C., “Study of the anchorage connections for buckling restrained braces part 1: Experimental investigation”, (2013), Advances in Structural Engineering 16 (4) , pp. 759-771.
- Guo, X.-K., Li, G.-Q., Sun, F.-F., Liu, Y.-S., “Study of the anchorage connections for buckling restrained braces part 2: Theoretical study”, (2013), Advances in Structural Engineering 16 (4) , pp. 773-789.
- Merzouq, S., Tremblay, R., “Seismic design of dual concentrically braced steel frames for stable seismic performance for multi-storey buildings”, (2006), Proc. 8 th U.S. Nat. Conf. on Earthquake Eng.
- Mitchell, D., Paultre, P., Tinawi, R., Saatcioglu, M., Tremblay, R., Elwood, K., Adams, J., Devall, R., “Evolution of seismic design provisions in the National building code of Canada”, Published by NRC Research Press (2010).

- Moghaddasi, N.S., Yunfeng Z., Xiaobin, H., “Seismic retrofitting of reinforced concrete frame structures using GFRP-tube-confined-concrete composite braces”, (2012), Earthquake Engineering and Engineering Vibration, Vol.11, No.1, pp. 91-105.
- NBCC 2010 – National Building Code of Canada – Issued by National Research Council of Canada (NRC).
- Nyi, N.Z., Tani, M., “Seismic evaluation and retrofit of existing reinforced concrete buildings”, (2013), Bulletin of the International Institute of Seismology and Earthquake Engineering 47, pp. 97-102.
- Ozbakkaloglu T., Lim, J.C., Vincent, T., “FRP confined concrete in circular sections: Review and assessment of stress-strain models”, (2013), Engineering Structures 49, pp. 1068-1088.
- Ozbakkaloglu, T., and Saatcioglu, M. “Tensile Behavior of FRP Anchors in Concrete.“ ASCE Journal of Composites, 13: 2, (2009), pp. 82-92.
- Ozcelik, R., Binici, B., Akpinar, U., ”Seismic retrofit of non-ductile reinforced concrete frames with chevron braces”, (2012), Proceeding of the Institution of Civil Engineers, Structures and Buildings, Vol. 166, Issue SB7, pp. 326-341.
- Pincheira, J.A. and Jirsa, J.0., “Post-tensioned bracing for seismic retrofit of RC frames. Proceedings of the Tenth World Conference on Earthquake Engineering”, (1992); 9:pp. 5199-5204; Madrid, Spain.
- Pincheira, J.A. and Jirsa, J.0., “Seismic response of RC frames retrofitted with steel braces or walls”, (1995), Journal of Structural Engineering 1995.121, pp. 1225-1235.
- Prinz, G.S., Richards, P.W., “Seismic performance of buckling-restrained braced frames with eccentric configurations”, (2012), Journal of Structural Engineering (United States) 138 (3) , pp. 345-353.
- Saatcioglu, M., Serrato, F., and Foo, S. “Seismic performance of masonry infill walls retrofitted with CFRP sheets.” ACI Special Publication SP-230, 230, (2005), pp. 341-354.
- Saatcioglu, M., Ozbakkaloglu, T. and Elnabelsy, G. “Seismic behavior and design of reinforced concrete columns confined with FRP stay-in-place formwork.” ACI-SP 257-09, American Concrete Institute, 230, (2008), pp. 149-170.

- Sarno L. and Manfredi G. “Experimental tests on full-scale RC unretrofitted frame and retrofitted with buckling-restrained braces”, Earthquake Engineering and Structural Dynamics, (2012), 41: pp. 315-333.
- Shalouf, F. and Saatcioglu, M. “Seismic retrofit of non-ductile reinforced concrete frames with diagonal prestressing.” Proceedings of the 8th U.S. National Conference on Earthquake Engineering, San Francisco, (2006).
- Shalouf, F., “Seismic retrofit of reinforced concrete frames with diagonal prestressing or FRP strips”, PhD dissertation (2005).
- Tremblay, R., Christopoulos, C., Erochko, J., Kim, H.J., “Experimental validations and design of self-centering energy dissipative (SCED) braced structures”, (2010), 9th US National and 10th Canadian Conference on Earthquake Engineering 2010, Including Papers from the 4th International Tsunami Symposium 2 , pp. 1300-1309.
- Thermou and Elnashai, “Seismic Retrofit schemes for RC structures and local-global consequences”, (2006), Progress in Structural Engineering and Materials, Vol. 8, Issue 1, pp. 1-15.
- Uang, C-M., and Bertero, V.V. “Use of energy as a design criterion in earthquake-resistant design.” Report No. UCB/EERC-88/18, University of California, Berkeley, (1988).
- Uang C.M., Nakashima M., “Earthquake Engineering: From Engineering Seismology to Performance Based Engineering.”, (2004) CRC Press LLC:NewYork.
- Varum, H., Teixeira-Dias, F., Marques, P., Pinto, A.V., Bhatti, A.Q., “Performance evaluation of retrofitting strategies for non-seismically designed RC buildings using steel braces”, (2013), Bulletin of Earthquake Engineering 11 (4), pp. 1129-1156.
- Xie Q., “State of the art of buckling-restrained braces. Journal of Constructional Steel Research”, (2005); 61:pp. 727–748.
- “Recommended provisions for buckling restrained braced frames”, Structural Engineers Association of Northern California (SEAONC) (2001).
- “Recommended Provisions for Seismic regulations for New Buildings and Other Structures” NEHRP Publications, FEMA-450 (2004).
- “Seismic Provisions for Structural Steel Buildings” AISC-2005.

Appendix A – Experimental Data

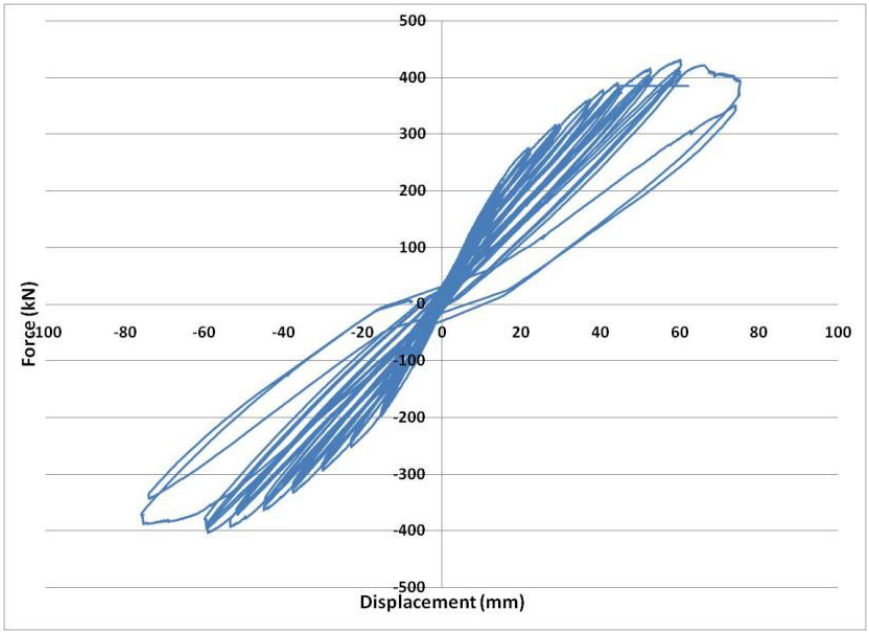

Fig. 4.1 – Hysteretic Lateral Load – Lateral Displacement Relationship for Frame No.1

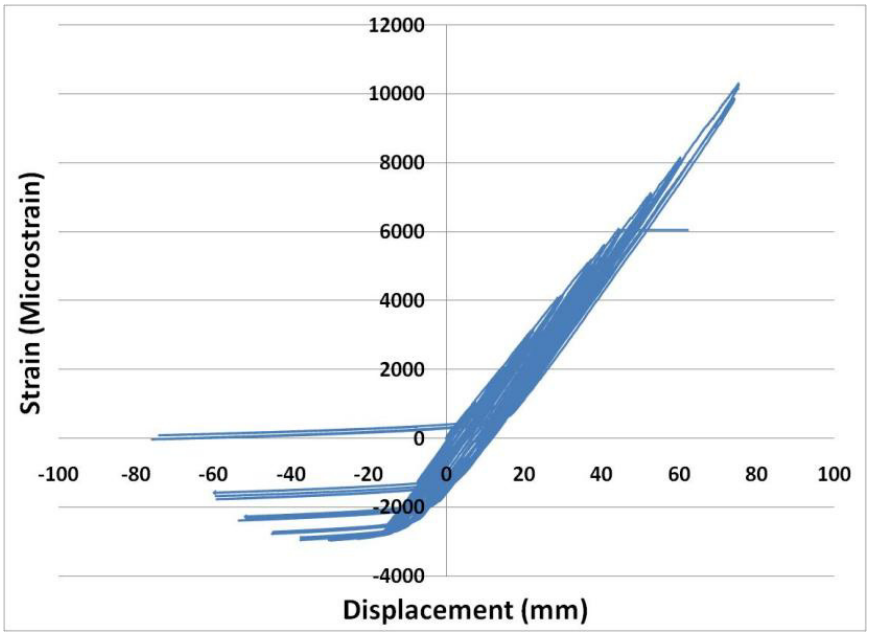

Fig. 4.2 – Lateral Displacement vs. Strain of Diagonal Cable (Push Direction) – Ch.23 (100kN)

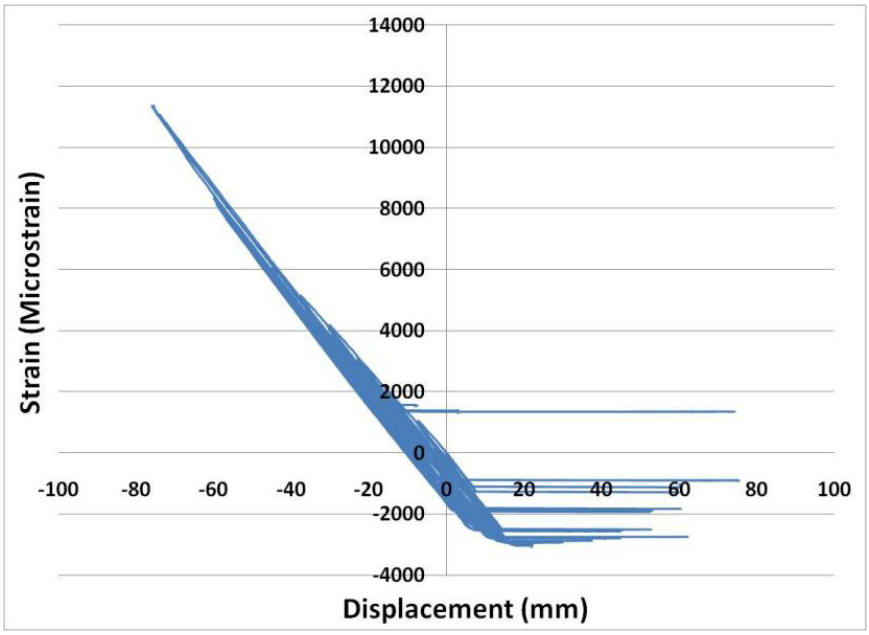

Fig. 4.3 – Lateral Displacement vs. Strain of Diagonal Cable (Pull Direction) – Ch.25 (100 kN)

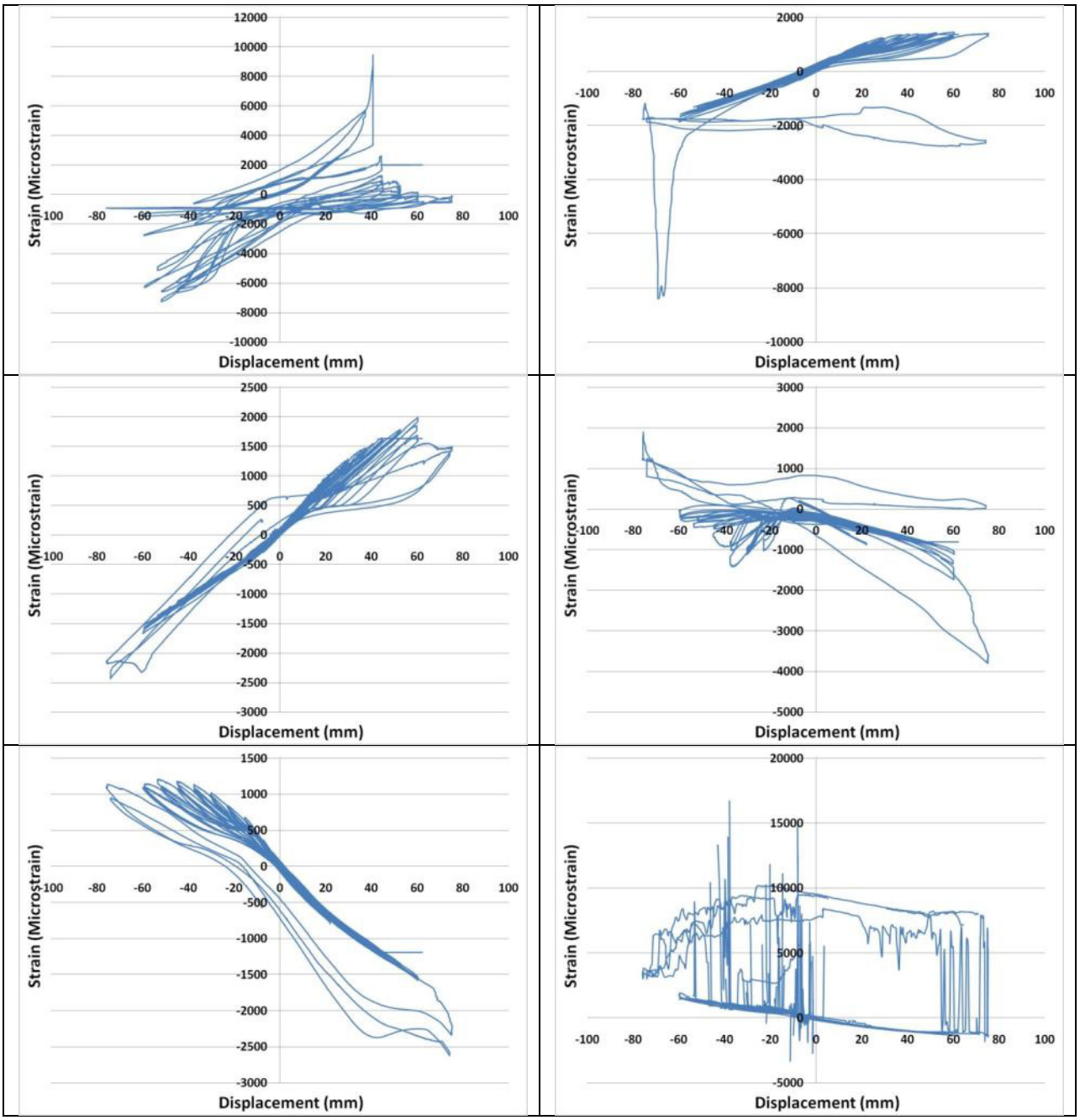
Strain (Microstrain)
Displacement (mm)
12000
10000
8000
6000
4000
2000
0
-2000
-4000
-6000
-8000
-10000
-100 -80 -60 -40 -20 0 20 40 60 80 100
Strain (Microstrain)
Displacement (mm)
2000
0
-2000
-4000
-6000
-8000
-10000
-100 -80 -60 -40 -20 0 20 40 60 80 100
Strain (Microstrain)
Displacement (mm)
2500
2000
1500
1000
500
0
-500
-1000
-1500
-2000
-2500
-3000
-100 -80 -60 -40 -20 0 20 40 60 80 100
Strain (Microstrain)
Displacement (mm)
3000
2000
1000
0
-1000
-2000
-3000
-4000
-5000
-100 -80 -60 -40 -20 0 20 40 60 80 100
Strain (Microstrain)
Displacement (mm)
1500
1000
500
0
-500
-1000
-1500
-2000
-2500
-3000
-100 -80 -60 -40 -20 0 20 40 60 80 100
Strain (Microstrain)
Displacement (mm)
20000
15000
10000
5000
0
-5000
-100 -80 -60 -40 -20 0 20 40 60 80 100
Strain (Microstrain)
Displacement (mm)

ch.1 to 6

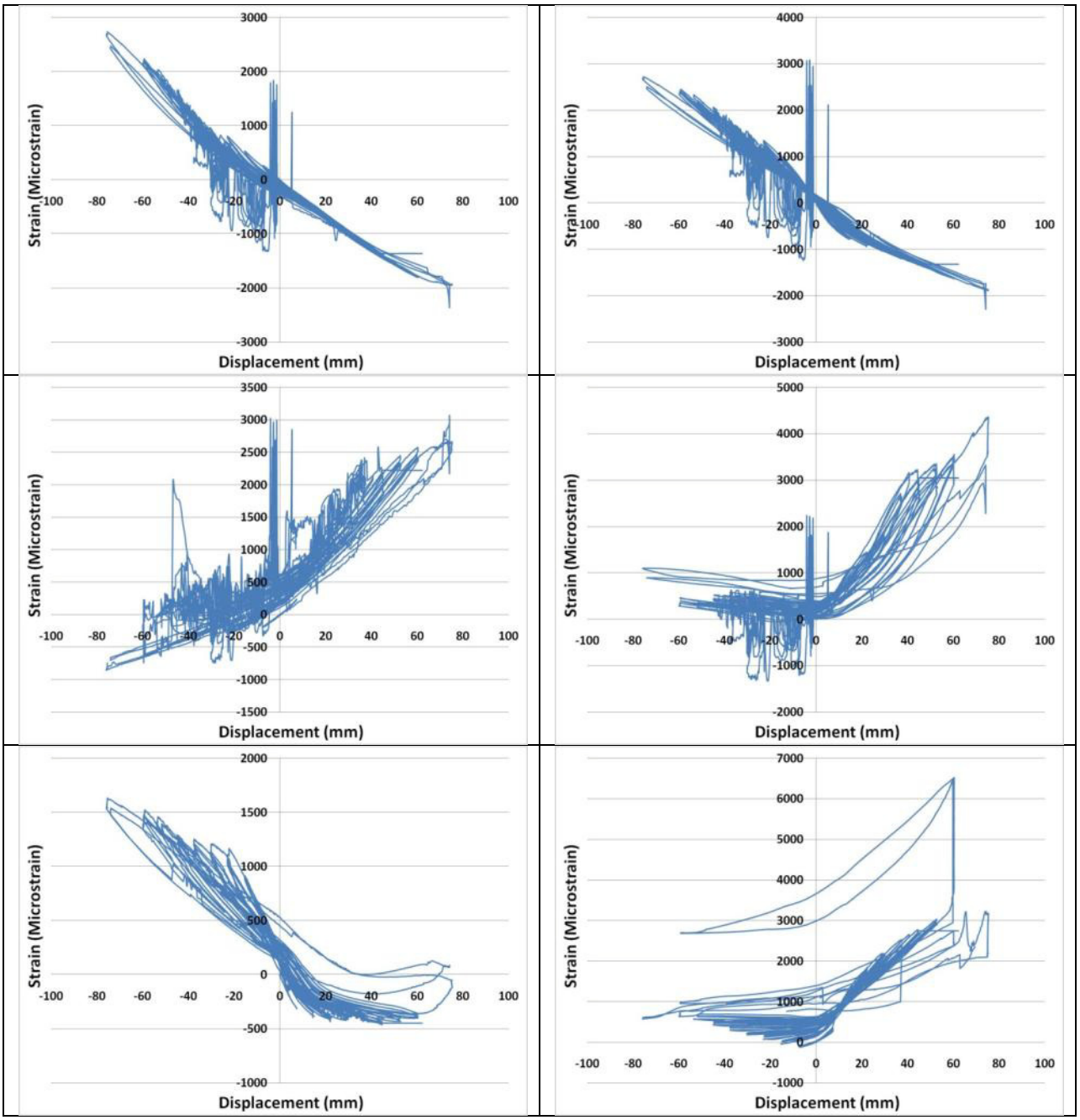
Strain (Microstrain)
Displacement (mm)
3000
2000
1000
0
-1000
-2000
-3000
-100 -80 -60 -40 -20 0 20 40 60 80 100
Strain (Microstrain)
Displacement (mm)
4000
3000
2000
1000
0
-1000
-2000
-3000
-100 -80 -60 -40 -20 0 20 40 60 80 100
Strain (Microstrain)
Displacement (mm)
3500
3000
2500
2000
1500
1000
500
0
-500
-1000
-1500
-100 -80 -60 -40 -20 0 20 40 60 80 100
Strain (Microstrain)
Displacement (mm)
5000
4000
3000
2000
1000
0
-1000
-2000
-100 -80 -60 -40 -20 0 20 40 60 80 100
Strain (Microstrain)
Displacement (mm)
2000
1500
1000
500
0
-500
-1000
-100 -80 -60 -40 -20 0 20 40 60 80 100
Strain (Microstrain)
Displacement (mm)
7000
6000
5000
4000
3000
2000
1000
0
-1000
-100 -80 -60 -40 -20 0 20 40 60 80 100
Strain (Microstrain)
Displacement (mm)

Ch.7 to 12

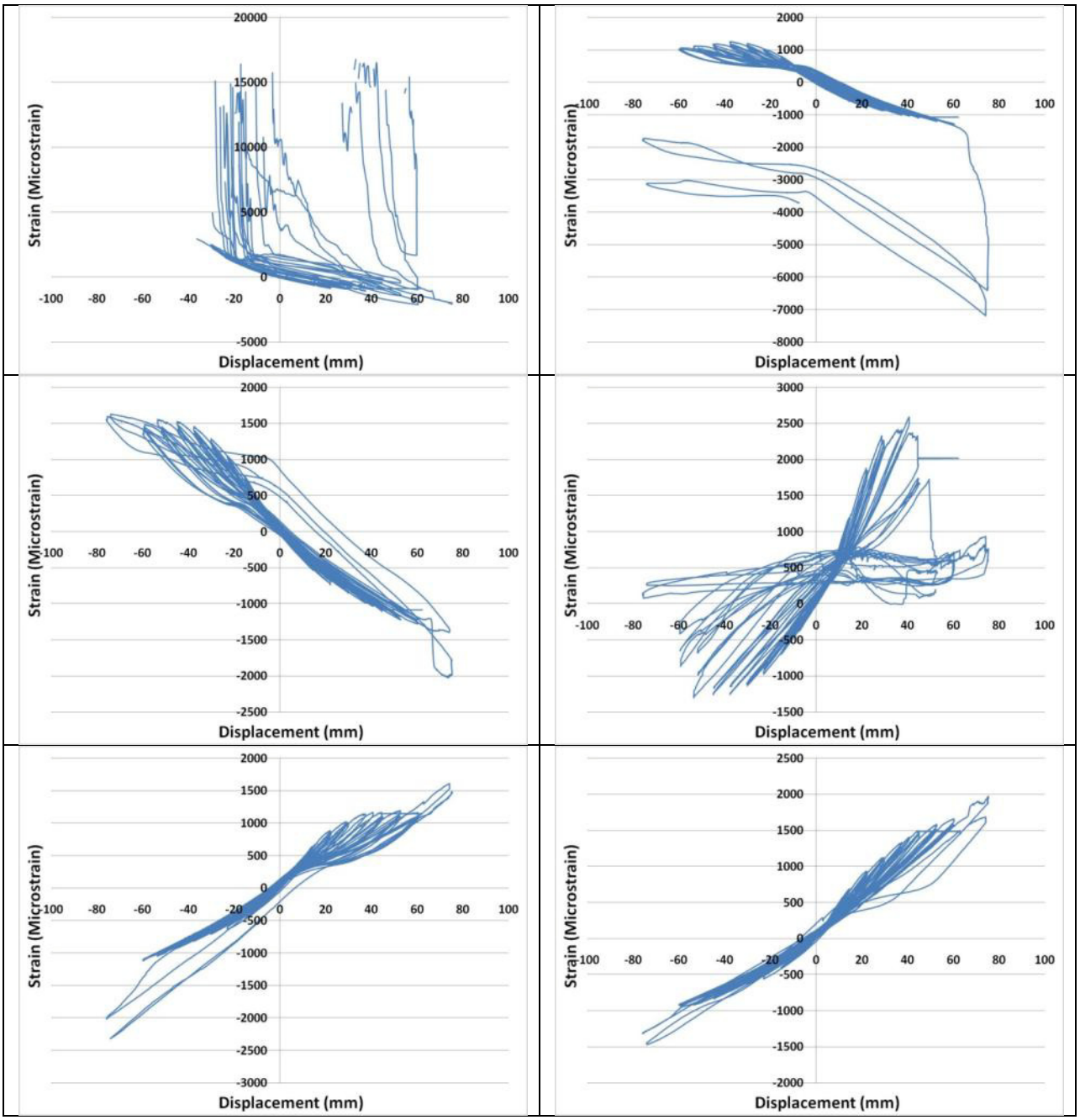
Strain (Microstrain)
Displacement (mm)
20000
15000
10000
5000
0
-5000
2000
1000
-1000
-2000
-3000
-4000
-5000
-6000
-7000
-8000
1500
500
-500
-1500
-2500
3000
2500
-3000
-100
-80
-60
-40
-20
0
20
40
60
80
100

Ch. 13-18

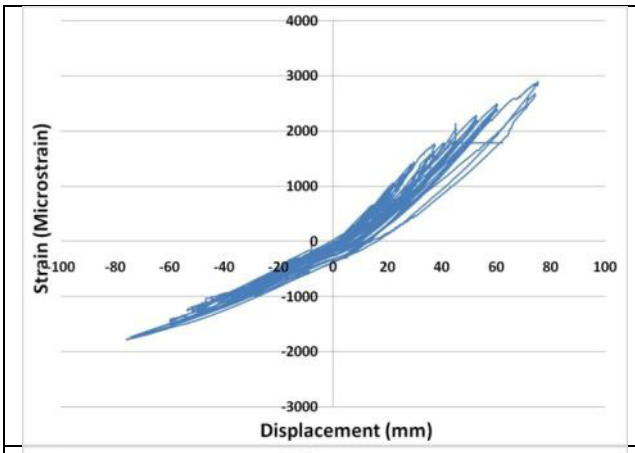

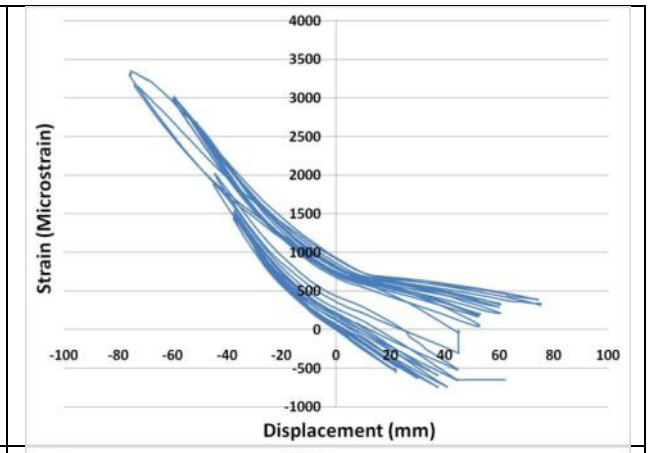

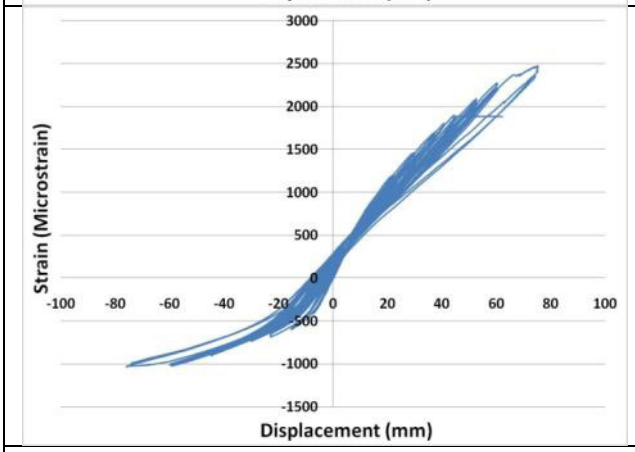

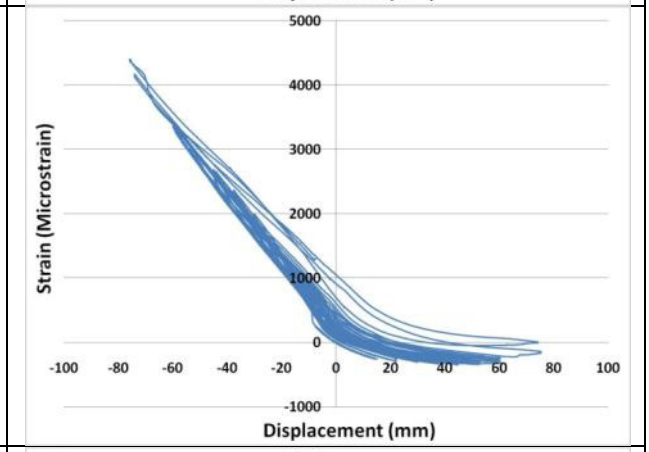

Cable No.1 (Push Direction)

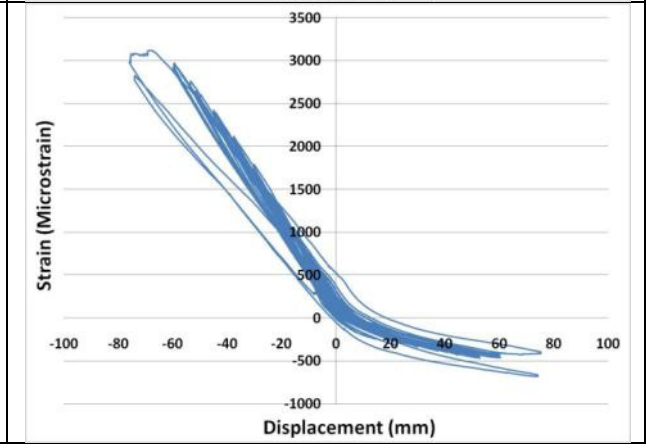

Ch.19-24

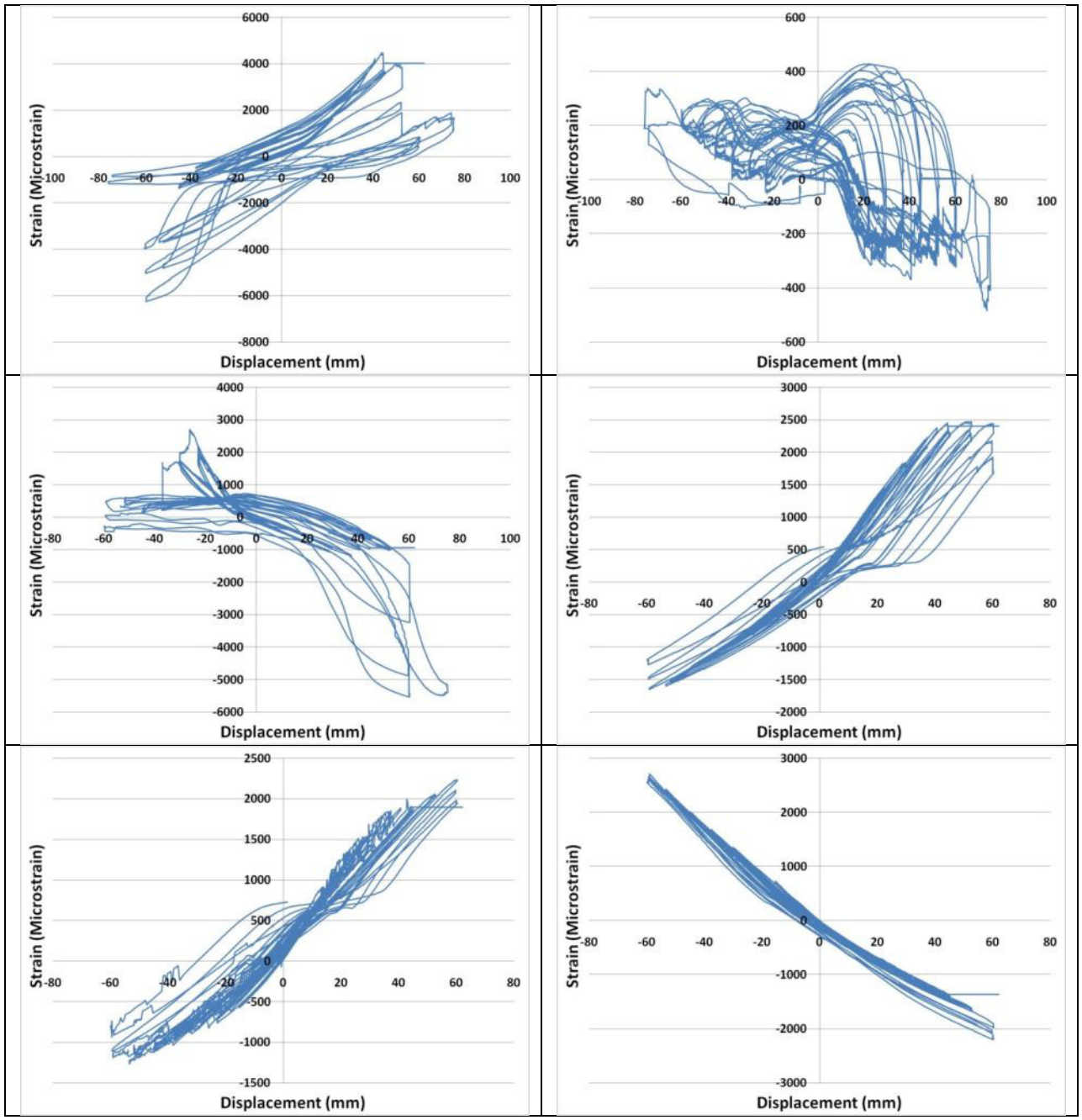
Strain (Microstrain)
Displacement (mm)
6000
4000
2000
0
-2000
-4000
-6000
-8000
-100
-80
-60
-40
-20
0
20
40
60
80
100
600
400
200
0
-200
-400
-600
3000
2500
2000
1500
1000
500
-500
-1000
-1500
-2000
-3000

Ch. 1 to 6

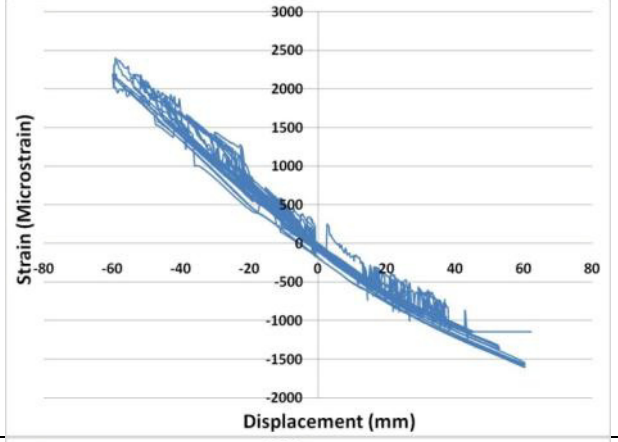

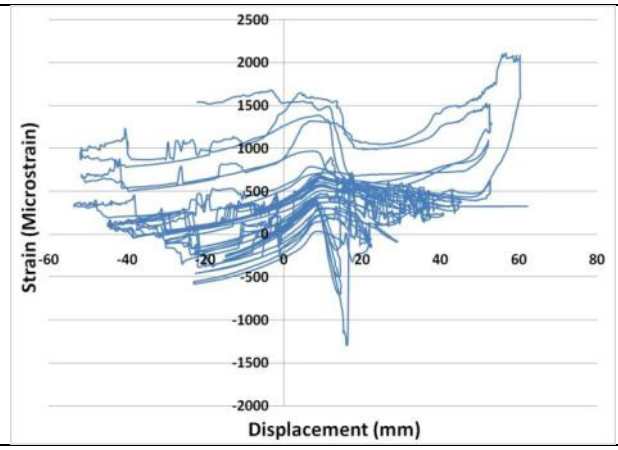

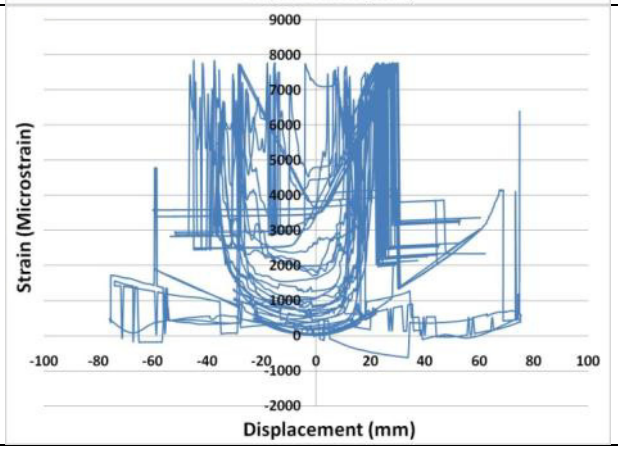

Channel 10 reading is corrupted.

Channel 11 reading is corrupted.

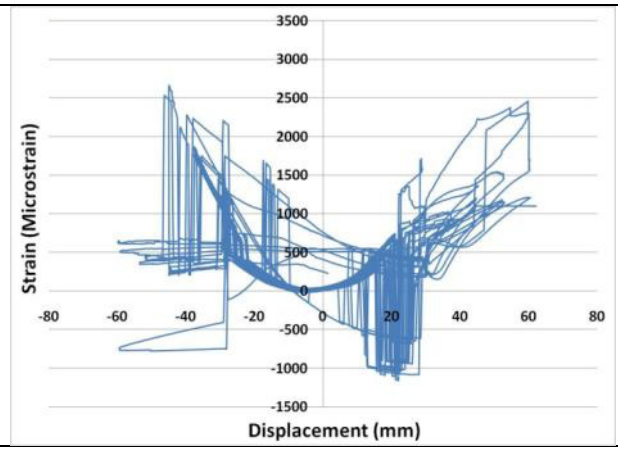

Ch. 7-12

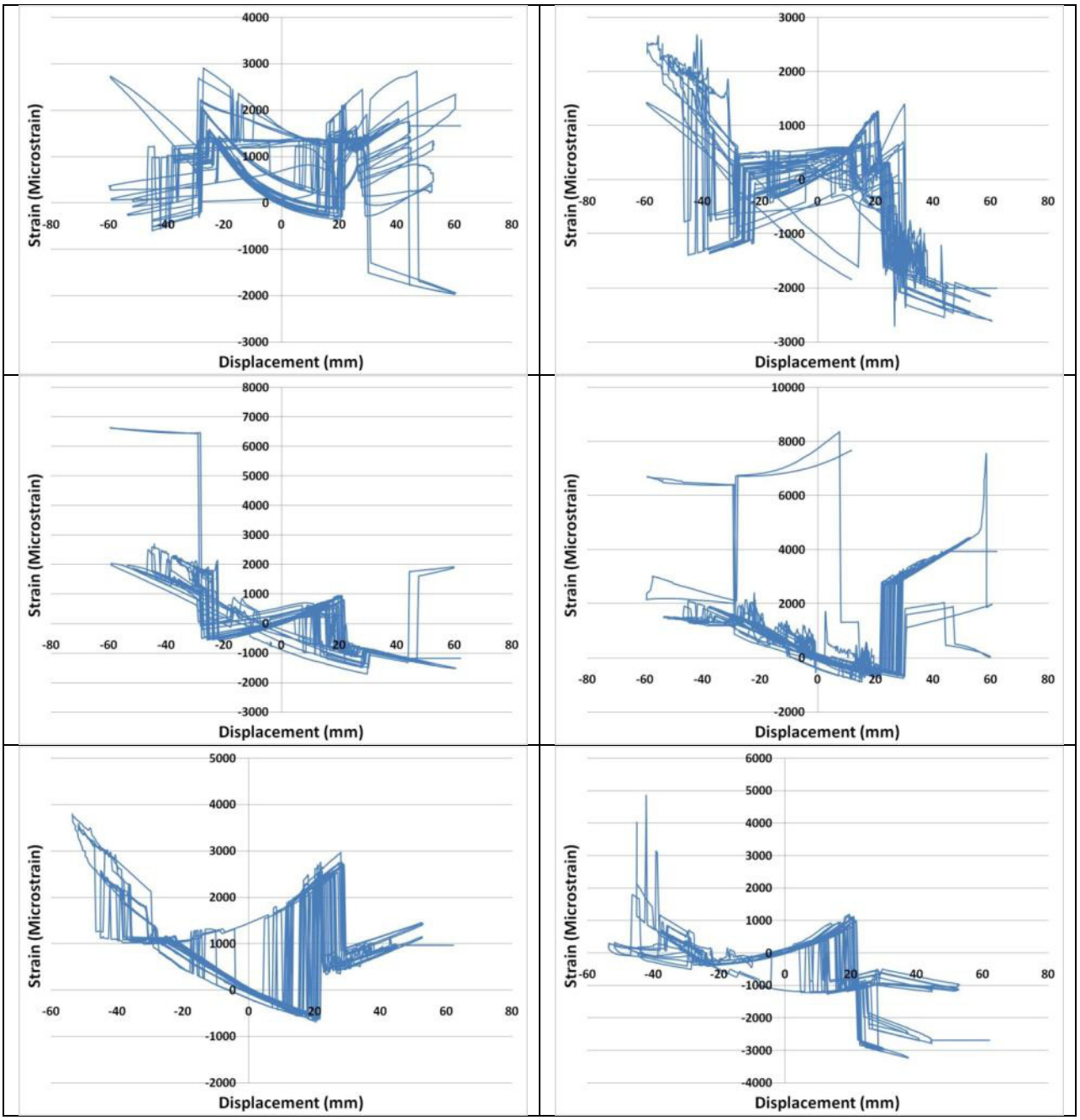
Strain (Microstrain)
Displacement (mm)
4000
3000
2000
1000
0
-1000
-2000
-3000
-80
-60
-40
-20
0
20
40
60
80
Strain (Microstrain)
Displacement (mm)
3000
2000
1000
0
-1000
-2000
-3000
-80
-60
-40
-20
0
20
40
60
80
Strain (Microstrain)
Displacement (mm)
8000
7000
6000
5000
4000
3000
2000
1000
0
-1000
-2000
-3000
-80
-60
-40
-20
0
20
40
60
80
Strain (Microstrain)
Displacement (mm)
10000
8000
6000
4000
2000
0
-2000
-80
-60
-40
-20
0
20
40
60
80
Strain (Microstrain)
Displacement (mm)
5000
4000
3000
2000
1000
0
-1000
-2000
-60
-40
-20
0
20
40
60
80
Strain (Microstrain)
Displacement (mm)
6000
5000
4000
3000
2000
1000
0
-1000
-2000
-3000
-4000
-60
-40
-20
0
20
40
60
80
Ch. 13-18

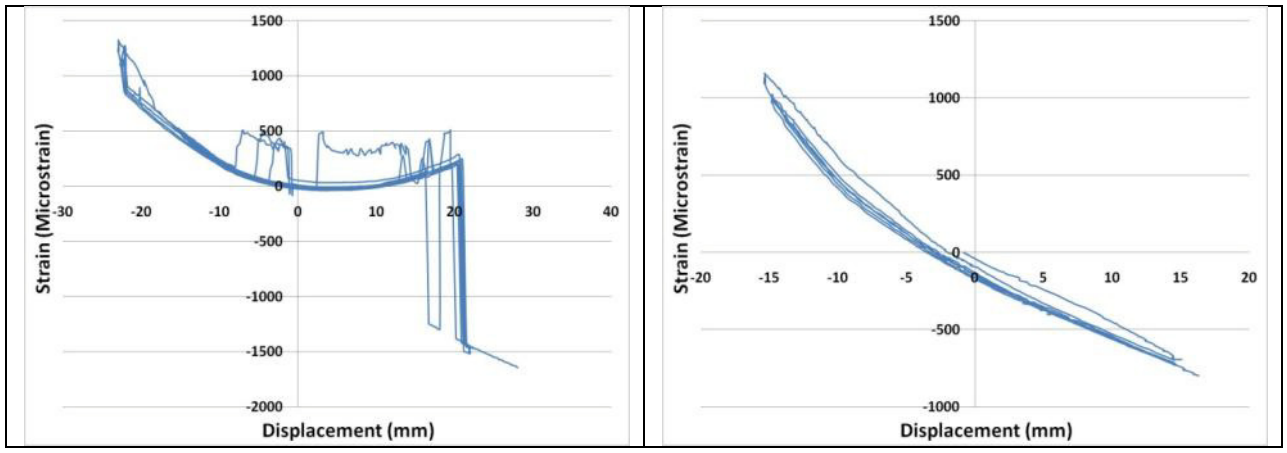
1500
1000
500
0
-500
-1000
-1500
-2000
-30
-20
-10
0
10
20
30
40
Strain (Microstrain)
Displacement (mm)
1500
1000
500
0
-500
-1000
-20
-15
-10
-5
0
5
10
15
20
Strain (Microstrain)
Displacement (mm)

Ch. 19-20

Second Frame Recorded Data – 1st Test

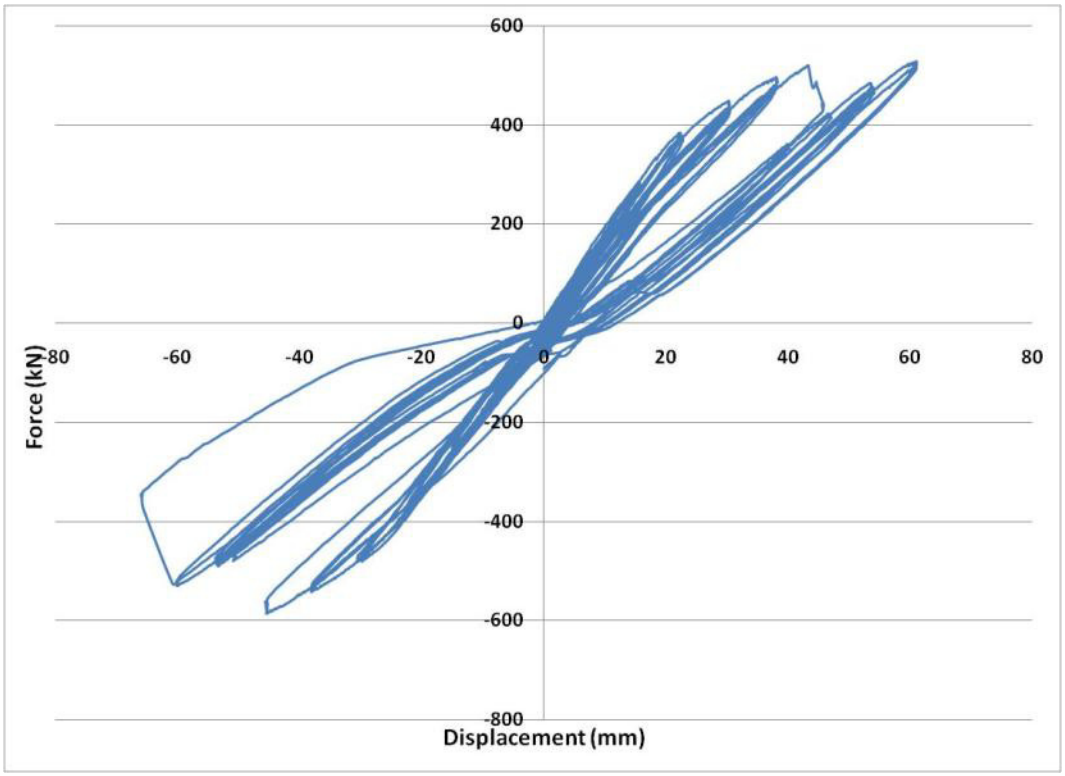

Fig. 4.5 – Hysteretic Lateral Load – Lateral Displacement Relationship for Frame No.2

(with prestressing – 100kN per cable – 200 kN prestressing per direction)

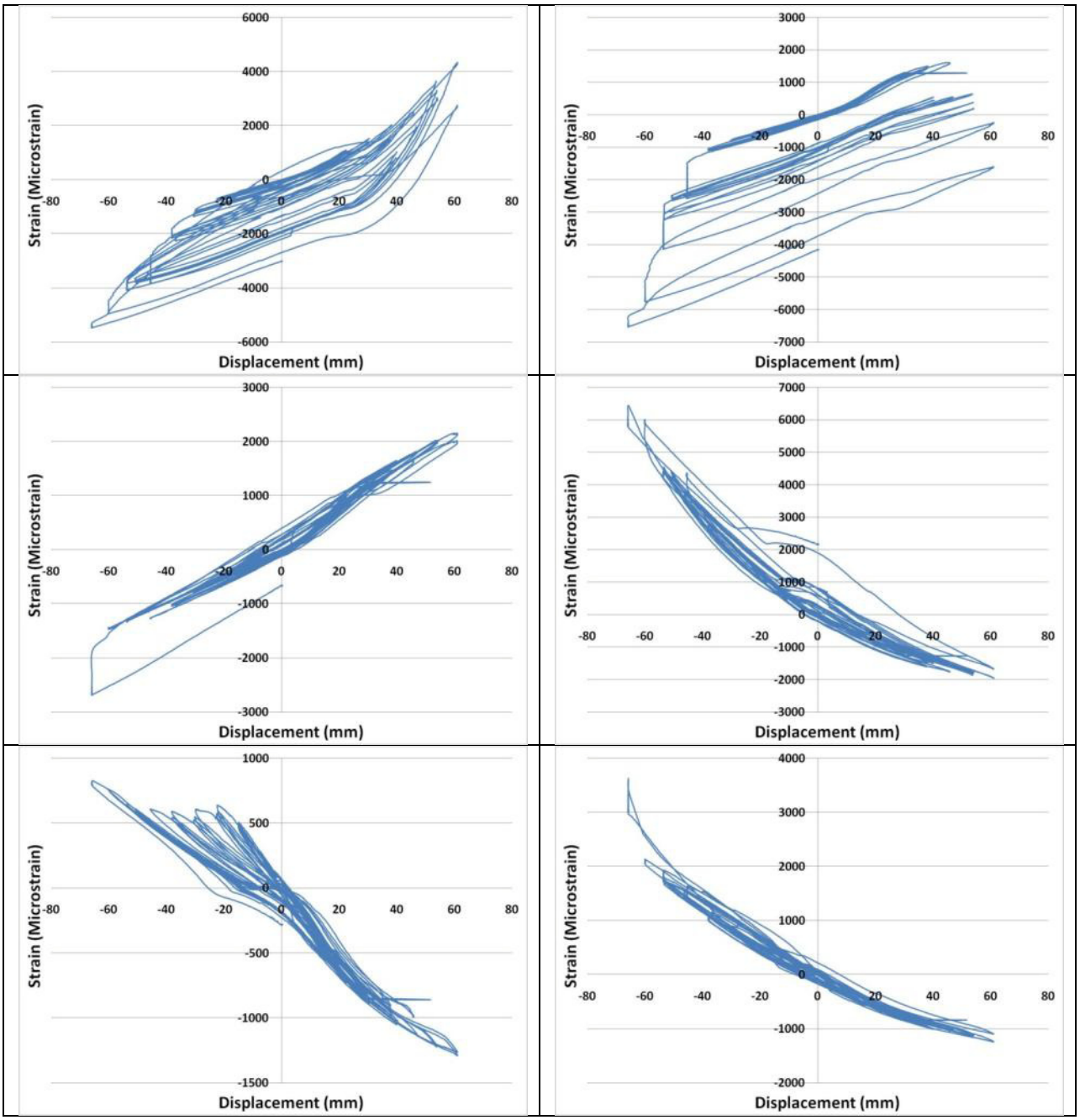
Strain (Microstrain)
Displacement (mm)
6000
4000
2000
0
-2000
-4000
-6000
-80
-60
-40
-20
0
20
40
60
80
3000
2000
1000
0
-1000
-2000
-3000
-4000
-5000
-6000
-7000
7000
6000
5000
4000
3000
2000
1000
0
-1000
-2000
-3000
500
-500
-1000
-1500

Ch. 1-6

Channel 7 reading is corrupted.	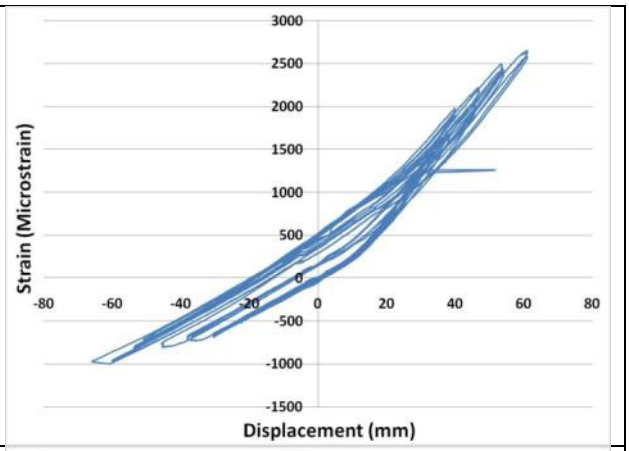
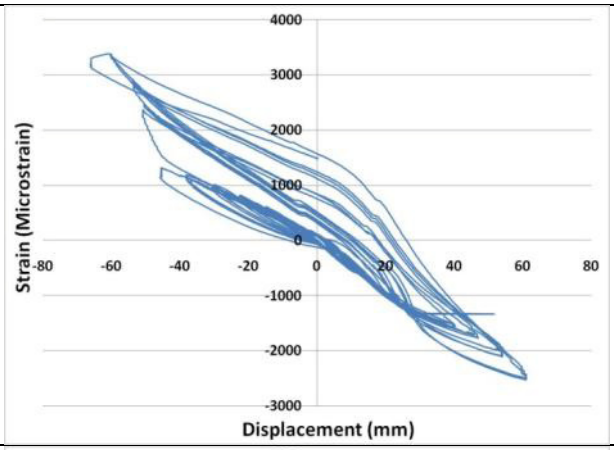	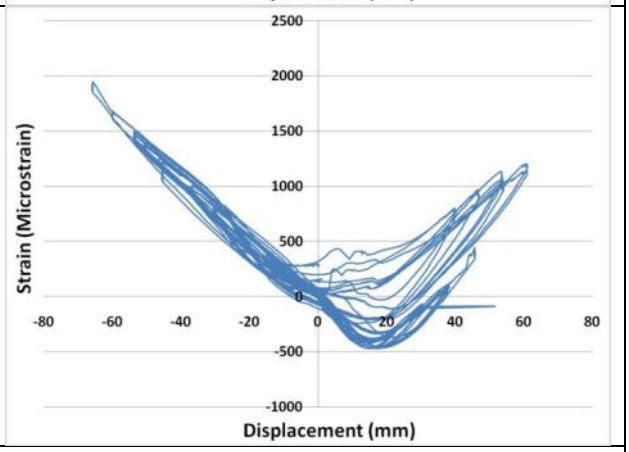
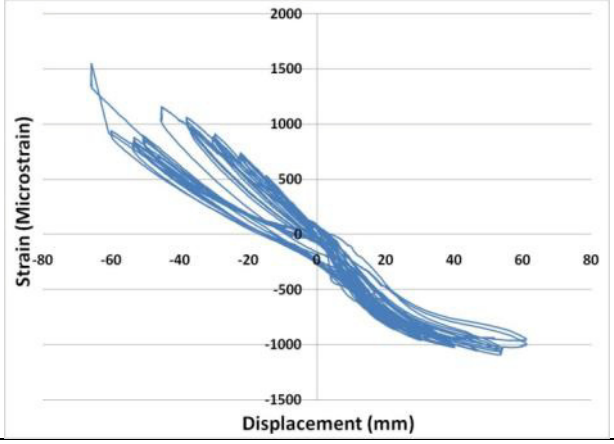	Channel 12 reading is corrupted.

Ch. 7-12

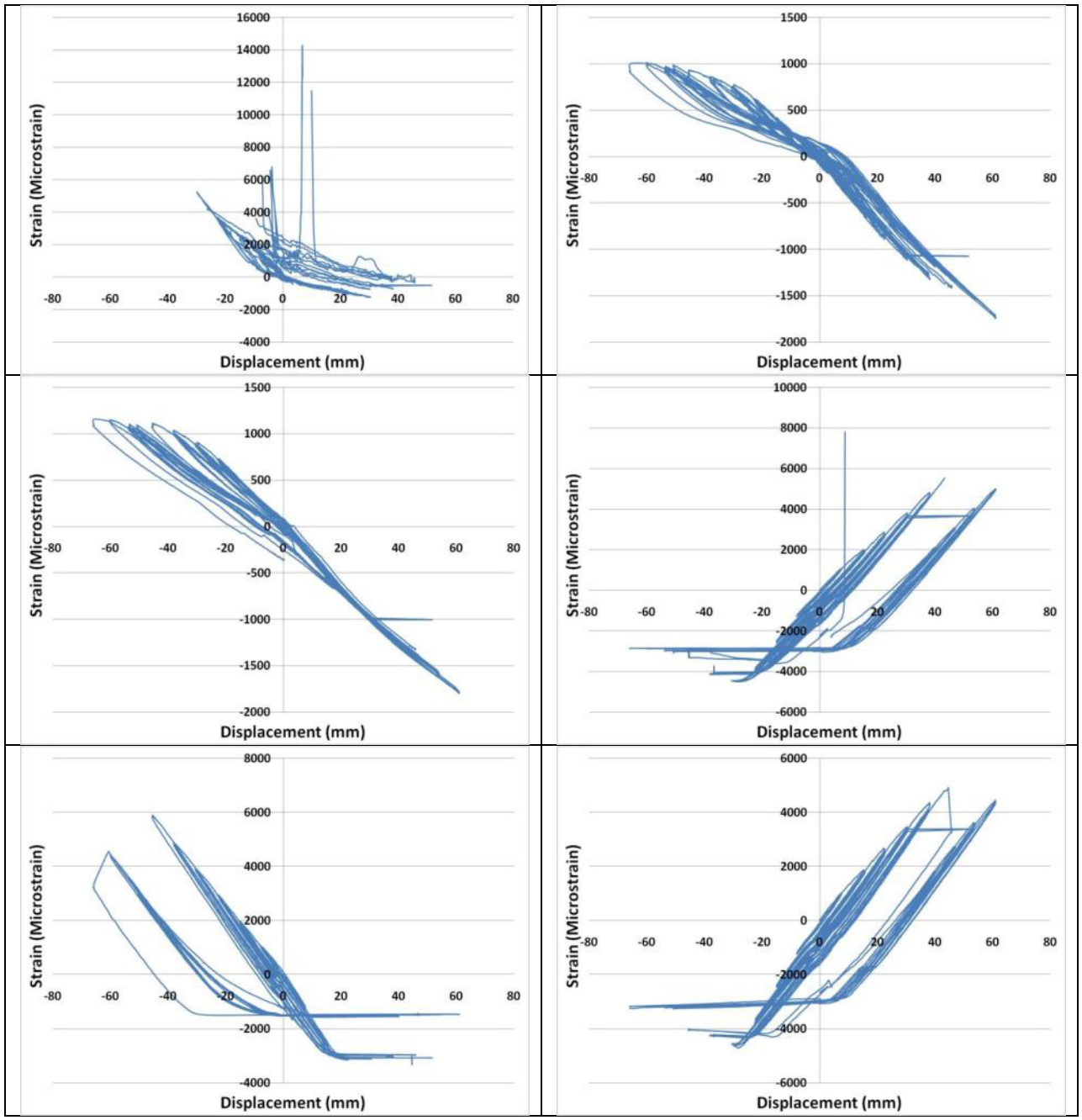
Strain (Microstrain)
Displacement (mm)
16000
14000
12000
10000
8000
6000
4000
2000
0
-2000
-4000
1500
1000
500
-500
-1000
-1500
-2000
10000
8000
6000
4000
2000
0
-2000
-4000
-6000
-80
-60
-40
-20
0
20
40
60
80

Ch. 13-18

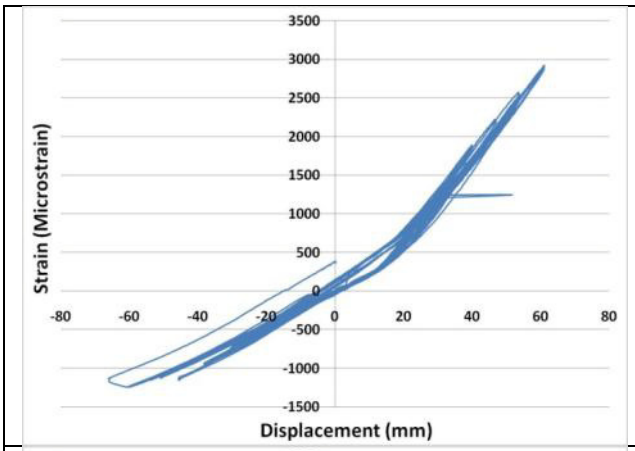

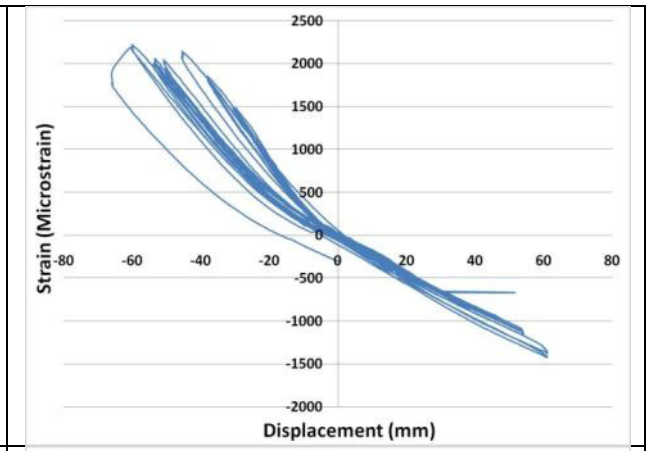

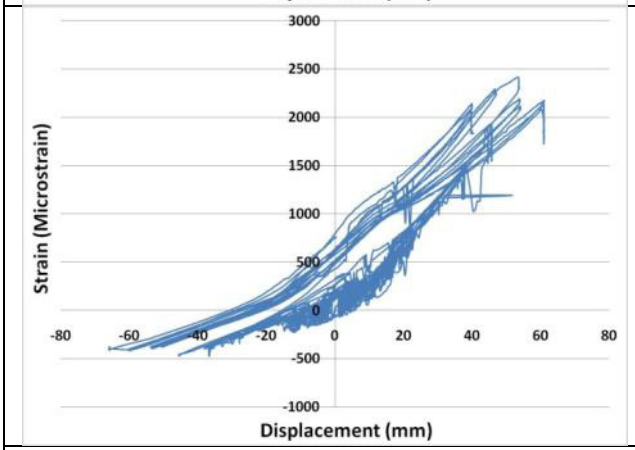

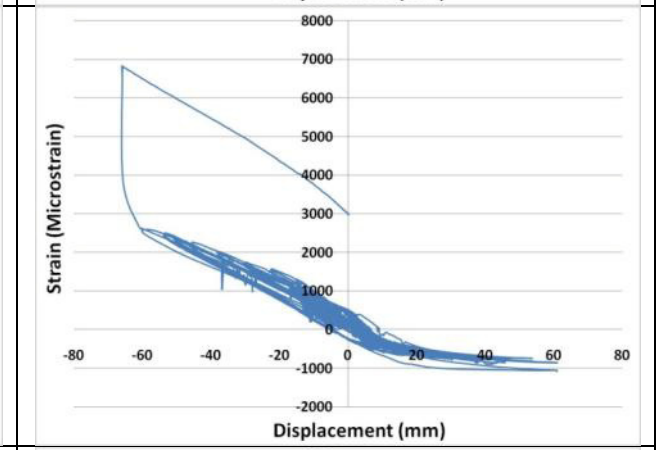

Channel 23 reading is corrupted.

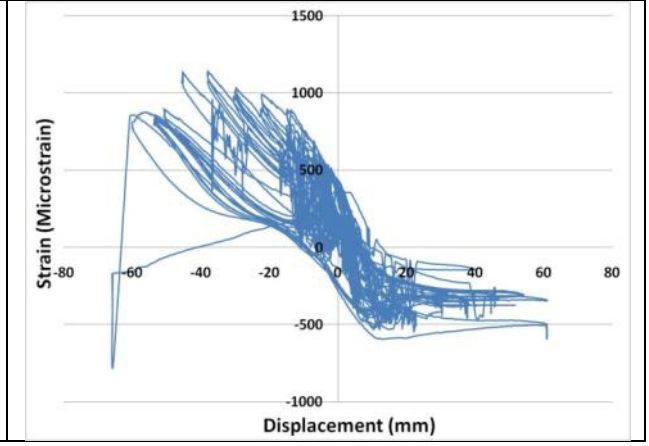

Ch. 19-24

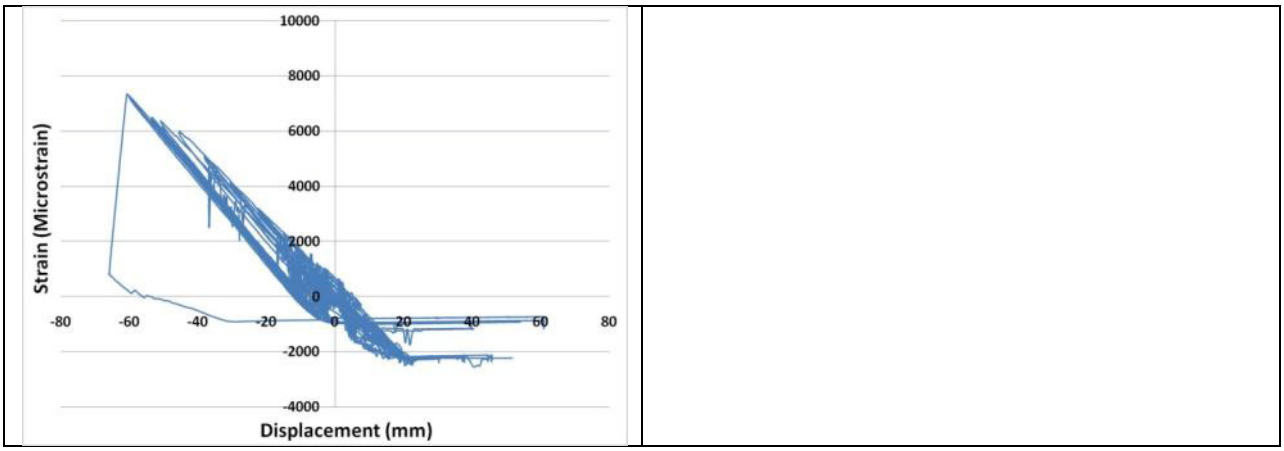

Channel 25 readings

Second Frame Recorded Data – 2nd Test

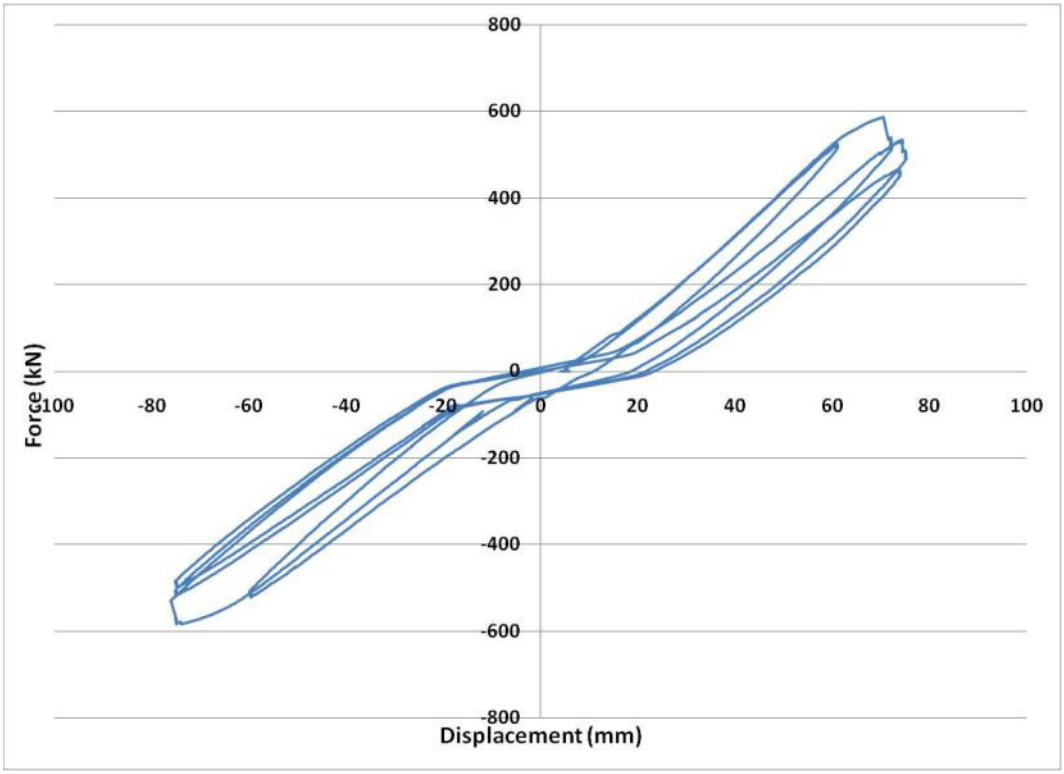

Fig. 4.6 – Hysteretic Lateral Load – Lateral Displacement Relationship for Frame No.2

(Without Prestressing the cables)

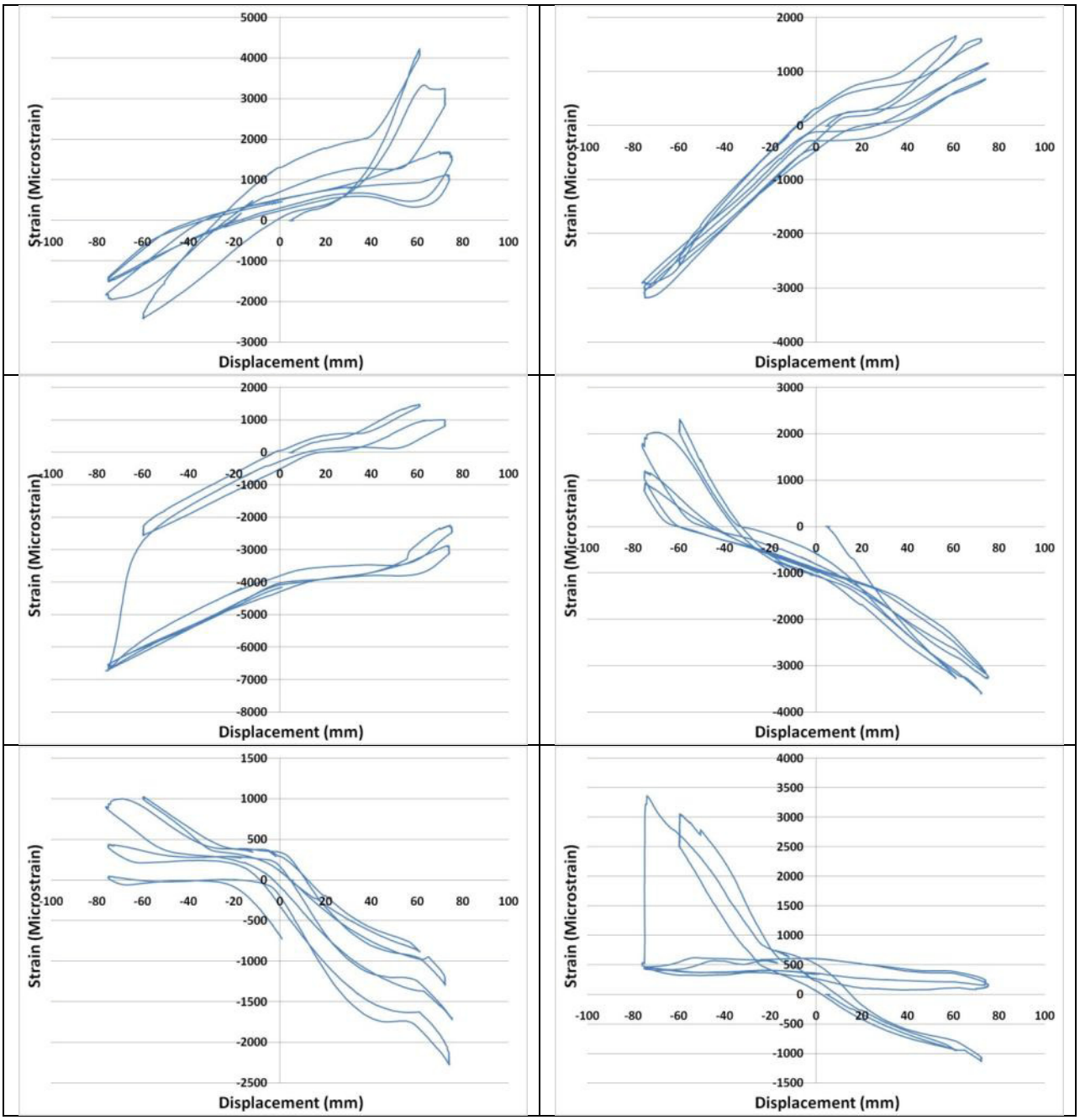
Strain (Microstrain)
Displacement (mm)
5000
4000
3000
2000
1000
0
-1000
-2000
-3000
-100 -80 -60 -40 -20 0 20 40 60 80 100
Strain (Microstrain)
Displacement (mm)
2000
1000
0
-1000
-2000
-3000
-4000
-100 -80 -60 -40 -20 0 20 40 60 80 100
Strain (Microstrain)
Displacement (mm)
2000
1000
0
-1000
-2000
-3000
-4000
-5000
-6000
-7000
-8000
-100 -80 -60 -40 -20 0 20 40 60 80 100
Strain (Microstrain)
Displacement (mm)
3000
2000
1000
0
-1000
-2000
-3000
-4000
-100 -80 -60 -40 -20 0 20 40 60 80 100
Strain (Microstrain)
Displacement (mm)
1500
1000
500
0
-500
-1000
-1500
-2000
-2500
-100 -80 -60 -40 -20 0 20 40 60 80 100
Strain (Microstrain)
Displacement (mm)
4000
3500
3000
2500
2000
1500
1000
500
0
-500
-1000
-1500
-100 -80 -60 -40 -20 0 20 40 60 80 100
Ch. 1-6

Channel 7 reading is corrupted.	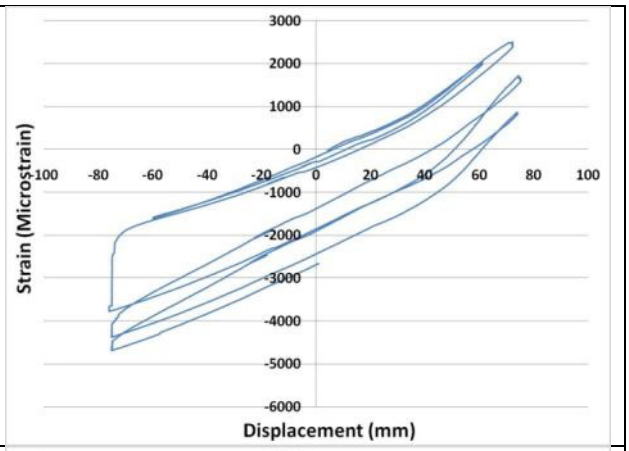
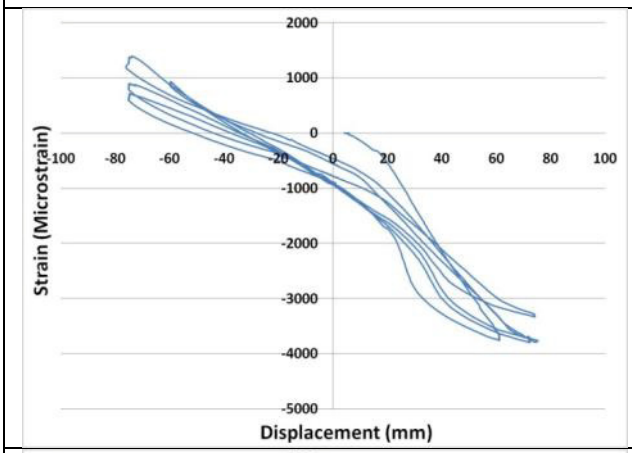	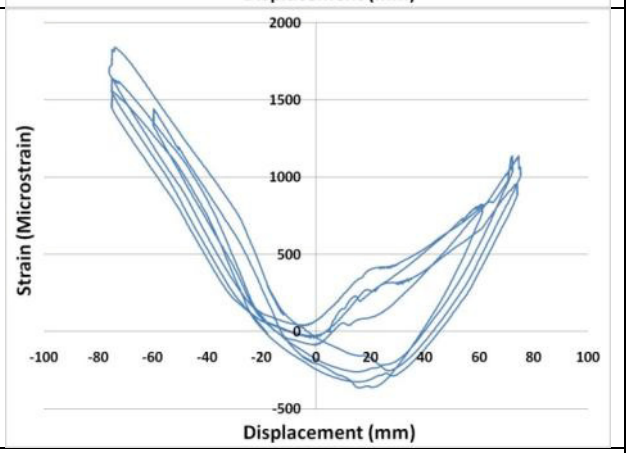
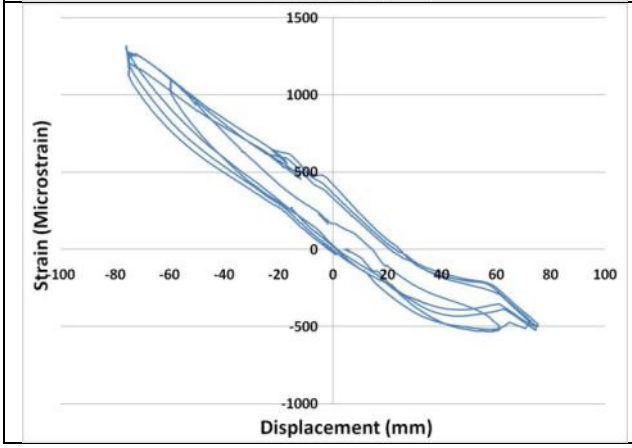	Channel 12 reading is corrupted.

Ch. 7-12

Channel 13 reading is corrupted.	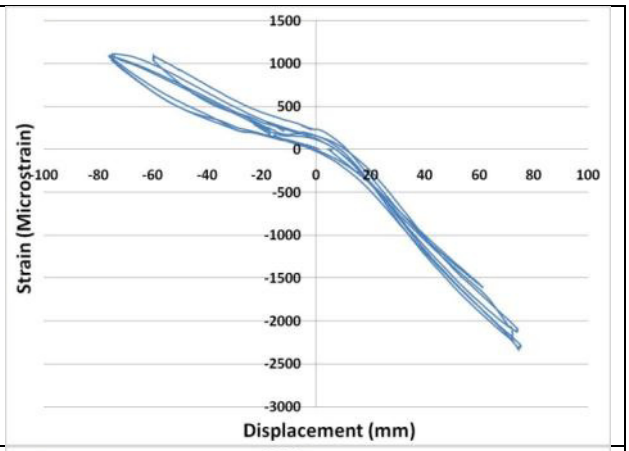
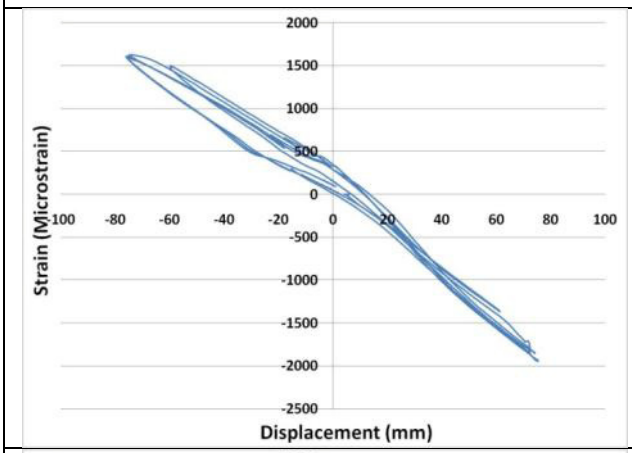	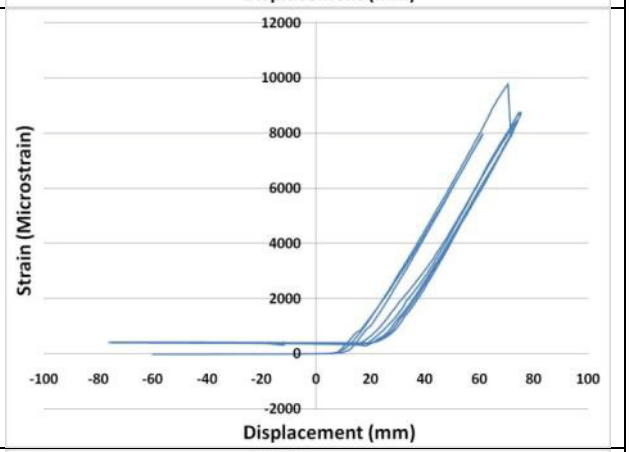
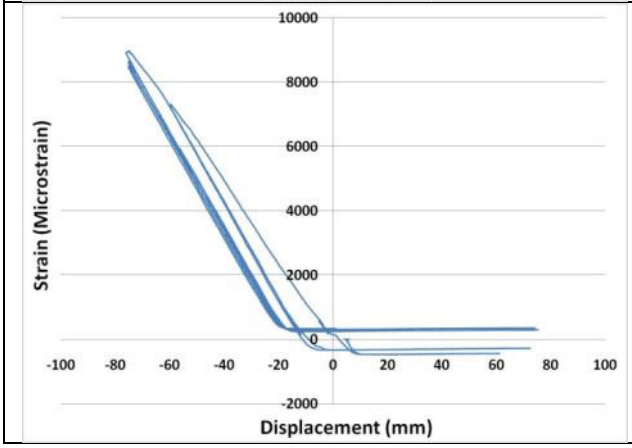	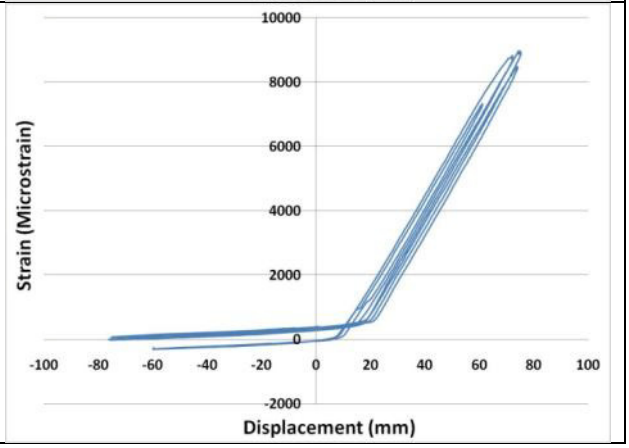

Ch. 13-18

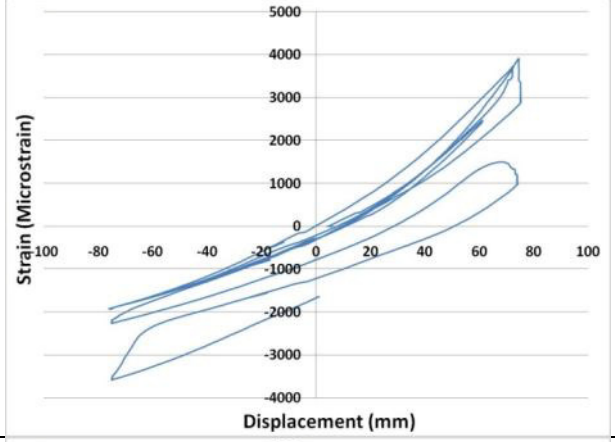

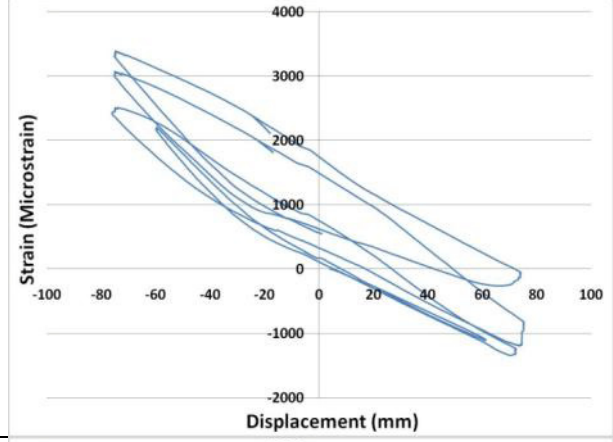

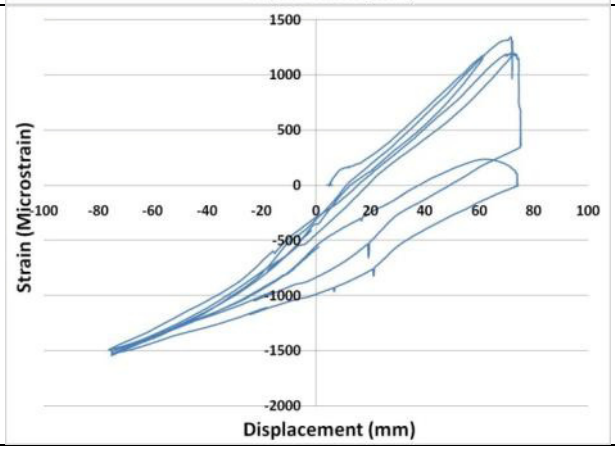

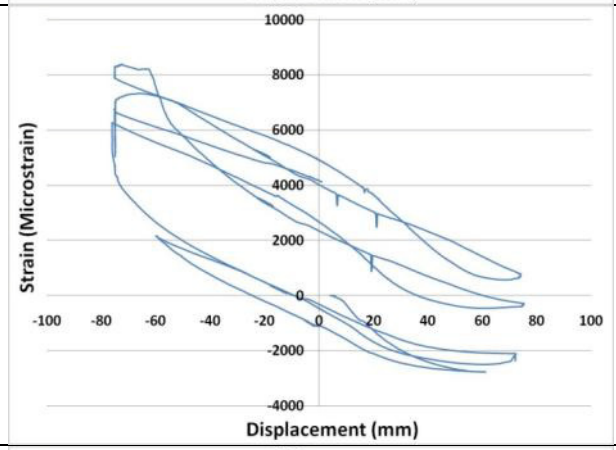

Channel 23 reading is corrupted.

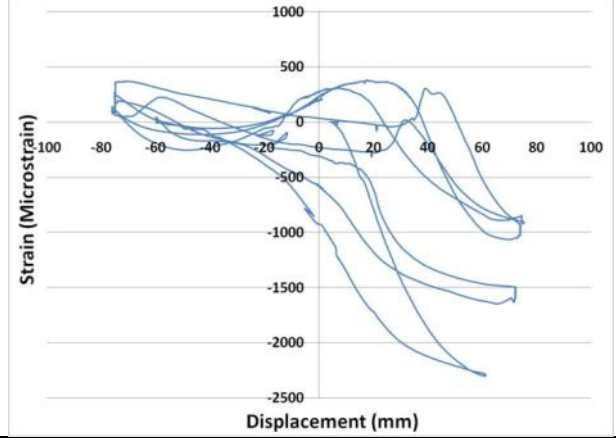

Ch. 19-24

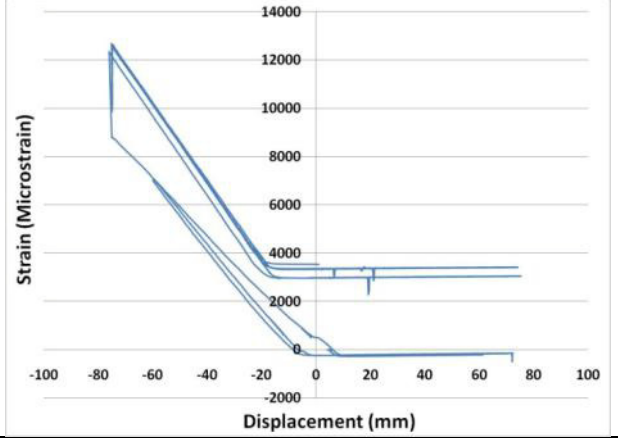

Channel 25 strain readings

LVDT Readings for Frames No. 1 and 2

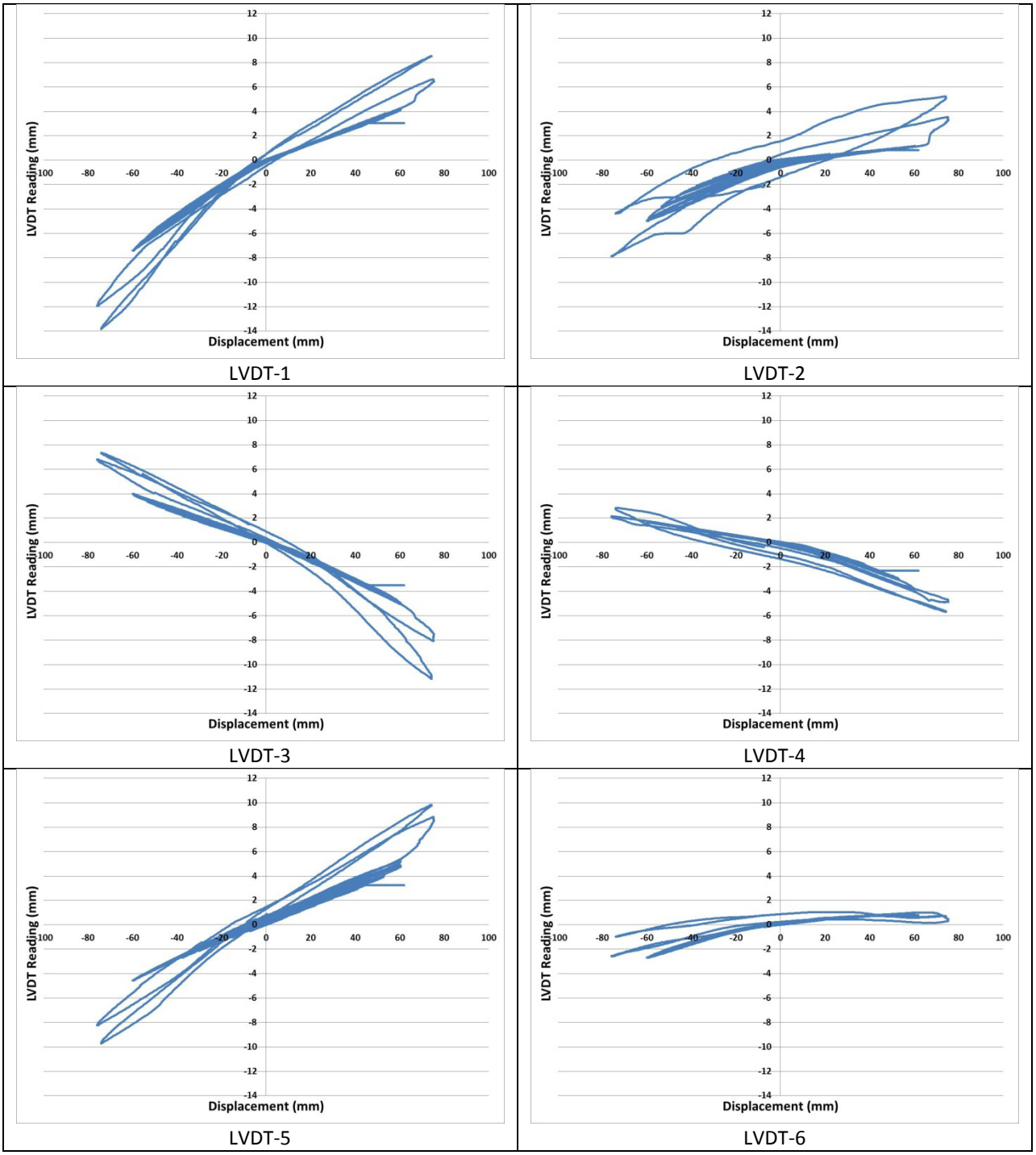

First Frame – LVDT Readings

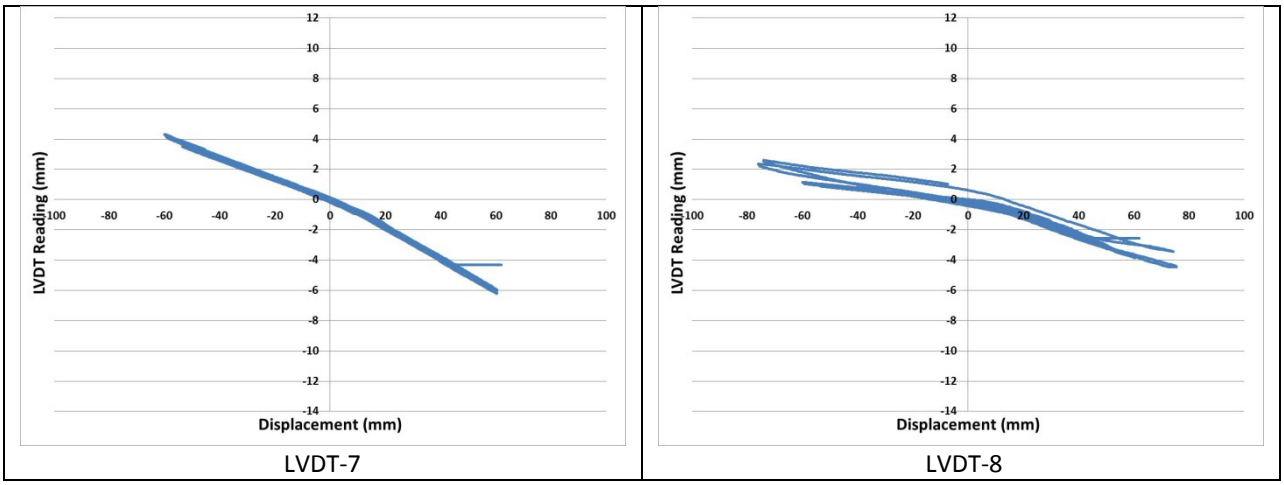

First Frame – LVDT Readings

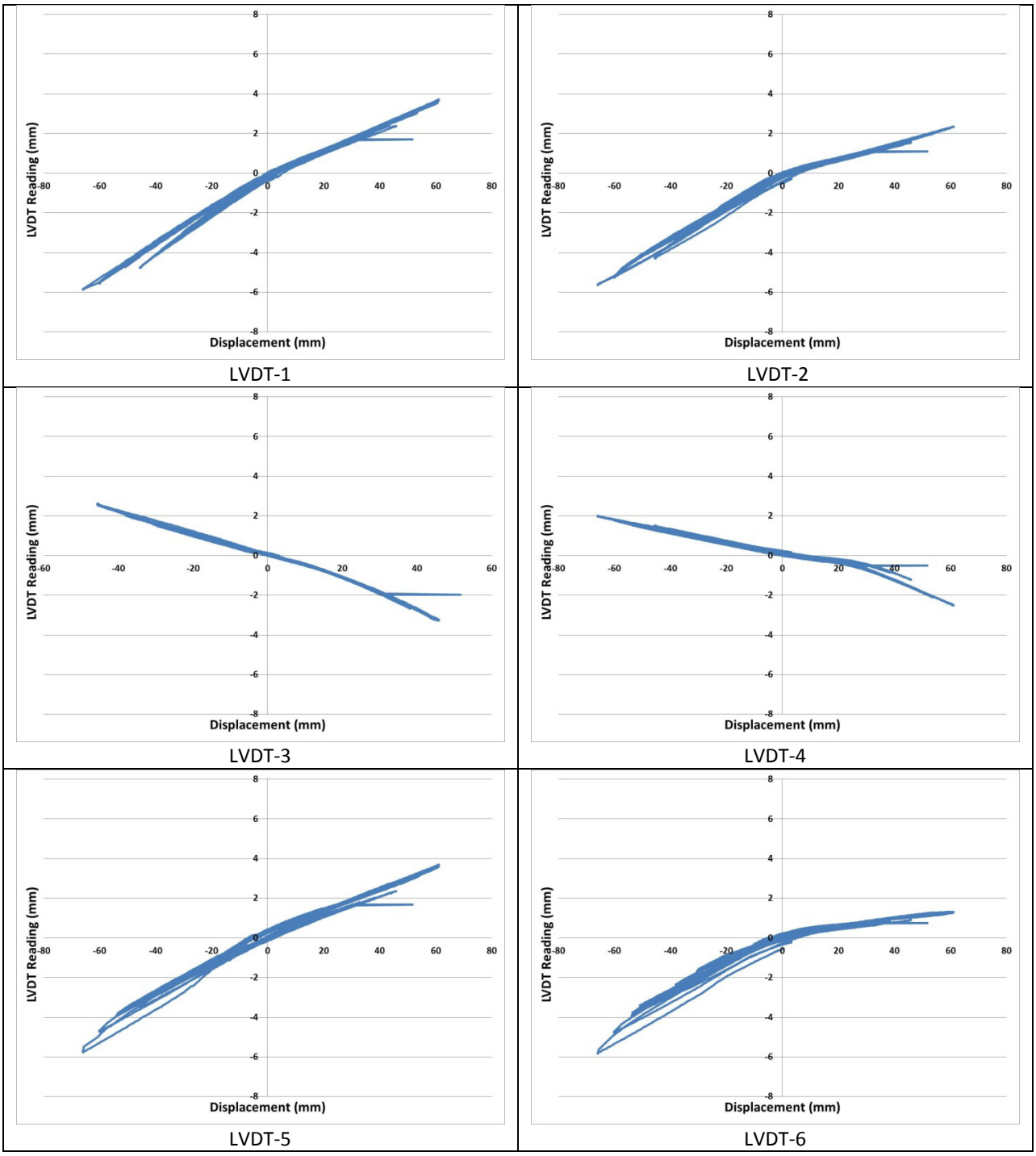

Second Frame – First Test with Prestressed Cables – LVDT Readings

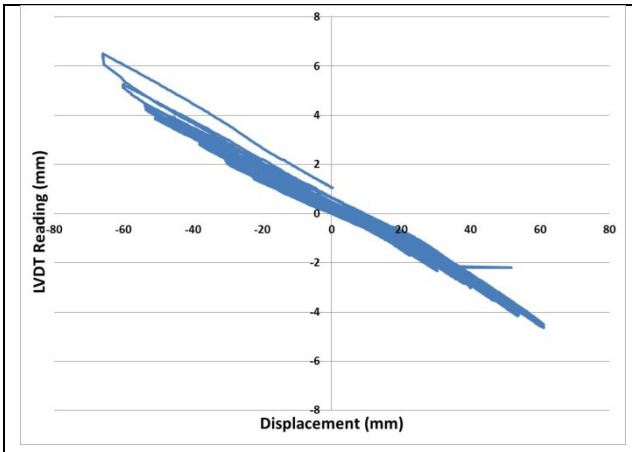

LVDT-7

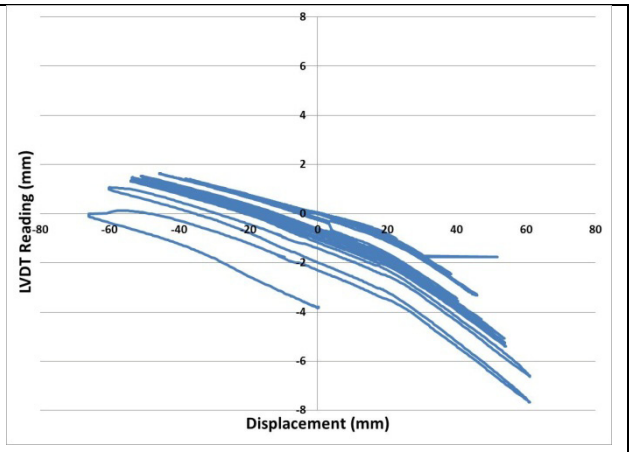

LVDT-8

Second Frame – First Test with Prestressed Cables – LVDT Readings

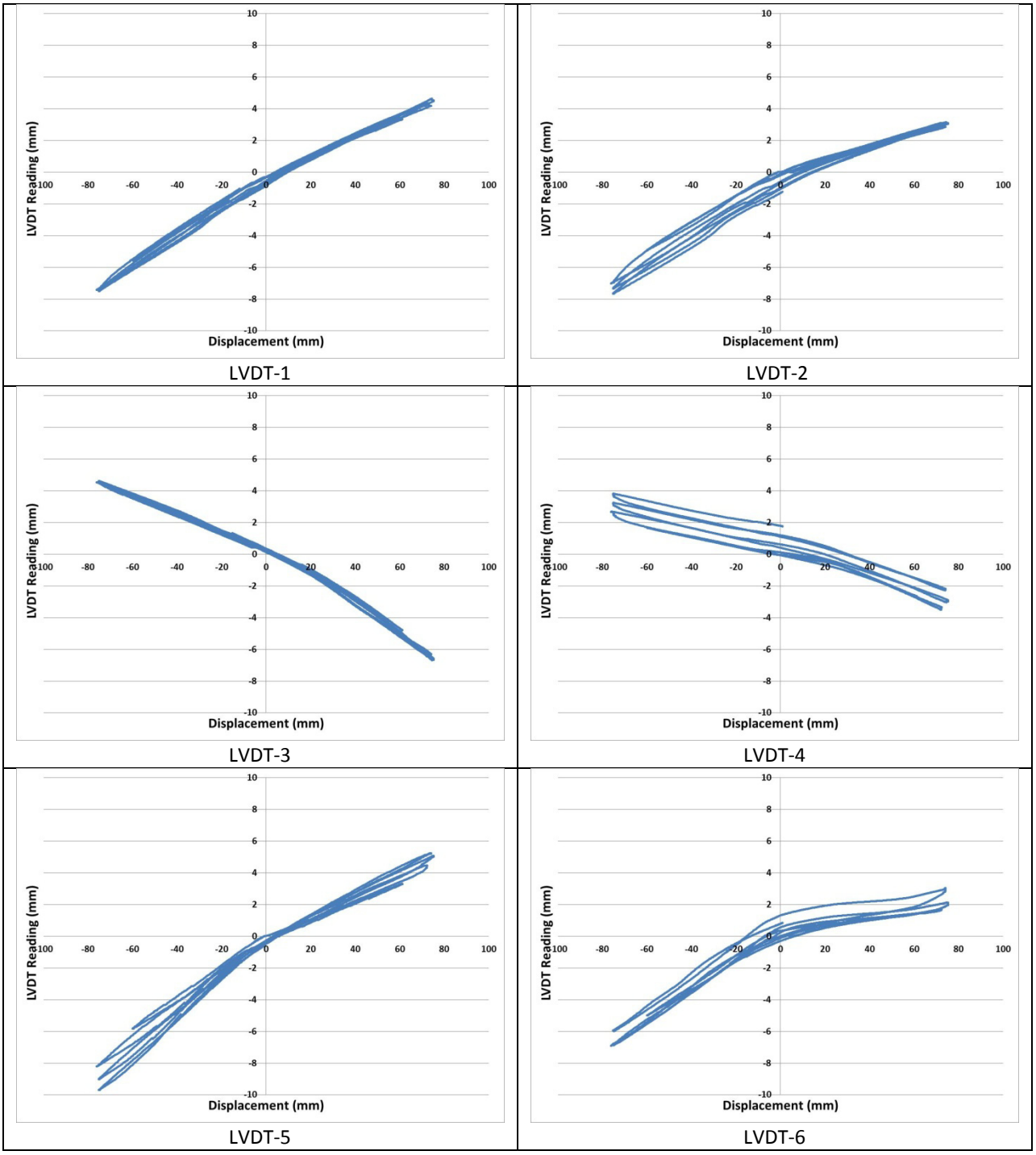

Second Frame – Second Test without Prestressing – LVDT Readings

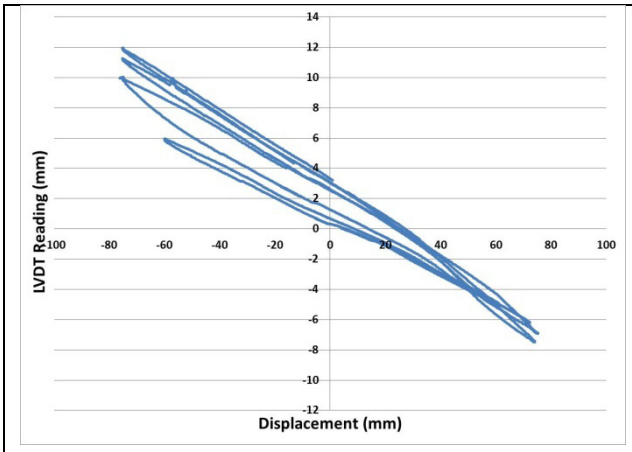

LVDT-7

Reading Error
LVDT-8

Second Frame – Second Test without Prestressing – LVDT Readings